UQAC
Université du Québec
à Chicoutimi

A THESIS SUBMITTED TO

THE UNIVERSITY OF QUEBEC AT CHICOUTIMI

IN PARTIAL FULFILMENT OF THE REQUIREMENTS

FOR THE DEGREE OF MASTERS

IN ENGINEERING

by

ANIL ARICI

DEVELOPMENT OF Al-SI-MG ALLOYS FOR PERMANENT MOLD CASTING AND HIGH-PRESSURE VACUUM DIE CASTING APPLICATIONS

Québec, Canada

UQAC
Université du Québec
à Chicoutimi

MÉMOIRE

PRÉSENTÉ À

L'UNIVERSITÉ DU QUÉBEC À CHICOUTIMI

COMME EXIGENCE PARTIELLE

DE LA MAITRISE EN INGÉNIERIE

par

ANIL ARICI

DÉVELOPPEMENT D'ALLIAGES D'AL-SI-MG POUR LES APPLICATIONS DE COULÉE DE MOULE PERMANENTES ET DE COULÉE SOUS PRESSION À HAUTE PRESSION

Québec, Canada

Abstract

The aim of this study is to design and to develop new aluminum alloys for high pressure vacuum die casting applications which can provide higher mechanical properties and superior light weighting solution for automotive body structures. In the meantime, the present study focuses on the effect of transition elements, namely, vanadium (V), zirconium (Zr) and molybdenum (Mo) on mechanical properties and microstructural features of permanent mold casting and high-pressure vacuum die casting AlSi10Mg and AlSi8Mg alloys.

In this work, eight distinct permanent mold casting alloys with different V, Zr and Mo addition combinations were designed and investigated to select the promising alloys for high pressure vacuum die casting (HPVDC) applications. After evaluation of mechanical properties on as-cast condition, the permanent mold casting alloys were solution heat treated at 500 °C and 540°C up to 8 hours, followed by water quenching, and then subjected to an aging treatment at 170°C for 4 hours. Hardness measurements were performed to reveal the effect of different addition combinations and define the optimum heat treatment parameters. The hardness evaluation of as cast permanent mold castings showed that additions of V and Zr (HPD-101) elements improve hardness, yield strength, ultimate tensile strength and elongation of AlSi10Mg alloy by 14%, 28%, 29% and 25% respectively. On the other hand, the additions of V, Mo (HPD-103) resulted in 7%, 21%, 12% and 3% improvement in those properties respectively. Moreover, the additions combination of V, Zr and Mo (HPD-103) into AlSi10Mg resulted in an improvement of hardness, yield strength, ultimate tensile strength and elongation by 7%, 21%, 12, and 2% respectively on as-cast condition. The V, Zr additions into AlSi8Mg (HPD-802) improved hardness, yield strength ultimate tensile strength and elongation by 11%, 24%, 27% and 33% respectively, whereas the additions of V, Mo (in HPD-801) enhance these properties by 5%, 19%,

23% and 23%. Meanwhile, the additions of V, Zr, Mo in AlSi8Mg (HPD-803) resulted an outstanding improvement in yield strength, ultimate tensile strength and elongation values with increase of 27%, 32% and 61% respectively.

In order to optimize heat treatment parameters, hardness values of the experimental alloys were evaluated in two different temperatures with different soaking times. According to hardness results, the heat treatment parameters are optimized as solution heat treatment at 540°C for 2 hours, followed by water quench and aging at 170°C for 4 hours. In consideration of hardness and tensile properties on as-cast and heat-treated conditions, HPD-101 (V, Zr), HPD-802(V, Zr) and also HPD-803 (V, Zr, Mo) were chosen for further microstructural investigations and high-pressure vacuum die casting investigation.

The microstructures of selected alloys were examined by optical microscopy, scanning electron microscopy and transmission electron microscopy. The results indicate that addition of V and Zr into permanent mold casting alloys (HPD-101 and HPD-802) is beneficial to refine eutectic Si particles in the microstructures. Moreover, it can reduce length of Fe-rich intermetallic phases up to 20%, and also decrease the aspect ratio of intermetallic phases, proving the beneficial impact of V, Zr elements on intermetallic phase modification. On the other hand, V, Zr and Mo (HPD-803) additions remarkably decreased the length of the intermetallic phases by 40% in comparison with AlSi8Mg alloy. It is established that the main influence of V, Zr and Mo additions appeared in the formation of new distinct intermetallic phases such as $(AlSi)_3(ZrTi)$ and (Al-Si-Fe-Mn-V-Mo), modification of present intermetallic phases and silicon particles on as-cast condition. Following the solution heat treatment, partial dissolution of intermetallic phases and precipitation of dispersoids were observed, which would play vital role to improve mechanical properties.

In consideration of permanent mold casting (PM) alloys, high pressure vacuum die casting (HPVD) alloys were produced in six different composition including two base alloys with different level of Si. It is established that additions of V, Zr (10-I) metals into AlSi10Mg HPVD castings resulted in improvement of hardness, yield strength and ultimate tensile strength by 10%, 8% and 8% respectively while no significant change was reported for elongation of the alloy on as-cast condition. The additions of (V, Zr) into AlSi8Mg improved the hardness yield strength and ultimate tensile strength by 5%, 13% and 5% respectively while a slight reduction was observed in elongation in comparison to base alloy. On the other hand, in 8-III alloy (V, Zr, Mo), hardness, yield strength and ultimate strength was improved by 9%, 15% and 8% respectively, whereas the elongation also increased by 6%. After evaluation of mechanical properties on as-cast condition, optimization of heat treatment parameters was studied for T5 and T6 tempers. For T6 temper, although highest hardness values for HPVD castings were achieved via solution heat treatment at 540°C x 3h + WQ + 170°C x 4h, the heat treatment parameters are optimized as solution heat treatment at 520°C x 3h + WQ + 170°C x 4h in consideration of blistering effect. For T5 temper, two different conditions were selected; (1) 170°C x 4h and (2) 210°C x 1h. According to evaluation of mechanical properties, 10-II (V, Zr), 8-II (V, Zr) and 8-III (V, Zr, Mo) alloys were selected for further microstructural investigations.

The microstructural features of selected alloys on as-cast and heat-treated conditions were studied via optical microscopy, scanning electron microscopy and SEM-EBSD mapping. The results showed that the additions of (V, Zr) into AlSi10Mg alloy reduced the average grain diameter from 87.7 µm to 43.1 µm, revealing beneficial impact of V, Zr metals on grain modification. Besides, two new distinct intermetallic phases were observed which are (1) $(AlSi)_3(ZrTi)$ and (Al-Si-Fe-V-Mn). Moreover, quantitative analysis of intermetallics indicated

that aspect ratio and equivalent diameter of intermetallic phases reduced by 20% and 15% respectively, proving the beneficial influence of V and Zr on modification of intermetallic phases. It is also seen that heat treatment can further induce a reduction in the size and volume fraction of intermetallics and results the spherodizitation of the eutectic Si particles. Moreover, it was observed that V, Zr additions can promote the formation of dispersoids and thereby further increase the mechanical properties of the alloys in comparison to as-cast condition. It is also found that number density of dispersoids in 8-III (V, Zr, Mo) alloy were higher than those in 8-II (V, Zr) and 8-I (Base) alloys, resulting further improvement in mechanical properties. The thermal analysis of HPVDC alloys showed that V, Zr and Mo additions resulted in formation of three different exothermic peaks in DSC curves and the additions can reduce the onset and peak temperatures of β'', β' and β precipitations in base alloys.

Résumé

Le but de cette étude est de concevoir et de développer de nouveaux alliages d'aluminium pour les applications de moulage sous pression à haute pression, capables de fournir des propriétés mécaniques plus élevées et une solution légère supérieure de pondération pour les structures de carrosserie automobile. Dans l'intervalle, la présente étude porte sur l'effet des éléments de transition, à savoir le vanadium (V), le zirconium (Zr) et le molybdène (Mo) sur les propriétés mécaniques et les caractéristiques microstructurales du moulage permanent et du moulage sous vide à haute pression AlSi10Mg et Alliages AlSi8Mg.

Dans ce travail, huit alliages de coulée en moule permanents distincts avec différentes combinaisons de V, Zr et Mo ont été conçus et étudiés pour sélectionner les alliages prometteurs pour les applications de moulage sous vide à haute pression (HPVDC). Après évaluation des propriétés mécaniques à l'état coulé, les alliages de coulée en moule permanents ont été soumis à un traitement thermique en solution à 500° C et jusqu'à 8 heures, suivi d'une trempe à l'eau, puis soumis à un traitement de vieillissement à 170° C pendant 4 heures. Des mesures de dureté ont été effectuées pour comparer la dureté de chaque alliage et définir les paramètres optimaux de traitement thermique. En fonction des résultats de dureté, les paramètres de traitement thermique sont optimisés en tant que traitement thermique en solution à 540 ° C pendant 2 heures, suivi d'une trempe à l'eau et d'un vieillissement à 170 ° C pendant 4 heures. Des essais de traction sur des alliages tels que moulés et traités thermiquement ont également été effectués. Compte tenu des propriétés mécaniques des conditions de coulée et de traitement thermique, les alliages HPD-101 (V, Zr), HPD-802 (V, Zr) et HPD-803 (V, Zr, Mo) ont été choisis pour des investigations microstructurales plus poussées. et les applications de moulage sous vide à haute pression.

Les microstructures des alliages sélectionnés ont été examinées par microscopie optique, par microscopie électronique secondaire et par microscopie électronique à transmission. Les résultats indiquent que l'ajout de V et de Zr (HPD-101 et HPD-802) dans un alliage de coulée en moule permanent est bénéfique pour affiner les particules de Si eutectiques dans les microstructures. Par ailleurs, les additions de V, Zr et Mo (HPD-803) n'ont pas apporté de modification supplémentaire aux particules de silicium. Il est établi que l'influence principale des additions de V, Zr et Mo est apparue dans la formation de phases intermétalliques distinctes, la modification de phases intermétalliques et de particules de silicium et le renforcement de la solution à l'état de coulée. Après le traitement thermique en solution, la dissolution partielle des phases intermétalliques et la précipitation de dispersoïdes ont joué un rôle essentiel dans l'amélioration des propriétés mécaniques.

En ce qui concerne les alliages de coulée en moule permanents, des alliages de moulage sous pression à haute pression ont été produits en six compositions différentes, y compris deux alliages de base avec une teneur différente en Si. Les mesures de microdureté des alliages HPVDC sont effectuées à l'état fondu, puis l'optimisation des paramètres de traitement thermique a été étudiée pour les états T5 et T6. Sur la base des valeurs de dureté et des possibilités de formation de cloques, les paramètres de traitement thermique sont optimisés en tant que traitement thermique en solution à 520 ° C pendant 3h, suivi d'une trempe à l'eau puis d'un vieillissement à 170 ° C pendant 4h. De plus, des alliages de 10-II (V, Zr), 8-II (V, Zr) et 8-III (V, Zr, Mo) ont été sélectionnés pour des investigations microstructurales plus poussées.

Les caractéristiques microstructurales de certains alliages dans des conditions de coulée et de traitement thermique ont été étudiées par microscopie optique, microscopie électronique secondaire et cartographie SEM-EBSD. Les résultats ont révélé que l'addition de métaux V, Zr et

Mo entraînait une réduction significative de la taille des grains et la formation de nouvelles phases intermétalliques. On voit également que le traitement thermique peut induire une réduction de la taille et de la fraction volumique des intermétalliques et entraîne la sphérodisation des particules de Si eutectiques. De plus, il est indiqué que les additions de V, Zr et V, Zr, Mo peuvent grandement favoriser la formation de dispersoïdes et augmenter ainsi davantage les propriétés mécaniques des alliages par rapport à l'état de coulée. L'analyse thermique des alliages HPVDC a montré que les additions de V, Zr et Mo entraînaient la formation de trois pics exothermiques dans les courbes DSC et que ces additions pouvaient réduire les températures de début et de pointe des précipitations β '', β 'et β dans les alliages de base.

Acknowledgment

First and foremost, I would like to express my sincere thanks to my supervisor Prof. X. Grant Chen for his continuous trust and support during this research project. As a mentor, his contributions to my personal and professional life are priceless. It has been an honour to be his student. I would also like to express my gratitude to my co-director Prof. Zhang Zhan for his significant contribution to my research project. Without his guidance, this study would have never been accomplished.

I would like to convey my sincere gratitude to Prof. Duygu Kocaefe, and Prof. Yasar Kocaefe for giving me a chance to make my dream come true. During my study, they have always been supportive and treated me as their son.

I am very grateful to my friend Ahmet Deniz Bas for his endless support and help. His dedication, diligence and helpfulness will always remain an inspiration in my future. I am also thankful to my dear friends Sena Ozturk and Kaan Berki Karabay who supported and helped me during my study. They made my life much more fun and easier. My gratitude and appreciation for their friendship cannot be expressed. Many thanks are also to my colleagues and friends Dany Racine, Dave Girard, Dr. Kun Liu, Pier-luc Prive, Samuel Dessureault, Xiaoming Qian, Redouane Farid, Siyu Tu, Mengyun Liu, Chen Li, Wei Xu, Erdem Tekin for their kind support, friendship and help.

Finally, but no means least, I cannot find words to express my gratitude to my parents and my brother whose love and guidance are with me in whatever I pursue. I also thank my future wife Gozde Kaptikacti for her unceasing encouragement and everlasting support during my study.

This project was financially supported by Natural Science and Engineering Research Council of Canada (NSERC) and Rio Tinto Aluminum through the NSERC Industry Research Chair in the Metallurgy of Aluminum Transformation at Université du Québec à Chicoutimi (UQAC). I would like to thank both organizations for their support during my study.

PUBLICATIONS

Conference Papers and Presentations

1. Effect of Zr and V Additions on Microstructure and Mechanical Properties of the AlSi10Mg Cast Alloy, 16th International Conference on Aluminum Alloys, Quebec, Montreal, Canada 17-21 June 2018

2. Effect of Zr, V, Mo Additions on Mechanical Properties and Microstructure of AlSi8Mg Cast Alloy, TMS 2020, San Diego, California, USA, 23-27 February 2020

"Dedicated to Republic of Turkey, the country of beauty and generosity…

"We only need one thing, to be hardworking…"

M. Kemal Ataturk

Table of Contents

Abstract i

Résumé v

Acknowledgment viii

Chapter 1 2

INTRODUCTION 2

1.1 Definition of the Problem 2

1.2 Objective 5

1.3 Methodology 5

REFERENCES 7

Chapter 2 10

LITERATURE REVIEW 10

2.1 Aluminum-Silicon Casting Alloys 10

2.1.1 Aural ™ Alloys 15

2.2 Casting Processes 16

2.2.1 Permanent Mold Casting (Pm) 16

2.2.2 High Pressure Die Casting (HPDC) 18

2.2.3 High Pressure Vacuum Die Casting (HPVDC) 21

2.3 Role of Alloying Elements 23

2.3.1 Effect of Cu Addition 23

2.3.2 Effect of Mg Addition 23
2.3.3 Effect of Mn Addition 24
2.3.4 Effect of Fe Addition 25
2.3.5 Effect of Zr Addition 26
2.3.6 Effect of Ti Addition 26
2.3.7 Effect of Mo Addition 26
2.3.8 Effect of V Addition 27
REFERENCES 29
Chapter 3 35
EXPERIMENTAL PART 35
3.1 Alloy Design 36
3.2 Alloy preparation 37
3.2.1 Preparation of permanent mold casting alloys 37
3.2.2 Preparation of high-pressure vacuum die casting alloys 38
3.3. Heat Treatments 40
3.4 Characterization of Microstructures 41
3.4.1. Sample preparation for microstructure observation 41
3.4.2 Optical Microscopy observation and image analysis 42
3.4.3 SEM observation and elemental analysis 43
3.4.4. TEM observation and elemental analysis 44

3.5 Electrical Conductivity Analysis 44

3.6 Evaluation of Mechanical Properties 45

3.6.1 Microhardness Measurements 45

3.6.2 Evaluation of Tensile Properties 46

3.7 Differential Scanning Calorimetry 48

Chapter 4 50

EFFECT OF ZR, V AND MO ADDITIONS ON MECHANICAL PROPERTIES AND MICROSTRUCTURE OF PERMANENT MOLD CASTINGS 50

4.1 The Mechanical Properties of the Experimental Alloys 50

4.1.1 Hardness and Tensile Properties on As-Cast Condition 50

4.1.2 Optimization of Heat Treatment Parameters 54

4.1.3 The Mechanical Properties on T6 Condition 56

4.2 Selection of the Promising Alloys 59

4.2.1 Promising Alloy Selection for 10% Si Containing Alloys 59

4.2.2 Promising Alloy Selection for 8% Si Containing Alloys 60

4.3 Microstructure Investigation of the Promising Alloys 61

4.3.1 Microstructure of 10% Si Containing Alloys 61

4.3.2 Microstructure of 8% Si Containing Alloys (Base-8, HPD 802, and HPD 803) 71

4.4 Summary 82

REFERENCES 86

Chapter 5 88

EFFECT OF V, ZR AND MO ON MICROSTRUCTURE AND MECHANICAL PROPERTIES OF HPVD CASTINGS 88

5.1 The Mechanical Properties of HPVD Castings 88

5.1.1 The Hardness Evaluation of HPVD Castings on As Cast Condition 88

5.1.2 The Tensile Properties of HPVD Castings on As-cast Condition 89

5.2 Optimization of the Heat Treatment Parameters 91

5.2.1 Hardness Evaluation of T5 Heat Treated Alloys 92

5.2.2 Tensile Properties of T5 Heat Treated Alloys 94

5.2.3 Hardness Evaluation of T6 Heat Treated Alloys 96

5.2.4 Tensile Properties of T6 Heat Treated Alloys 99

5.3 Microstructure Investigation of HPVDC Alloys 101

5.3.1 Microstructure Analysis of 10%Si Containing Alloys on As-Cast Condition 102

5.3.2 Microstructure Analysis of 10% Si Containing Alloys on T6 Heat-Treated Condition 105

5.3.3 Microstructure Analysis of 8%Si Containing Alloys on As-Cast Condition 111

5.3.4 Microstructure Analysis of 8% Si Containing Alloys on T6 Heat-Treated Condition 115

5.4 Thermal Analysis of High-Pressure Vacuum Die Casting Alloys 122

5.5 Summary 125

REFERENCES 128

Chapter 6 130

GENERAL CONCLUSIONS AND RECOMMENDATIONS FOR FUTURE WORK 130

6.1 Conclusions 130

6.2 Recommendation for future work 135

List of Figures

Figure 2-1: Al-Si-Mg ternary phase diagram [4]. 11

Figure 2-2: Optical images of cast A356 alloys in unmodified (a) and 200ppm modified (b) conditions [12] 12

Figure 2-3: Illustration of T6 heat treatment steps on Al-Cu phase diagram [13]. 14

Figure 2-4: Schematically illustration of a permanent mold casting process [18]. 17

Figure 2-5: A typical micrograph of AlSi10Mg alloy produced by permanent mold casting method 18

Figure 2-6: Schematic illustration of high pressure die casting application [18]. 19

Figure 2-7: A schematic illustration of high-pressure vacuum die casting application [29]. 21

Figure 2-8: Optical microscopic images of Al-8% Si alloys, showing the porosity distribution in high pressure die casting (a) and high pressure vacuum die casting (b) 22

Figure 2-9: A typical micrograph of AlSi10Mg alloy produced by HPVDC method. 22

Figure 2-10: Effect of Mg content on T6 yield strength of Al-Si alloys [36] 24

Figure 2-11: Brittle Fe-rich intermetallic phase in AlSi10Mg casting 25

Figure 2-12: TEM micrograph of Al-(Fe,Mo)-Si dispersoids in interdendritic regions (a) and EDS spectrum of the dispersoids (b) [45]. 27

Figure 3-1: Electrical resistance furnace that used to produce the experimental alloys 37

Figure 3-2: Permanent mold that was used to produce the experimental alloys and cast plates of the Base10 alloy 38

Figure 3-3: High pressure vacuum die casting machine and produced cast plates of a sample ... 40

Figure 3-4: Electrical resistance furnace that was used for the heat treatments 41

Figure 3-5: Mounting and polishing machines that used for the metallographic sample preparation 42
Figure 3-6: Nikon Eclipse ME600 Optical Microscope 43
Figure 3-7: Scanning electron microscope used for microstructure observations 43
Figure 3-8: TEM, JEM-2100 transmission electron microscope. 44
Figure 3-9: Portable Fisher Sigmacope Electrical Conductivity Measurement System 45
Figure 3-10: Vickers microhardness machine used for the hardness measurements 45
Figure 3-11: Schematic illustration of Tensile Test Specimen 46
Figure 3-12: Instron-8801 tensile testing machine. 47
Figure 3-13: Differential scanning calorimetry system (DSC 8000) used in thermal analysis. ... 48
Figure 4-1: Hardness results of 10% Si containing alloys on as-cast condition 50
Figure 4-2: Hardness results of 8% Si containing alloys on as-cast condition 51
Figure 4-3: Tensile properties of 10% Si containing alloys on as-cast condition 52
Figure 4-4: Tensile properties of 8% Si containing alloys on as-cast condition 54
Figure 4-5: Evaluation of the hardness as function of holding times at the solution temperature 500°C (a,b) and at the solution temperature of 540°C (c,d) 55
Figure 4-6: Hardness evaluation of the experimental alloys on as-cast and T6 heat treated conditions. 56
Figure 4-7**:** Tensile properties of 10% Si containing alloys on T6 (540 °C x 2h + 170 °C x 4h) condition 57
Figure 4-8: Tensile properties of 8% Si containing alloys on T6 (540 °C x 2h + 170 °C x 4h) treated condition. 58

Figure 4-9**:** Optical microstructure images of the Base10 (a,c) and HPD 101 (b,d) alloys on as cast condition. 62

Figure 4-10**:** SEM backscattered electron image of the base alloy (a) and EDS spectrum of Fe-rich phase (b) 63

Figure 4-11**:** SEM backscattered electron image of HPD101 alloy (a), and EDS spectrum of Zr-rich intermetallic phase (b), and V-rich intermetallic phase (c) 63

Figure 4-12**:** Optical images of the Base10 (a) and HPD101 (b) alloys on heat-treated condition 64

Figure 4-13: SEM backscattered electron images of the Base10 (a) and HPD101 (b) alloys. 65

Figure 4-14**:** Equivalent Diameter of Si particles for Base-10 and HPD 101 alloy in both as-cast and heat-treated conditions 66

Figure 4-15: Volume Fraction (a) and aspect ratio (b) of the intermetallic phases in the Base10 and HPD 101 alloys on both as cast and heat-treated conditions 67

Figure 4-16: Length of the intermetallic phases in Base-10 (a) and HPD-101 (b) alloys. 67

Figure 4-17**:** Dispersoid zone and dispersoid free zone in the solution heat treated Base-10 (a) and HPD-101 (b) microstructures. 68

Figure 4-18: Secondary electron images of etched Base-10 (a) and HPD-101 alloys after solution heat treatment 69

Figure 4-19: Number density of dispersoids (a) and area fraction of dispersoid zones (b) 69

Figure 4-20: TEM images of Base-10 (a) and HPD-101 (b) alloys on solid- solution state. 70

Figure 4-21: Optical microscope images of Base8 (a), HPD802 (b) and HPD803 (c) alloys respectively. 72

Figure 4-22**:** SEM image (a), EDS spectrum (b) and present phases (c) in Base-8 alloy on as-cast condition 73

Figure 4-23: SEM image (a), EDS spectrums (b,c,d) and present phases (e) in HPD-802 alloy on as-cast condition. 74

Figure 4-24: SEM image, EDS spectrum and present phases in HPD-803 alloy on as-cast condition 75

Figure 4-25: Optical images and SEM micrographs of Base8 (a, d), HPD802 (b, e) and HPD803 (c, f) on heat-treated condition (540 °C x 2h + 170 °C x 4h). 76

Figure 4-26: Equivalent diameter of Si particles on as cast and heat-treated conditions for 8% Si containing alloys 77

Figure 4-27: Volume fraction (a), aspect ratio (b) and length of the intermetallic phases (c) in the experimental alloys on as cast and heat-treated conditions 79

Figure 4-28: Dispersoid zone and dispersoid free zone in the solution heat treated Base-8 (a), HPD-802 (b) and HPD-803 (c) microstructures 80

Figure 4-29**:**Secondary electron images of etched Base-8 (a), HPD-802 (b) and HPD-803 (c) alloys after solution heat treatment..... 81

Figure 4-30: Number density of dispersoids and area fraction of dispersoid zones in Base-8, HPD-802 and HPD-803 alloys. 81

Figure 5-1**:** Hardness of the 10% (a) and 8% (b) Si containing alloys on as-cast condition 89

Figure 5-2**:** The tensile properties of 10 % (a) and 8 % (b) Si containing HPVD castings on as-cast condition. 91

Figure 5-3: The hardness evaluation of the experimental alloys at 170°C (a,b) and 210°C (c,d) heat treated conditions 93

Figure 5-4: Tensile properties of HPVD castings on 170°C x 4h (a,c) and 210°C x 1h (b,d) conditions 95

Figure 5-5**:** Hardness evaluation of 10 % Si (a, c, e) and 8 % Si (b, d, f) containing alloys on T6 heat treated conditions 97

Figure 5-6: Tensile properties of HPVD castings on T6 heat treated condition at 500°C..... 100

Figure 5-7**:** Tensile properties of HPVD castings on T6 heat treated condition at 520°C. 101

Figure 5-8: Optical microscopic images of Aural-3 (a,c) and 10-II (b,d) alloys at the center of samples on as-cast condition..... 103

Figure 5-9: SEM backscattered image of Aural™-3 (a) and EDS spectrum of Fe-rich phase (b) 103

Figure 5-10**:** Backscattered SEM image of 10-II (a) and EDS spectrums (b,c) 104

Figure 5-11: EBSD mappings of Aural™-3 (a) and 10-II (b) alloys on as-cast condition..... 105

Figure 5-12: Optical microscopic images of Aural™-3 (a) and 10-II (b) alloys in T6 solution heat treated condition at X500 magnification..... 106

Figure 5-13: Backscattered SEM images of AuralTM-3 (a) and 10-II (b) inT6 heat treated condition 106

Figure 5-14: Aspect ratio (a) equivalent diameter (b) and volume fraction (c) of intermetallic phases in Aural-3 and 10-II alloys in as-cast and T6 treated conditions 108

Figure 5-15**:** Distribution of dispersoid zone and dispersoid free zone in Aural™-3 and 10-II alloys 109

Figure 5-16: Secondary electron images of etched Aural™-3 (a) and 10-II (b) alloys after solution heat treatment..... 110

Figure 5-17: Number density of dispersoids (a) and area fraction of DFZ (b) in 10% Si containing alloys 110
Figure 5-18: Optical microscopic images of 8-I, 8-II (V, Zr) and 8-III (V, Zr, Mo) alloys in as-cast condition 111
Figure 5-19: Backscattered SEM image (a) of 8-I alloy and EDS spectrum of Fe-rich phase (b) 112
Figure 5-20: Backscattered SEM image of 8-II (V, Zr) alloy and EDS spectrum of intermetallics 113
Figure 5-21**:** Backscattered SEM image of 8-III alloy and EDS spectrum of intermetallics 113
Figure 5-22: EBSD mapping of 8-I (a), 8-II (b) and 8-III (c) alloys at the center on as-cast condition 114
Figure 5-23**:** Optical microscopic images of 8-I (a), 8-II (b) and 8-III (c) alloys at the center of the sample on T6 condition at 520°C x 3h + 170°C x 4h 116
Figure 5-24: Backscattered SEM images of 8-I (a), 8-II (b) and 8-III(c) in T6 heat treated condition. 117
Figure 5-25: Quantitative analysis of intermetallic phases on as-cast and T6 heat treated conditions. 118
Figure 5-26: Distribution of dispersoid zone and dispersoid free zone in 8-I (a), 8-II (b) and 8-III (c) alloys..... 119
Figure 5-27: Secondary electron images of etched 8-I (a), 8-II (b) and 8-III (c) alloys after solution heat treatment 120
Figure 5-28: Number density of dispersoids and area fraction of DFZ in 8% Si containing alloys 120

Figure 5-29: Differential scanning calorimetry curves of 10% Si containing alloys 122

Figure 5-30: Differential scanning calorimetry curves of 8-I (a), 8-II (b) and 8-III (c) alloys.. 124

Table 2-1: Characteristics of aluminum - silicon casting alloys [9]. 12

Table 2-2: Aural ™ family alloy compositions (%wt) [17]. 16

Table 2-3: Advantages and disadvantages of permanent mold casting process 17

Table 2-4: Advantages and disadvantages of high pressure die casting applications..... 20

Table 3-1: Chemical composition of the experimental alloys (wt.%) 38

Table 3-2**:** Chemical composition of the high-pressure vacuum die casting alloys (wt.%) 39

Table 3-3: Heat treatment parameters and conditions for the experimental alloys. 41

Table 4-1**:** Electrical conductivity of the 10% and 8% Si containing alloys on as-cast and solution heat treated conditions 52

Table 4-2: The effect of addition elements on tensile properties of 10% Si containing alloys 53

Table 4-3: Effect of addition elements on tensile properties of 8%Si containing alloys..... 54

Table 4-4: Electrical conductivity of T6 heat treated experimental alloys..... 57

Table 4-5: The main phases and their morphology identified using SEM/EDS in HPD101 alloy. 65

Table 4-6: The suggested alloys for high pressure vacuum die casting investigation. 85

Table 5-1: Electrical conductivity variation of the HPVD castings 89

Table 5-2**:** Electrical conductivity of HPVD castings at peak hardness values..... 99

Table 5-3: The average grain diameter of 10% Si containing alloys..... 105

Table 5-4: The main phases and their morphology identified using SEM/EDS in AuralTM-3 alloy. 107

Table 5-5: The main phases and their morphology identified using SEM/EDS in 10-II(V, Zr) alloy. 107

Table 5-6: Electrical conductivity of Aural^{TM}-3 and 10-II (V, Zr) alloys on T6 treated condition at 520°C x 3h + 170°C x 4h 109

Table 5-7: The average grain diameter of 8% Si containing HPVD castings 114

Table 5-8: Electrical conductivity of HPVD castings on T6 heat treated condition at 520°C x 3h + 170°C x 4h 121

Table 5-9: The onset and peak temperatures of β'', β' and β phases in 10% Si containing alloys 123

Table 5-10: The average values of onset and peak temperatures for A and B peaks in 10-II alloy 123

Table 5-11: The onset and peak temperatures of β'', β' and β phases in 8% Si containing alloys 125

Table 5-12: The average onset and peak temperatures for A and B peaks in 8-II and 8-III alloys. 125

CHAPTER 1

INTRODUCTION

Chapter 1

INTRODUCTION

1.1 Definition of the Problem

Growing concern on the requirements of fuel economy and vehicle emissions has forced producers to find out new ways of improving fuel efficiency. One way of increasing the fuel efficiency is to reduce to total mass of the product by using light weight alloys for structural components and applying superior manufacturing technologies with short heat treatment cycles. Therefore, the use of aluminum alloys is steadily increasing to reduce the weight of the structural applications. In this regard, the Aural alloys are Al-Si based alloys that specifically designed for high integrity structural die castings. These alloys offer a wide range of property levels to meet durability, high mechanical properties as well as the crash performance requirements [1]. Beside their excellent corrosion resistance, Aural alloys can be used to cast thin and large structural components due to their very high fluidity. [2].

It is established that the casting process plays a vital role on mechanical properties of the alloys due to its influence on microstructural features. Therefore, extensive studies were performed on the different casting processes to reveal the effect of casting processes as well as their similarities and main differences. Al-Si alloys are widely used to produce permanent mold (PM) and high-pressure vacuum die casting (HPVDC) components. In permanent mold casting applications, molten metal is poured into a metal mold cavity and then solidified under relatively low cooling rate (<10 Ks^{-1}). Permanent mold castings can provide desirable grain structure with high mechanical properties and stiffness. Addition to that, heat treatment can be applied for the

permanent mold castings [3-4]. On the other hand, in HPVDC, the molten metal is injected into the mold cavity with higher speed (30-50m /s) and solidified under high pressures (up to 200MPa) with high cooling rate (up to ~103 Ks–1) in comparison with permanent mold casting. High pressure vacuum die casting can provide excellent dimensional accuracy and high casting tensile strength for the final product. Due to the presence of vacuum valve, gas pores and shrinkage can be hinder which allows to perform heat treatment applications for the castings. [5-6].

It is well known that the alloying elements such as Cu, Mn, Fe, Mg are traditionally added into Al-Si alloys to improve their mechanical properties. The studies showed that Cu and Mg are used in Al-Si alloys to obtain common precipitation hardening phases such as Al_2Cu, Mg_2Si and Al_2CuMg which can provide higher mechanical properties for the alloy. [7-8]. For instance, Dunn and Dickert [9] proved that the addition of Mg up to 0.55% has favorable effect on tensile properties and hardness of A380 and 383 alloys. Also, further improvement in hardness can be achieved via heat treatment. On the other hand, some studies indicate that excessive addition of Mg may result in reduction of ductility and fracture toughness of the materials. It is also reported that the strength of the Al-Si alloys after aging can be significantly increased by the addition of Cu element [10]. Iron is another additive element that frequently used in commercial Al-Si alloys. Komiyama et al. observed that in Al-Si-Cu-Mg alloy, increasing Fe content can improve the hardness of Al-Si alloys whereas it resulted in a significant reduction of tensile strength and elongation when the iron content exceeds %0.5. Manganese is commonly used as Fe neutralization in order to inhibit harmful effect of iron. It can lead to the formation of Fe-rich skeleton-like phases as opposed to the needle-like shape phases. On the other hand, Shabestari et al. showed that high amount of Mn content can resulted in sludge formation which would affect the machinability of the alloy [11].

The morphology and size of eutectic silicon particles is another key factor to determine mechanical properties of Al-Si alloys. The presence of brittle, acicular silicon particles in as cast microstructure results a major decrease in mechanical properties whereas fine, fibrous silicon particles lead a significant improvement in ultimate tensile strength and ductility of alloy. In order to modify size and morphology of silicon particles, strontium is commonly added into Al-Si alloys.

Nowadays, the attention has been paid to the effect of the transition elements such as Zr, V, Mo and Ti in Al-Si-Cu-Mg alloys. The presence of minor level trace elements, such as Ti, Mn, Fe and Cr in Al-Si alloys may induce changes in the solid-state precipitation sequence due to their possible interactions with purposely added transition metals, such as Zr, V and Mo, thus resulting the formation of various types of dispersoids and precipitates inside α-Al grains at higher volume fractions [12]. In this regard, several studies reported that V, Zr and Ti additions in Al-Si-Cu alloys can improve mechanical properties at high temperature by forming thermally stable intermetallics and precipitates on as-cast and heat-treated conditions [13-14]. Another finding indicates that the minor additions of Zr in aluminum alloys can modify the eutectic silicon particles which supports the improvement of the tensile strength and wear resistance. Knippling et al. [15] reported that Mo addition to Al-Si alloys results in the formation of Mo-containing dispersoids which can resist the coarsening process at high temperatures and thus improve the mechanical properties of the alloy. Also, it is established that the creep resistance of Al-Si-Cu alloys can be improved via addition of Mo transition element [16].

Although several studies on the additions of V, Zr and Mo in Al-Si-Cu alloys provide important input for fundamental understanding of the influence of these elements, a clear insight has not been achieved for the roles of Zr, V and Mo in microstructure features and mechanical properties of Al-Si cast alloys which is one of the most used alloys for aerospace and automotive industry. Hence,

this study attempts to investigate the effect of Zr, V and Mo additions and various heat treatment applications on microstructural features and mechanical properties for permanent mold casting and high-pressure vacuum die casting alloys.

1.2 Objective

The aim of this study is to reveal the effect of V, Zr and Mo additions on microstructure features and mechanical properties of permanent mold casting and high-pressure vacuum die casting Al-Si alloys. Addition to that, this study is performed to design and develop new aluminum alloys for high pressure vacuum die casting applications which can provide higher mechanical properties and superior light weighting solution for automotive body structures. In order to achieve the objectives, several research works will be performed and discussed as follows;

1. To investigate the effect of different chemical compositions on mechanical properties;
2. To optimize the heat treatment parameters;
3. To evaluate mechanical properties of the experimental alloys on as cast and heat-treated conditions;
4. To characterize microstructure of the alloys in order to have better understanding on the strengthening mechanisms.

1.3 Methodology

1. Experimental alloys were produced by permanent mold casting.
2. Mechanical properties of permanent mold casting alloys were evaluated via tensile testing and microhardness measurements in as cast and heat-treated conditions.
3. Microstructure analysis and electrical conductivity measurements were carried out in order to understand strengthening methods. As cast and heat-treated microstructures were observed by optical microscope. A scanning electron microscopy (SEM,

equipped with energy-dispersive X ray spectroscopy) was used to identify intermetallic phases.

4. Promising alloys were selected and produced by high pressure vacuum die casting.
5. Mechanical properties of high-pressure vacuum die casting alloys were evaluated in as-cast, T5 and T6 heat treated conditions.
6. Heat treatment parameters were optimized.
7. Microstructure characterization of high-pressure vacuum die casting alloys was performed via optical microscope, scanning electron microscope.
8. Electron backscatter diffraction (EBSD) was performed to study grain size.

REFERENCES

[1] Breton, F., Fourmann, J., (2016) Alloys with high strength and ductility for high pressure vacuum die casting in automotive body structure applications, (NADCA,2016)

[2] Tinto, R., Aluminium Your guide to automotive innovation. 2016: p. 12, 13.

[3] Ji, S., et al., Microstructural evolution and solidification behavior of Al-Mg-Si alloy in high-pressure die casting. Metallurgical and Materials Transactions A, 2013. 44(7): p. 3185-3197.

[4]. Gourlay, C., H. Laukli, and A. Dahle, Defect band characteristics in Mg-Al and Al-Si high-pressure die castings. Metallurgical and Materials Transactions A, 2007. 38(8): p. 1833-1844.

[5] Wang, L.-Y., Zheng, L.-S., Qu,W.-T., Zhou, X.-C., Xu, J.-W. , Special casting processes. Industry Press, Beijing, China, 1984: p. 196.

[6] Hamasaiid, A., et al., Effect of mold coating materials and thickness on heat transfer in permanent mold casting of aluminum alloys. Metallurgical and materials Transactions A, 2007. 38(6): p. 1303-1316.

[7] Moustafa M, Samuel FH, Doty HW, Valtierra S. Effect of Mg and Cu additions on the microstructural characteristics and tensile properties of Sr-modified Al–Si eutectic alloys. Int J Cast Met Res 2002;14: 235–53.

[8] Ouellet P, Samuel FH. Effect of Mg on the ageing behavior of Al–Si–Cu 319 type aluminum casting alloys. J Mater Sci 1999; 34:4671–97.

[9] Dunn R, Dickert W. Magnesium effect on the strength of A380.0 and 383.0 aluminum die casting alloys. Die Cast Eng 1975; 19:2–20.

[10] Zeren M., (2005). Effect of copper silicon content on mechanical properties Materials Processing Technology, 292-298

[11] S.G. Shabestari, H. Moemeni Effect of copper and solidification conditions on the microstructure and mechanical properties of Al–Si–Mg alloys Journal of Materials Processing Technology 153–154 (2004) 193–198

[12] Shaha, S.K., Czerwinski, F., Kasprzak, W., Chen, D.L. (2014). Tensile and compressive deformation behavior of the Al–Si–Cu–Mg cast alloy with additions of Zr, V and Ti. Materials & Design 59 (pp. 352–358).

[13] Shaha, S.K., Czerwinski, F., Kasprzak, W., Friedman, J., Chen, D.L. (2015). Microstructure and mechanical properties of Al-Si cast alloy with additions of Zr-V-Ti. Materials & Design 30, (pp. 801- 812).

[14] Mahmudi, R., Sepehrband, P., Ghasemi, H.M. (2006). Improved properties of A319 aluminum casting alloy modified with Zr, Materials Letters 60 (pp. 2606- 2610).

[15] K.E. Knipling: Development of a Nanoscale Precipitation- Strengthened Creep-Resistant Aluminum Alloys Containing Trialuminide Precipitates, Northwestern University, Evanston, IL, 2006.

[16] A.R. Farkoosh, X. Grant Chen, M. Pekguleryuz, Mater. Sci. Eng. A 620 (2015) 181- 189.

CHAPTER 2

LITERATURE REVIEW

Chapter 2

LITERATURE REVIEW

2.1 Aluminum-Silicon Casting Alloys

Aluminum casting alloys with high content of silicon are one of the most widely used alloys in the automotive, aerospace and electronics industries. Due to their light weight, low thermal expansion coefficient, high corrosion resistant and superior casting characteristics, aluminum alloys became center of attention of producers and are replacing cast iron components.

Due to high content of silicon, Al-Si alloys provide excellent castability. This attributes to the high fluidity of the molten metal and it is described as an ability to flow into a mold and fill the areas before molten metal solidified. It is known that fluidity of molten metal can be increased via increasing silicon content. Although higher amount of Si increases fluidity, formation of primary silicon particles in the melt can block the flow when Si content exceed 18-20%. Therefore, most of the Al-Si casting alloys contain no more than 18- 20% Si [1-3]. It is also reported that increasing Si content improves the strength and stiffness of the alloy while it reduces ductility. According to silicon content in microstructure, the cast aluminum alloys can be classified into three groups. Hypoeutectic aluminum alloys contain 5% - 10% Si containing alloys while eutectic alloys contain 11% - 13% Si and hypereutectic alloys contain 14% - 20% Si.

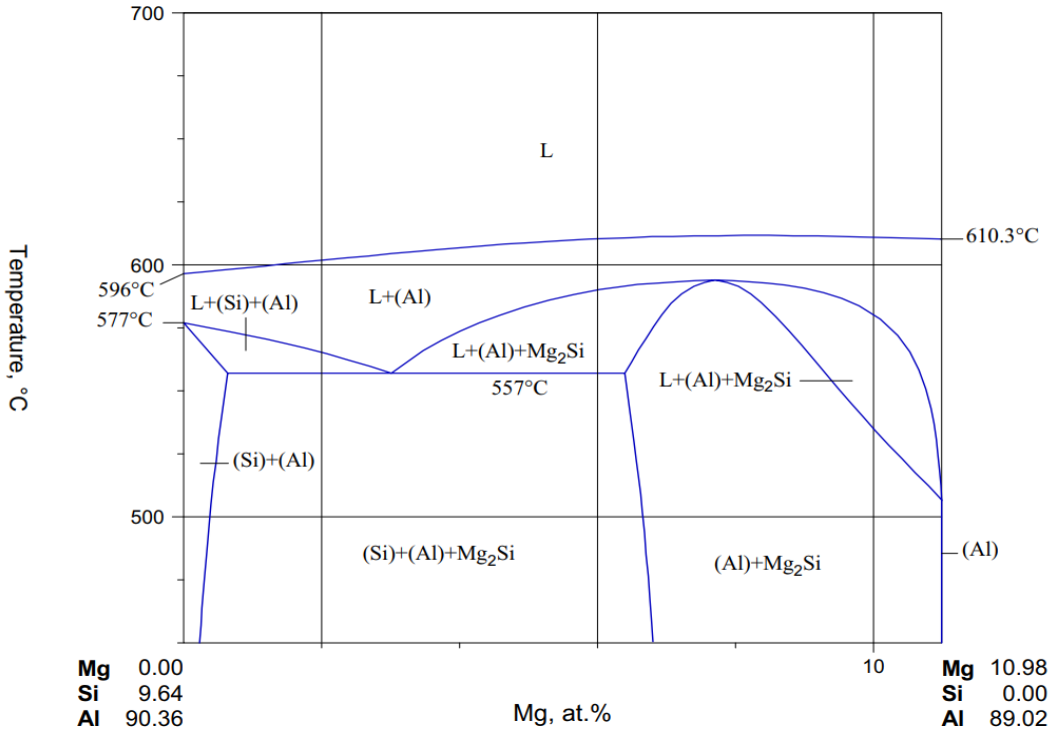

Figure 2-1: Al-Si-Mg ternary phase diagram [4].

High silicon containing hypereutectic alloys have very good casting characteristics, low thermal expansion coefficient and very high wear resistance. On the other hand, eutectic alloys offer high corrosion resistance and good weldability, while hypoeutectic and near eutectic aluminum alloys provide good castability and high corrosion resistance. In addition to that small amount of Mg and Cu might be added to increase their mechanical properties. These alloys are usually heat treated in order to further increase mechanical properties and to obtain desired combination of strength and ductility. Therefore, these Al- Si alloys can extensively use in automotive, aerospace and military industries [5-8].

Table *2-1* represents the characteristics of some major Al-Si alloys. The characteristics are rated from 1 to 5, which indicates the worst and best respectively.

Table 2-1: Characteristics of aluminum - silicon casting alloys [9].

Alloy	Casting Method	Resistance To Tearing	Pressure Tightness	Flui-dity	Shrinkage Tendency	Corrosion Resistance	Machin-ability	Weld-ability
319.0	S,P	2	2	2	2	3	3	2
332.0	P	1	2	1	2	3	4	2
355.0	S,P	1	1	1	1	3	3	2
A356.0	S,P	1	1	1	1	2	3	2
A357.0	S,P	1	1	1	1	2	3	2
380	D	2	1	2	-	5	3	4
390	D	2	2	2	-	2	4	2
413.0	D	1	2	1	-	2	4	4
443.0	P	1	1	2	1	2	5	1

S: sand casting; P: permanent mold casting; D: high pressure die casting
Rating: 1 Best, 5 Worst

The mechanical properties of Al-Si alloys can also be improved due to modification of eutectic silicon particles. The additions of chemical modifiers such as Sr or Na can lead the modification of silicon particles from their acicular brittle form to a more fibrous and rounded form and thereby significantly increase strength and elongation of the alloys [10-11]. Figure *2-2* shows the influence of Sr-modifier on eutectic silicon particles. As seen clearly, in unmodified state (a), the eutectic silicon particles are in acicular flakes form whereas the silicon particles in Sr-modified microstructure (b) represents fine and fibrous morphology.

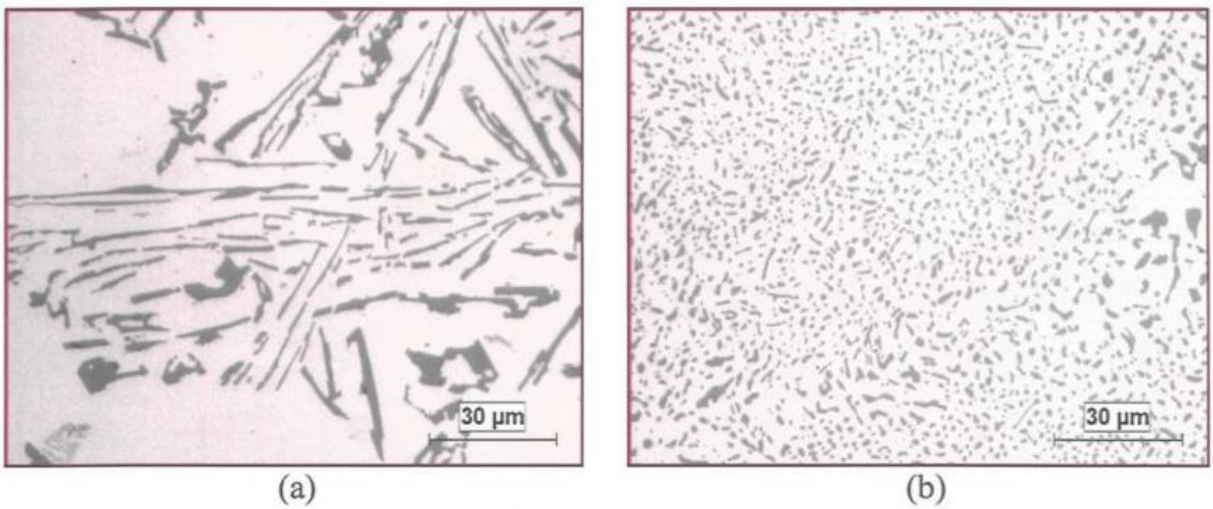

Figure 2-2: Optical images of cast A356 alloys in unmodified (a) and 200ppm modified (b) conditions [12]

The tensile properties of the Al-Si alloys can also be correlated with presence of intermetallic phases and porosities in the microstructure. Generally, increasing size and volume fraction of intermetallic phases causes to decrease tensile properties. In addition, porosity which forms due to the remaining gas gaps during casting process has a harmful influence on tensile properties.

Heat treatment is a process that a metal is heated to a specific temperature, then cooled in a certain way to change the microstructure in order to obtain desired mechanical properties. Therefore, the aluminum alloys that can be exposed to heat treatment referred as heat-treatable alloys. Generally, aluminum alloys are subjected to variety of heat treatments such as T4, T5, T6 and T7.

Mainly, T5 temper used for the castings which are artificially aged at temperatures between 170°C and 210°C. Due to precipitation hardening, higher mechanical properties can be achieved by T5 heat treatment applications. Also, low heat treatment temperatures avoid to formation of distortion or blistering therefore reduce the cost compared to T6 and T7 heat treatments.

In T4 heat treatment process an aluminum alloy is subjected to solution heat treatment at elevated temperatures between 460 °C - 540 °C then, exposed to immediately quenching. The high solution heat treatment temperatures allow addition elements such as Mg and Cu to become supersaturated in solid solution. Subsequent the solution heat treatment, the quenching is performed to prevent the excess solute from precipitating. Quenching is usually conducted in water. Typically, T4 heat treated alloys provides very high ductility.

T6 heat treatment procedures are applied to achieve the highest strength and good ductility for a given alloy. This heat treatment includes three cycles; solution heat treatment (1), quenching (2) and artificial aging (3). As distinct from T4 treatment, additional artificial aging process in T6

treatment allows hardening constituents to re-precipitate in the matrix and thus, producing a hardening effect for alloy.

A typical T6 heat treatment procedure is given in Figure *2-3* and schematically explained on Al-Cu phase diagram. As it is seen, the aluminum alloy is firstly heated (1) to a certain temperature which is above its solvus temperature, then kept at that temperature long enough to maximize the solid solubility of Cu in the matrix and to produce homogenous solid solution. During solution heat treatment, increasing soaking time allows to partial or complete dissolution of intermetallic phases and leads to achieve a uniform microstructure. Subsequent the solution heat treatment, the heated alloys immediately quenched (2) in water, oil or any other suitable environment in order to form a supersaturated solid solution and to inhibit the precipitation of phases such as Mg_2Si and Al_2Cu. As a last step of T6 treatment, quenched alloy is exposed to artificial aging procedure which indicates keeping alloy for certain period of time at temperature below solvus line. During artificial aging process, finely dispersed precipitates are obtained in the microstructure. These precipitates play crucial role to prevent the dislocation movements, thereby improve the mechanical properties of aluminum alloy [13].

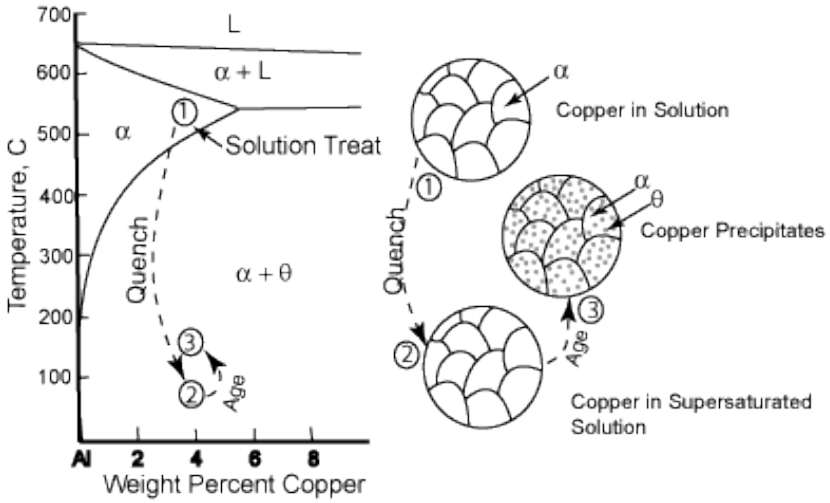

Figure 2-3: Illustration of T6 heat treatment steps on Al-Cu phase diagram [13].

On the other hand, T7 heat treatment can be carried out for the alloy that requires higher ductility in comparison to T6 heat treatment. In T7 process, an artificial ageing follows the solution heat treatment cycle. The main difference between T6 and T7 heat treatments is a higher ageing temperature which results slightly over aging of the alloy, thereby lower strength but higher ductility features [14-16].

2.1.1 Aural ™ Alloys

Growing concern on the requirements of fuel economy and vehicle emissions has forced producers to find out new ways of improving fuel efficiency. One way of increasing the fuel efficiency is to reduce to total mass of the product by using light weight alloys for structural components and applying superior manufacturing technologies with short heat treatment cycles. In order to fulfill the growing demand for lightweight alloys with high mechanical properties, large number of studies focused to develop new aluminum alloys. In this regard, Aural ™ alloys are particularly designed for high integrity structural die castings. These alloys offer a wide range of property levels to meet durability, high mechanical properties as well as the crash performance requirements. Beside their excellent corrosion resistance, Aural ™ alloys can be used to cast thin and large structural components due to their very high fluidity [17].

Table *2-2* shows the chemical composition of Aural ™ alloys. As can be seen from the table, Aural™-2 and Aural™-3 alloys contain 10% silicon while Aural™-5 alloy contains 7.4% silicon. Although the lower amount of silicon results in a reduction in strength, Aural™-5 alloy is an outstanding candidate for high elongation required applications due to its lower content of silicon. On the other hand, in Aural™-2 alloy, the presence of Mg leads to obtain magnesium silicide (Mg_2Si) in the microstructure which is a main strengthening phase for Aural ™ alloys. Aural™-2 alloy contains higher amount of Mg and also Sr is added to modify the eutectic silicon

particles. Due to higher amount of Mg and presence of Sr, ductility and strength of the alloy are expected to be higher than those in Aural™-2 alloy.

Table 2-2: Aural ™ family alloy compositions (%wt) [17].

Variants	Aluminum	Silicon	Iron	Copper	Manganese	Magnesium	Zinc	Titanium	Strontium
Aural-2™	Remaining	10.3	0.16	<0.01	0.52	0.31	<0.01	0.05	-
Aural-3™	Remaining	10.1	0.18	0.01	0.49	0.55	<0.01	0.06	0.012
Aural-5™	Remaining	7.4	0.17	<0.01	0.49	0.20	<0.01	0.08	0.018

2.2 Casting Processes

In recent years, growing demand for production of specific components with more complex shapes has resulted in attempt to develop new casting process. Beside the superior technological developments, increasing knowledge and experience on the relations between microstructure and mechanical properties of the alloys and the casting processes have brought varied solutions for the problems in casting and manufacturing industry. Therefore, extensive studies were performed on the casting processes to reveal the effect of casting methods as well as their similarities and main differences.

2.2.1 Permanent Mold Casting (PM)

Permanent mold casting is a casting method that the molten metal is poured into a metal mold cavity with a low speed (< 1.5 m/s) and then solidified under relatively low cooling rate (<10 Ks–1). In permanent mold casting, the molten metal is either directly poured into mold cavity by gravity or poured with a special equipment which is attached to the mold. A permanent mold casting process is schematically shown in Figure *2-4* [18].

Due to presence of metal mold, the liquid metal can be solidified quickly thereby, permanent mold castings can provide desirable grain structure with high mechanical properties and stiffness. Addition to these, heat treatment can be applied for permanent mold castings in order

to further increase mechanical properties. Although the metal mold allows to have better surface qualities in comparison with sand castings, it requires high production volumes to reduce the production cost. Also, the thermal fatigue and erosion occurred during the process can significantly reduce the life of the molds, indicating additional cost. Therefore, in industrial aspect, permanent mold castings are considered as medium - cost efficient per part. The main advantages and disadvantages of permanent mold castings are given in Table *2-3* [19-20].

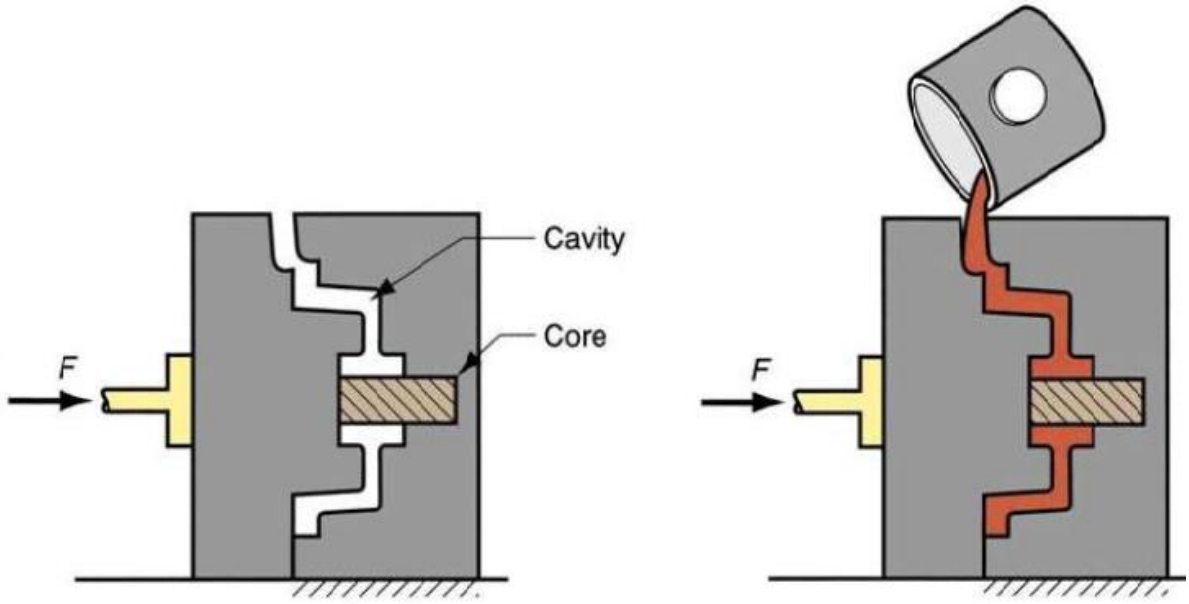

Figure 2-4: Schematically illustration of a permanent mold casting process [18].

Table 2-3: Advantages and disadvantages of permanent mold casting process

Advantages	Disadvantages
Good surface finish and dimensional accuracy	High tooling cost for mold
Allowing heat treatment	Medium- cost efficiency
Reusable mold	Low mold life

Mainly, the casting process starts with preheating of metal mold to 150 °C - 210 °C in order to ease the molten flow as well as to inhibit thermal damage to the casting. Subsequently, the

preheated metal mold is coated with a refractory material to prevent possible sticking issues which may occur between the mold and casting. The coating process can also increase the mold life. Following the coating, sand or metal cores is placed if needed and then, molten metal is poured into the mold. After solidification is completed, the casting is removed from the mold. For production of following castings, same process is repeated, however preheating of the mold is not required due to heat from last previous casting [21]. A typical optical microscopic image of permanent mold casting AlSi10Mg alloy is given in Figure *2-5*.

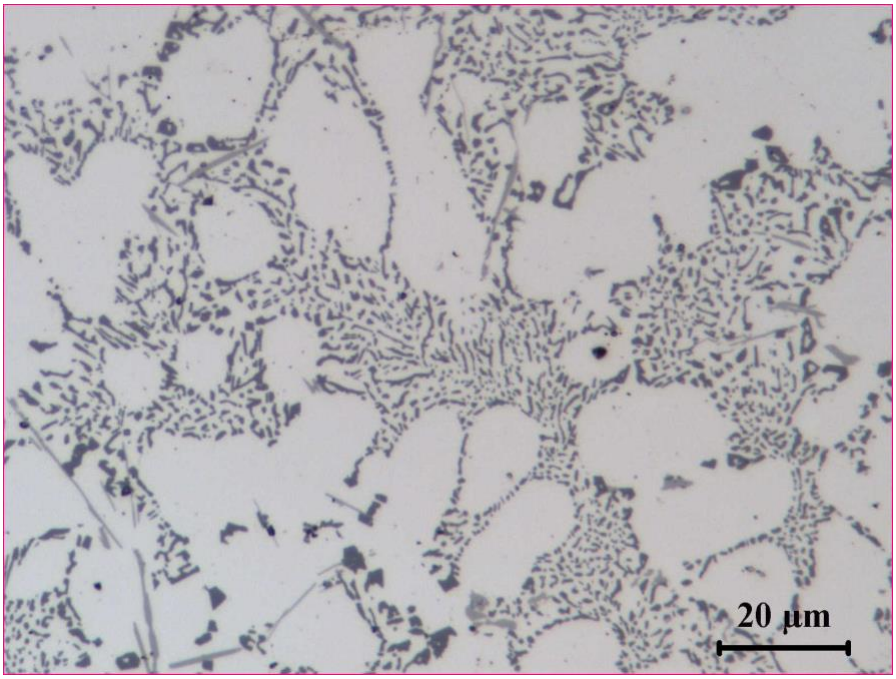

Figure 2-5: A typical micrograph of AlSi10Mg alloy produced by permanent mold casting method

2.2.2 High Pressure Die Casting (HPDC)

The high pressure die casting (HPDC) is a process that molten metal is injected very fast into the water-cooled die where it rapidly solidifies under hydraulic pressure. Although the actual

pressures depend on specific equipment configurations, it could increase up to 120 MPa with the melt flow velocity between 30 – 50 m/s at gates [22- 23].

In comparison with permanent mold casting process, geometrically more complex metal parts can be produced with better dimensional accuracy and the smooth surfaces via high pressure die casting. Also, large quantity of small or medium sized parts can be produced with lower cost through high pressure die casting applications [24]. An example illustration of high pressure die casting is given in Figure *2-6* .In addition, the advantages and disadvantages of high pressure die casting applications are listed in Table *2-4*.

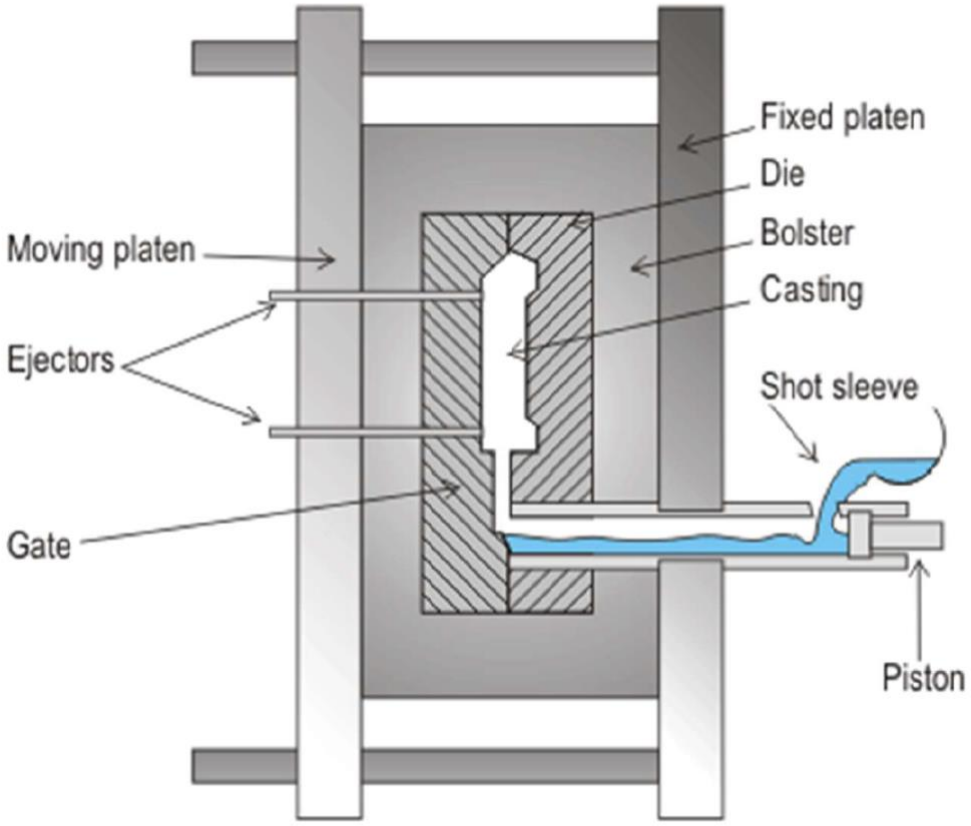

Figure 2-6: Schematic illustration of high pressure die casting application [18].

Table 2-4: Advantages and disadvantages of high pressure die casting applications

Advantages	Disadvantages
Excellent surface finish and dimensional accuracy	High tooling cost for mold
Higher mechanical properties in comparison PM	Large parts cannot be cast
Rapid production	Porosity due to turbulence

As it is similar in permanent mold casting applications, the high pressure die casting production begins with the pre-heating of the dies. In high pressure die casting, the molds are made by two or more metal parts named as cavity or die halves. Following the placement and pre-heating of die halves, a refractory material is applied to the die halves in order to prevent sticking issues. The liquid metal is then injected with high pressure into die cavity. After solidification is completed, the casting is removed from the mold. Finally, finishing steps such as removal of gating, flash or surface machining can be applied for the product if it is required.

Due to subjected high pressures during casting process, turbulence issues can be observed in liquid metal. The complex shape of casting mold and the turbulence of liquid metal often result in porosity which occurs due to the trapped air and other gasses in the metal. As well known, the presence of porosity has harmful effect on mechanical properties of the alloy. Moreover, the present gas pores (porosities) expands during solution heat treatment and causes the formation of blisters. Therefore, heat treatment applications are not recommended for the casting that produced via high pressure die casting method. However, this problem can be solved with the addition of assistant vacuum system. The presence of vacuum system allows to evacuate the remaining air and gases in the mold, thereby significantly reduces the porosity. [25-28]

2.2.3 High Pressure Vacuum Die Casting (HPVDC)

High pressure vacuum die casting method is developed in order to bring solutions for porosity problems in high pressure die casting applications. Although two casting process based on same principles, an assistant vacuum system is installed to evacuate remaining air in the cavity. Therefore, this method is named as high-pressure vacuum die casting. Due to the presence of vacuum system, the possible porosity issues are remarkably decreased. Since the trapped air can be evacuated due to vacuum system, blistering issues may not occur during high temperature heat treatment process, indicating that the vacuum system allows to perform heat treatment for the castings. Hence, high pressure vacuum die casting method can be used to produce high integrity die casting components that mechanical properties can be further improved due to heat treatment applications. An example schematic illustration of high-pressure vacuum die casting method is given in Figure *2-7*.

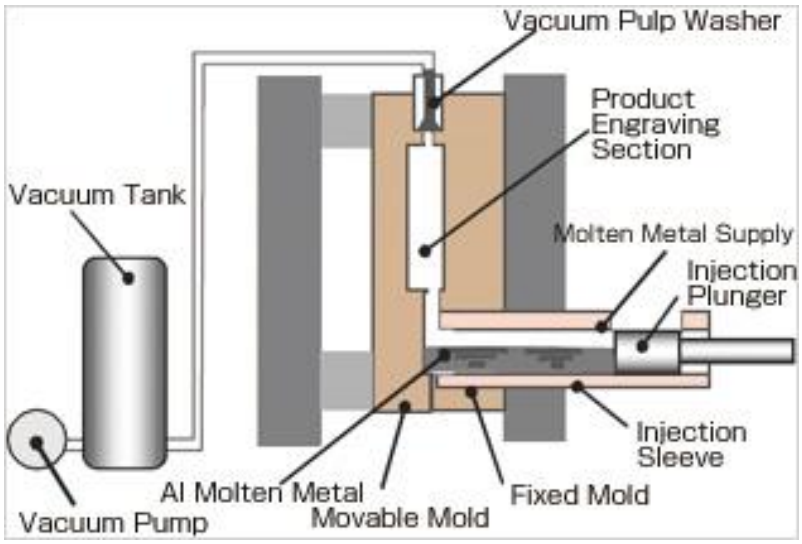

Figure 2-7: A schematic illustration of high-pressure vacuum die casting application [29].

As can be seen from Figure *2-7*, in high pressure vacuum die casting applications, a vacuum system is actively used to evacuate remaining air from the die cavity during the process. In order

to reveal the influence of vacuum assistant, two optical microscopic images are shown in Figure *2-8*. According to micrographs, microstructure of the high pressure die casting alloy (Figure *2-8*.a) contains significantly higher amount of gas porosity than that in high pressure vacuum die casting alloy, proving the beneficial effect of vacuum assistant on porosity formation in high pressure die casting applications.

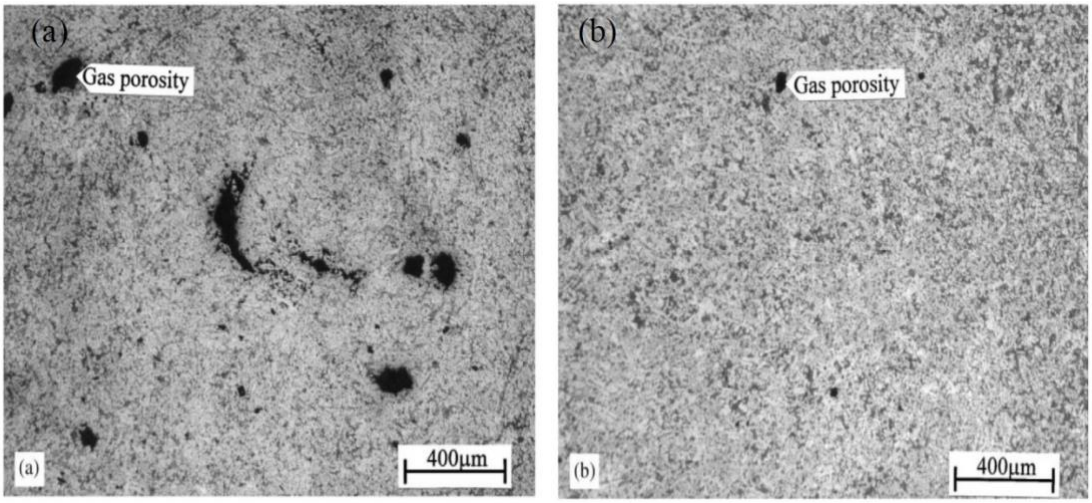

Figure 2-8: Optical microscopic images of Al-8% Si alloys, showing the porosity distribution in high pressure die casting (a) and high pressure vacuum die casting (b)

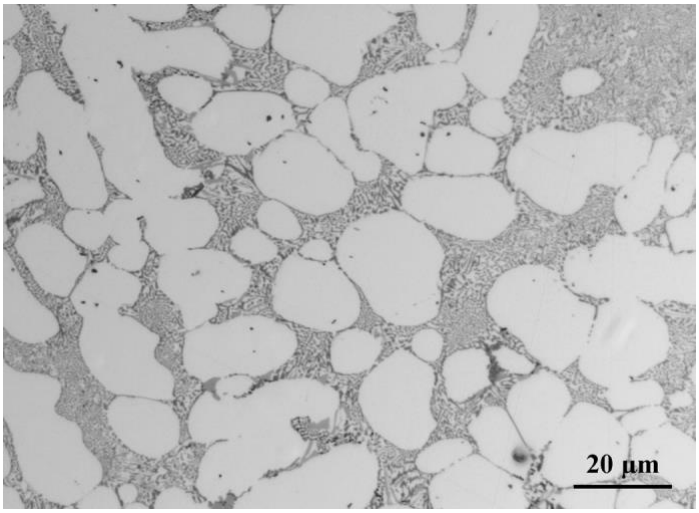

Figure 2-9: A typical micrograph of AlSi10Mg alloy produced by HPVDC method.

2.3 Role of Alloying Elements

Alloying elements such as Cu, Mg, Fe, Zr, Ni, Mn and Mo are traditionally added to Al-Si cast alloys for decades to modify the microstructural features, thereby increase the mechanical properties. In the following subsections, the alloying elements that commonly used in alloying and their influence on aluminum will be presented.

2.3.1 Effect of Cu Addition

It is well established that Cu addition has impact on strength and hardness of aluminum in both as cast and heat-treated conditions. It is also reported that the presence of Cu can increase the machinability of alloy due to solution strengthening potential of Cu. Shabestari et al. [30] investigated the effect of copper on mechanical properties and microstructure features. They found that in Al-Si-Mg alloys, addition of 0.2 - 0.5 % wt. Cu can significantly increase ultimate tensile strength of the alloy on T6 heat treated condition. This is attributed to the precipitation of copper bearing intermetallic phases in inter dendritic regions. On the other hand, the studies proved that addition of Cu reduces the corrosion resistance of aluminum and in specific alloys, it increases stress corrosion sensitivity [31].

2.3.2 Effect of Mg Addition

Magnesium is one of the most commonly used addition elements for aluminum alloying. Many studies indicate that Mg can increase the corrosion resistance, weldability and strengthening ability of the alloy [32,33]. In industrial applications, magnesium is generally combined with silicon in order to form hardening Mg_2Si phase which can significantly improve the yield strength (YS) and ultimate tensile strength (UTS) of the alloy in both as-cast and T6 heat treated condition. Moreover, higher level of Mg can further increase the yield strength and ultimate tensile strength.

Several investigations [34-35] reported that an improvement in yield strength and ultimate tensile strength is accompanied with a reduction in ductility, revealing the down side effect of Mg additions in aluminum alloys. The influence of magnesium additions on T6 heat treated yield strength in Al-Si alloys is shown in Figure *2-10*.

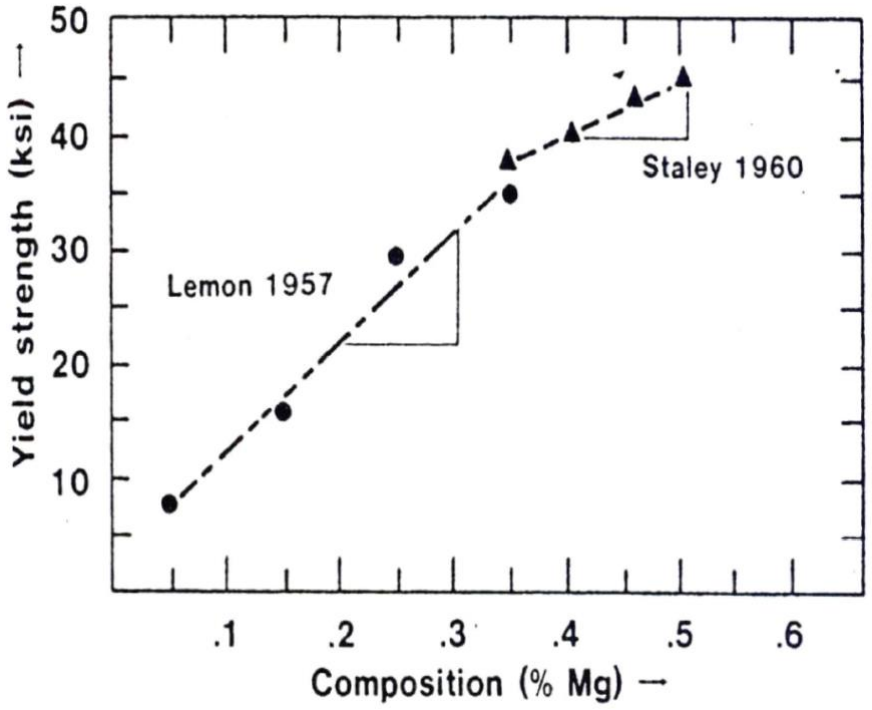

Figure 2-10: Effect of Mg content on T6 yield strength of Al-Si alloys [36]

2.3.3 Effect of Mn Addition

It is reported that the presence of Mn element in aluminum alloy, increases the yield strength and ultimate tensile strength of the alloy due to solid solution or modification of the intermetallic phases on as cast and heat-treated conditions. In addition to that Mn helps to reduce die soldering during the casting process. Manganese is commonly combined with iron in order to modify Fe-rich phases which can reduce the harmful effect of these intermetalics on mechanical

properties of the alloys. On the other hand, excess amount of manganese can result in reduction of mechanical properties [37-38]

2.3.4 Effect of Fe Addition

As known well Fe is one of the main impurities and leads the formation of Fe-rich intermetallic phases in Al-Si alloys. Wang et al. [39] indicated that addition of Fe content up to 0.2% resulted in an improvement of yield strength whereas ultimate tensile strength and elongation of the alloy was slightly decreased. Although presence of Fe element can contribute yield strength, Fe-rich intermetallic phases are considered as one of the most detrimental formations for mechanical properties of Al-Si alloys. Due to their brittle features and needle-like shape, Fe intermetallic phases can result significant reduction in tensile properties, especially for elongation. Figure *2-11* illustrates an example of brittle Fe-rich intermetallic phase containing micrograph of AlSi10Mg alloy.

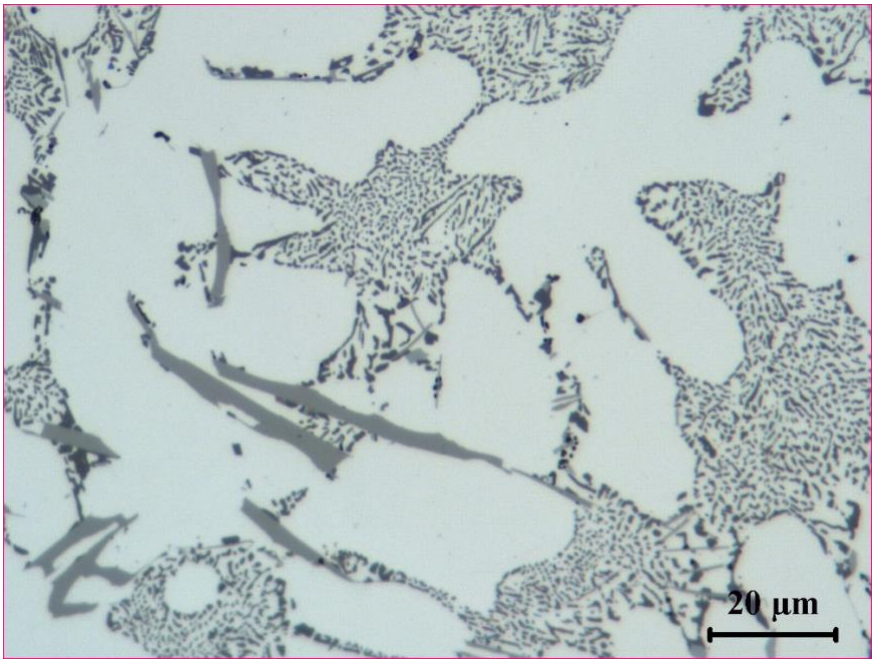

Figure 2-11: Brittle Fe-rich intermetallic phase in AlSi10Mg casting

2.3.5 Effect of Zr Addition

The studies show that of addition of Zr metal into aluminum alloys results in the modification of silicon particles as well as reduction in as-cast grain size, thereby improve the strength and ductility of the alloy. Moreover, it is reported that the presence of Zr allow to form fine coherent precipitates named as Al_3Zr. These particles are very stable at elevated temperature and can resist coarsening which attributed to their high thermal stability [40].

It has been established that minor addition of Zr element (less than 0.25% wt.) in aluminum alloys can improve the tensile properties and wear resistance. Also, Shaha et al. [41] indicated that mechanical properties of aluminum alloys at elevated temperatures can be enhanced by minor additions of Zr due to thermally stable intermetallic phases and precipitates.

2.3.6 Effect of Ti Addition

In general, Ti element is used for grain refinement purposes in aluminum casting alloys. However, Majed et al [42] reveal that increasing Ti content can improve the corrosion properties. On the other hand, it is reported that the Ti content higher than 0.15% wt. can cause casting difficulties. Another study on effect of Ti showed that Ti addition up to 4% wt. can significantly increase the microhardness and wear resistance of the alloy due to precipitation of Al_3Ti compounds. In addition to that wear resistance can further increase via T5 heat treatment applications [43].

2.3.7 Effect of Mo Addition

Mo element is known as dispersoid former in Al-Si casting alloys due to its ability to form large volume of thermally stable dispersoids even when added at low levels. The literature review shows that minor additions of Mo into Al-Si-Cu-Mg casting alloys leads remarkable improvement in creep resistance due to formation of Mo containing dispersoids [44, 45]. From microstructure

modification aspect, a significant impact of Mo elements on grain size was not reported. However, it is found that Mo addition in Al-Si casting alloys pushed down to presence of brittle β-Al5FeSi intermetallic phases whereas it promoted the formation of blocky Al-(Fe,Mo)-Si compounds, thus significantly improve the tensile elongation [45].

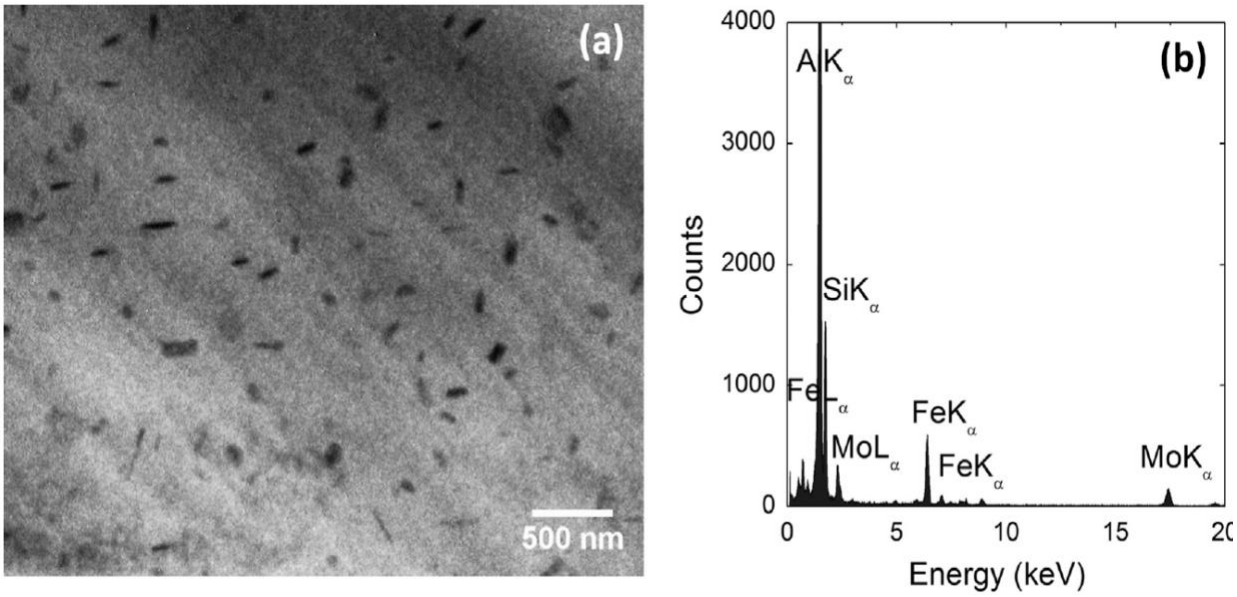

Figure 2-12: TEM micrograph of Al-(Fe,Mo)-Si dispersoids in interdendritic regions (a) and EDS spectrum of the dispersoids (b) [45].

According to another study, it is found that the addition of 0.3% Mo into aluminum - titanium cast alloys results enhancement in hardness and flow stress. In addition to that Mo helps to improve the surface quality of the alloy [46].

2.3.8 Effect of V Addition

Although many studies were carried out to reveal the influence of transition metals additions on mechanical properties and microstructural features, a fully understanding of the indivudual effect of V addition is not actualized yet. It is established that V element enhance the alloy performance by forming Al_3V and Al_{10} compounds which is indeed originated from master alloys. In the previous studies, V is usually combined with other transition elements such as Zr, Ti

and Mo. It is well known that V, Zr and Ti elements have very low diffusivity and solubility in aluminum, form thermally intermetallic phases, thereby help to maintain mechanical properties at elevated temperatures. In addition, Al-Si casting alloys contain a certain amount of Fe impurities which lead the formation of needle-like Fe-rich intermetallic phases. These intermetallic phases are known as detrimental for mechanical properties, particularly for elongation. In this regard, a study proved that additions of V and Zr elements can modify needle-like intermetallic phases, thereby improve the mechanical properties in as-cast condition. [40, 46].

REFERENCES

[1] John E. Hatch, Aluminum: Properties and Physical Metallurgy, American Society for Metals, Metals Park, Ohio, USA, 1984, p. 339.

[2] Zhang, D. and L. Zheng, The quench sensitivity of cast Al-7 wt pct Si 0.4 wt pct Mg alloy. Metallurgical and Materials Transactions A, 1996. 27(12): p. 3983-3991.

[3] J.L. Jorstad, "Hypereutectic Al-Si Casting Alloys: 25 Years, What's Next?", Silver Anniversary Paper, AFS Transactions, Vol. 104, 1996, pp. 669-671.

[4] Shaha, S.K., PhD. Thesis: Development and Characterization of Cast Modified Al-Si-Cu Alloys for Heat Resistant Power Train Applications, 2015.

[5] Lee, F., J. Major, and F. Samuel, Effect of silicon particles on the fatigue crack growth characteristics of Al-12 Wt Pct Si-0.35 Wt Pct Mg-(0 to 0.02) Wt Pct Sr casting alloys. Metallurgical and Materials Transactions A, 1995. 26(6): p. 1553- 1570.

[6] Hoskin, G., J. Provan, and J. Gruzleski, The in-situ fatigue testing of a cast aluminum-silicon alloy. Theoretical and applied fracture mechanics, 1988. 10(1): p. 27-41.

[7] C. Kammer, Aluminum Handbook, Vol. 1: Fundamentals and Materials, Aluminium-Verlag, Inc., 1999.

[8] M. Warmuzek, Aluminum-silicon casting alloys, Ohio, USA: ASM International, 2004.

[9] M. Lebyodkin, A. Deschamps and Y. Bréchet, "Influence of Second-Phase Morphology on Mechanical and Fracture Properties of Al-Si Alloys", Materials Science and Engineering, Vols A234-236, 1997, pp. 481-484.

[10] Heusler, L. and W. Schneider, Recent Investigations of Influence of P on Na and Sr Modification of Al-Si Alloys (97-97). Transactions of the American Foundrymen's Society, 1997. 105: p. 915-922.

[11] Hess, P. and E. Blackmun, Strontium as a modifying agent for hypoeutectic aluminum-silicon alloys. Paper from" Transactions of the Americal Foundrymen's Society., 1975. 83.

[12] Hu C. Master Thesis: Effect of cooling rate, strontium modification, melt thermal treatment and solution heat treatment on the eutectic silicon particle characteristic and tensile properties of A356 alloy, 2005

[13] D. Askeland, P. Fulay and W. Wright, The Science and Engineering of Materials, 6th Edition, Cengage Learning (Pub.), Stamford, 2011, pp. 458-484.

[14] D. Apelian, S. Shivkumar and G. Sigworth, "Fundamental Aspects of Heat Treatment of Cast Al-Si-Mg Alloys," AFS Transactions, Vol. 97, 1989, pp. 727- 742.

[15] Breton F., Fourmann J., "Alloys with High Strength and Ductility for High Pressure Vacuum Die Casting in Automotive Body Structure Applications: Impact of Heat Treatment on Mechanical Properties", NADCA congress 2016

[16] Amiotte C., Desrosiers S., Beaulieu S., Hartlieb M., "Heat Treatment of Structural High Integrity Die Castings", NADCA Transactions 2015.

[17] Aluminum Your guide to automotive innovation, Rio Tinto

[18] Casting metals. Open university.

[19] Todd, R.H., D.K. Allen, and L. Alting, Manufacturing processes reference guide. 1994: Industrial Press Inc.

[20] Degarmo, E.P., J. Black, and R.A. Kohser, Materials and processes in manufacturing, 1997. Prentice-Hall, Englewood Cliffs, New Jersey.

[21] Kalpakjian, Serope; Schmid, Steven (2006), *Manufacturing Engineering and Technology* (5th ed.),

[22] F. Bonollo, N. Gramegna, G. Timelli, High-pressure die-casting: contradictions and challenges, JOM 67 (5) (2015) 901–908.

[23] F. Czerwinski,M. Mir,W. Kasprzak, Application of cores and binders in metalcasting, Int. J. Cast Met. Res. (2014).

[24] 34. Kendall, K., A. Howard, and J.D. Birchall, The relation between porosity, microstructure and strength, and the approach to advanced cement-based materials. Phil. Trans. R. Soc. Lond. A, 1983. 310(1511): p. 139-153.

[25] Street, A., The Die Casting Books. Portcullis Press Ltd., 1977: p. 625-641.

[26] Kendall, K., A. Howard, and J.D. Birchall, The relation between porosity, microstructure and strength, and the approach to advanced cement-based materials. Phil. Trans. R. Soc. Lond. A, 1983. 310(1511): p. 139-153.

[27] Lee, S., et al., Effect of process parameters on porosity distributions in high pressure die-cast AM50 Mg-alloy. Materials Science and Engineering: A, 2006. 427(1-2): p. 99-111.

[28] Zaki, A.G., Master Thesis: On the performance of low pressure die cast Al-Cu- based automotive alloys; role of additives (2014)

[29] http://www.kikuwa.net/global/feature/22/

[30] S.G. Shabestari, H. Moemeni Effect of copper and solidification conditions on the microstructure and mechanical properties of Al–Si–Mg alloys Journal of Materials Processing Technology 153–154 (2004) 193–198

[31] http://wpedia.goo.ne.jp/enwiki

[32] Davis, J. R., Corrosion of Aluminum and Aluminum alloys, 1999, Ohio,ASM International.

[33] Mondolfo, L. F., Aluminum alloys: Structure and Properties, 1976, London, Butterworths

[34] C.H. Caceres, C.J. Davidson, J.R. Griffiths and Q.G. Wang, "The Effect of Mg on the Microstructure and Mechanical Behavior of Al-Si-Mg Casting Alloys," Metallurgical and Materials Transactions A, 1999, Vol. 30A, pp. 2611-2618.

[35] Q.G. Wang, "Microstructural Effects on the Tensile and Fracture Behavior of Aluminum Casting Alloys A356/357," Metallurgical and Materials Transactions A, Vol. 34A, Dec. 2003, pp. 2887-2899.

[36] A. Granger and R.R. Sawtell, "Effect of Beryllium on the Properties of A357 Castings," AFS Transactions, Vol. 115, 1984, pp. 579-586.

[37] Cho, Y.H., Joo, D.H., Kim, C.H. and Lee, H.C., 2006. The effect of alloy addition on the high temperature properties of over-aged Al-Si (CuNiMg) cast alloys. In Materials Science Forum (Vol. 519, pp. 461-466). Trans Tech Publications Switzerland.

[38] Seifeddine, S., Johansson, S. and Svensson, I.L., 2008. The influence of cooling rate and manganese content on the β-Al 5 FeSi phase formation and mechanical properties of Al–Si-based alloys. Materials Science and Engineering: A, 490(1), pp.385-390.

[39] Wang, Q.G., P.E. Jones, and M. Osborne, Effect of Iron on the Microstructure and Mechanical Properties of an Al-7%Si-0.4%Mg Casting Alloy. SAE- Technical Publication,. 2003-01-0823.

[40] Totten, G.E. and MacKenize, D.S. (Eds.), Handbook of Aluminum - vol. 1: Physical Metallurgy and Process, Marcel Dekker Inc., N ew York, NY, 2003.

[41] Shaha, S.K., Czerwinski, F., Kasprzak, W., Chen, D.L. (2014). Tensile and compressive deformation behavior of the Al–Si–Cu–Mg cast alloy with additions of Zr, V and Ti. Materials & Design 59 (pp. 352–358).

[42] Majed Jaradeh, Torbjorn Carlberg “Effect of titanium additions on the microstructure of DC-cast aluminium alloys”, Materials Science and Engineering A 413–414 (2005) 277–282

[43] N. Saheb, T. Laoui, A.R. Daud, M. Harun, S. Radiman, R. Yahaya “Influence of Ti addition on wear properties of Al–Si eutectic alloys”Wear 249 (2001) 656–662

[44] A.R. Farkoosh, X. Grant Chen, M. Pekguleryuz, Mater. Sci. Eng. A 620 (2015) 181- 189.

[45] A.R. Farkoosh, X.G. Chen, M. Pekguleryuz, Mater. Sci. Eng. A 627 (2015) 127-138.

[46] Davies I G, Dennis J M and Hellawell A 1970 Metal. Trans. A 1 275-279

[47] Shaha, S.K., Czerwinski, F., Kasprzak, W., Friedman, J., Chen, D.L Effect of Cr, Ti, V and Zr micro additions on microstructure and mechanical properties of the Al-Si-Cu-Mg alloy

CHAPTER 3

EXPERIMENTAL PART

Chapter 3

EXPERIMENTAL PART

The use of aluminum alloys is steadily increasing to decrease the weight of the structural applications. In this regard, a large demand emerged to develop new aluminum alloys that can offer wide range of property levels to meet required durability and high mechanical properties. In this study, combinations of V, Zr and Mo transition metals were used to modify microstructural features and thereby to improve mechanical properties.

The literature review reveals that the main types of intermetallic phases in permanent mold casting and high-pressure vacuum die castings are very similar but have different size. From this point of view, the experimental alloys were designed with different V, Zr and Mo combination and then produced by permanent mold casting method in order to choose promising alloys for high pressure vacuum die casting investigation and reduce the cost of research study. After producing experimental alloys, microstructural features and mechanical properties of the alloys were investigated on as-cast condition. Meanwhile, the heat treatment parameters were also optimized to further improve the mechanical properties and to evaluate precipitation potential. Electrical conductivity analysis was also carried out to understand strengthening mechanism. Following the overall consideration on microstructural features and mechanical properties on as-cast and heat-treated conditions, few Al-Si-Mg alloys were chosen as candidate for high pressure vacuum die casting investigation. Then, selected Al-Si-Mg alloys were produced by high pressure vacuum die casting method. The microstructural features and mechanical properties of experimental alloys were analyzed on as-cast condition. In order to optimize heat treatment parameters, T5 and T6 heat treatments were applied to experimental alloys and microstructural features and mechanical properties were analyzed on heat treated conditions as well. EBSD studies were performed to

measure grain size. Besides, electrical conductivity of the alloys was analyzed on as cast and heat-treated condition in order to understand strengthening method. Also, differential scanning calorimetry analysis was performed to understand the effect of transition elements on precipitation kinetics.

3.1 Alloy Design

As known well, addition elements are commonly used to obtain desired mechanical properties for aluminum alloys. In the present study, the addition elements were selected based on four strengthening methods; phase modification, solute solution strengthening, precipitation strengthening and intermetallic phase strengthening.

The literature review on addition elements suggests that transition elements such as V, Zr and Mo can significantly increase the amount of solute atom in the matrix and lead the formation of thermally stable precipitates, thereby higher mechanical properties. Moreover, these elements can refine the aluminum grains and modify the eutectic Si and intermetallic phases in the microstructure. From this point of view, eight experimental alloys with different combination of V, Zr and Mo additions were designed and produced. As mentioned earlier, the main purposes of this study are (1) to develop a new Al-Si-Mg alloy for high pressure vacuum die casting applications, and (2) to reveal the effect of V, Zr and Mo additions on mechanical properties and microstructural features.

The experimental alloys classified into two groups according to their Si content. First group experimental alloys contain 10% Si and designed to obtain high hardness, yield strength and ultimate tensile strength. On the other hand, the second group experimental alloys contain 8% Si with the aim of higher elongation at break (%).

3.2 Alloy preparation

3.2.1 Preparation of permanent mold casting alloys

Commercially pure Al (99.7%), pure Mg (99.9), Al-25%Mn, Al-25%Fe, Al-50%Si, Al-5V and Al-15Zr master alloys were used in the alloy preparation. For each batch, approximately 3 kg of materials were melted in an electrical resistance furnace. The melt was kept at 750 °C for 30 min and degassed for 15 min. The melt was then poured into a copper permanent mold preheated at 250°C.

Figure 3-1: Electrical resistance furnace that used to produce the experimental alloys

The dimensions of the cast plates are 100mm x 80 mm with a wall thickness of 4 mm. Following the casting process, chemical composition of the experimental alloys was analyzed using an optical emission spectrometer and the results are listed in ***Table** 3-1*.

Figure 3-2: Permanent mold that was used to produce the experimental alloys and cast plates of the Base10 alloy

Table 3-1**:** Chemical composition of the experimental alloys (wt.%)

Alloy	Si	Mn	Mg	Fe	Ti	Sr	Zr	V	Mo	Al
Base 10	10.20	0.52	0.31	0.16	0.08	0.011	0.00	0.02	0.01	bal.
HPD101	10.17	0.48	0.36	0.16	0.08	0.011	**0.27**	**0.19**	0.00	bal.
HPD102	10.02	0.51	0.43	0.17	0.07	0.014	0.00	**0.14**	**0.14**	bal.
HPD103	9.96	0.48	0.35	0.17	0.07	0.012	**0.27**	**0.13**	**0.11**	bal.
Base 8	8.04	0.55	0.36	0.18	0.11	0.005	0.00	0.00	0.01	bal.
HPD801	8.18	0.53	0.28	0.16	0.08	0.014	0.00	**0.26**	**0.21**	bal.
HPD802	8.19	0.52	0.30	0.14	0.09	0.013	**0.17**	**0.33**	0.02	bal.
HPD803	7.68	0.51	0.30	0.14	0.05	0.012	**0.19**	**0.25**	**0.15**	bal.

3.2.2 Preparation of high-pressure vacuum die casting alloys

High pressure vacuum die casting method is developed in order to bring solutions for porosity problems in high pressure die casting applications. Although two casting process based on same principles, an assistant vacuum system is installed to evacuate remaining air in the cavity. Therefore, this method is named as high-pressure vacuum die casting. Due to the presence of vacuum system, the possible porosity issues are remarkably decreased. Since the trapped air can

be evacuated due to vacuum system, blistering issues may not occur during high temperature heat treatment process, indicating that the vacuum system allows to perform heat treatment for the castings.

The high-pressure vacuum die casting (HPVDC) alloys were produced by a cold chamber vacuum die casting machine at Centre de Métallurgie du Quebec (QMC). Five HPVDC samples with different compositions were produced with commercially pure Al (99.7%), pure Mg (99.9), Al-25%Mn, Al-25%Fe, Al-50%Si, Al-10V and Al-10Zr and Al-10Mo master alloys. The molten metal temperature was 780°C whereas the both fixed and mobile molds were 200°C. In addition to produced samples, Aural-3^{TM} HPVDC plates are provided by the Rio Tinto Aluminum. The dimensions of the plates are 220 mm x 65 mm with a thickness of 2.5 mm. Table *3-2* lists the output from an analysis of chemical composition of five castings using an optical emission spectrometer.

Table 3-2: Chemical composition of the high-pressure vacuum die casting alloys (wt.%)

Alloy	Si	Mn	Mg	Fe	Ti	Sr	Zr	V	Mo	Al
Aural-3	10.10	0.49	0.55	0.18	0.06	0.012	-	-	-	bal.
10-I	10.87	0.50	0.63	0.19	0.07	0.013	**0.14**	**0.20**	-	bal.
10-II	9.38	0.45	0.54	0.17	0.06	0.013	**0.21**	**0.27**	-	bal.
8-I	7.69	0.48	0.34	0.13	0.02	0.013	-	-	-	bal.
8-II	7.53	0.46	0.34	0.15	0.02	0.012	**0.14**	**0.14**	-	bal.
8-III	7.4	0.45	0.33	0.15	0.20	0.012	**0.14**	**0.16**	**0.14**	bal.

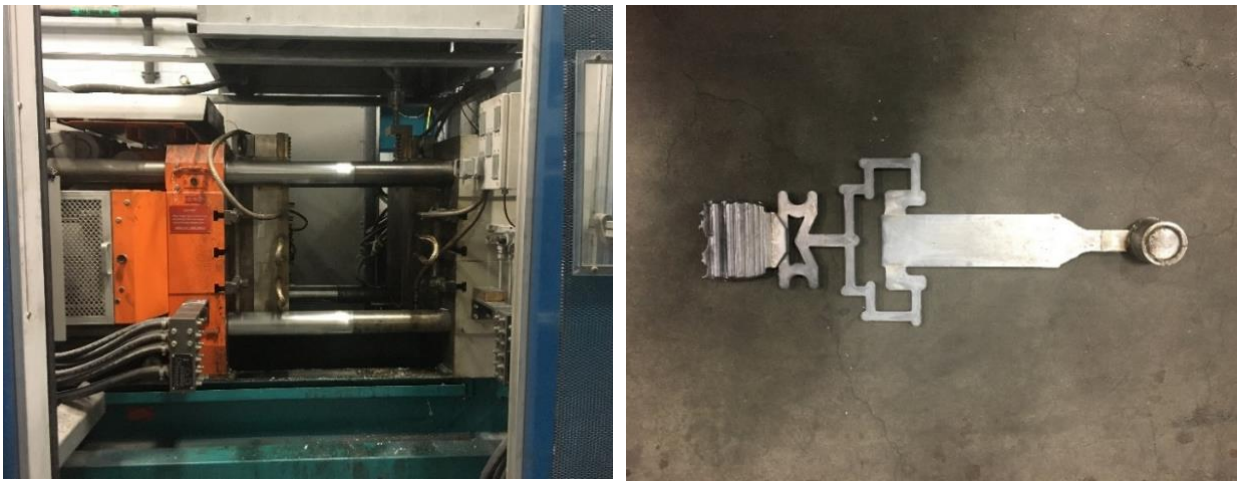

Figure 3-3: High pressure vacuum die casting machine and produced cast plates of a sample

3.3. Heat Treatments

In order to improve the mechanical properties and define the optimum heat treatment parameters for permanent mold and high-pressure vacuum die casting alloys, several heat treatments were performed under different conditions. All heat treatments of the cast samples were carried out in an electrically resistance furnace with air-circulating chamber and the heating rate was fixed at 5°C/ min. For the permanent mold casting samples, T6 solution heat treatments were performed at 500°C and 540°C for different holding times followed by water quench and aging at 170°C for 4 hours whereas T5 at 170°C and 210°C and T6 at 500°C, 520°C and 540°C followed by water quench and aging were applied to the high-pressure vacuum die casting alloys. (details indicated in Table *3-3*.)

Table 3-3: Heat treatment parameters and conditions for the experimental alloys.

	H.T.	Temperature (°C)	Holding Time (h)	Aging Cond.
PM	T5	-	-	-
	T6	500	2, 4, 8	170°C x 4h
		540	2, 4, 8	170°C x 4h
HPVDC	T5	170	1 to 14	-
		210	0.5, 1, 2.5, 3.5	-
	T6	500	1, 2, 3, 4, 8, 12, 24	170°C x 4h
		520	1, 2, 3, 4, 8, 12, 24	170°C x 4h
		540	1, 2, 3, 4, 8, 12, 24	170°C x 4h

Figure 3-4: Electrical resistance furnace that was used for the heat treatments

3.4 Characterization of Microstructures

3.4.1. Sample preparation for microstructure observation

Conventional metallographic polishing method was used to prepare the samples for microstructure observations. The samples were first mounted by using Strues / Labopress-3 mounting machine then polished with Strues / Tetrapol-100 polishing machine.

Figure 3-5: Mounting and polishing machines that used for the metallographic sample preparation

3.4.2 Optical Microscopy observation and image analysis

The both microstructures on as cast and heat-treated conditions were examined by using Nikon, Eclipse ME600 optical microscope equipped with CLEMEX software. Optical microscopy images were taken with 200X and 500X magnifications to represent the general microstructures. In order to carry out the quantitative analysis of the microstructures, 25 backscattered SEM images were taken at 500X magnification for each sample and then the images were analyzed with CLEMEX software in optical microscopy.

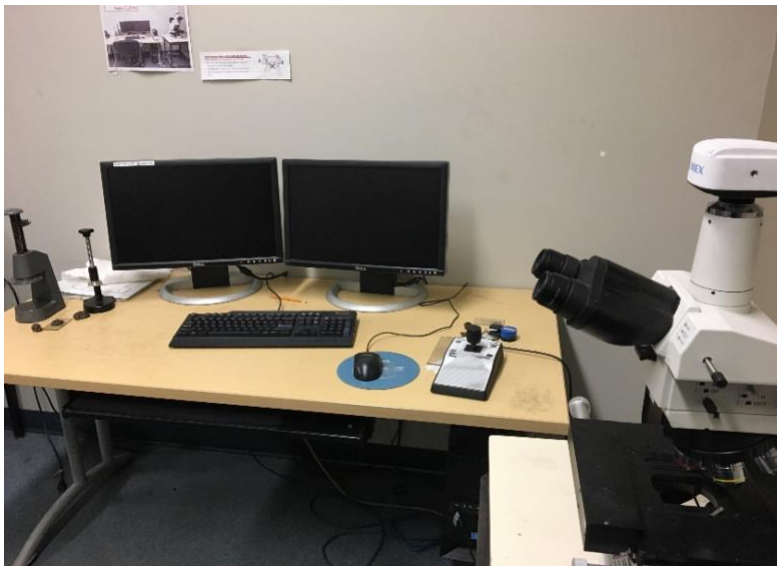

Figure 3-6: Nikon Eclipse ME600 Optical Microscope

3.4.3 SEM observation and elemental analysis

Microstructure features such as morphology of the present phases, grain structures and composition of intermetallic phases was studied by using a scanning electron microscope (SEM, JSM-6480LV) equipped with an energy dispersive x-ray spectrometer (EDS).

Figure 3-7: Scanning electron microscope used for microstructure observations

3.4.4. TEM observation and elemental analysis

A transmission electron microscope (TEM, JEM-2100) operated at 200kV was also used to identify the dispersoids and precipitates in microstructure of the experimental alloys. The TEM samples were prepared with traditional method. The samples first punched and then thin of until 70-90 µm with 600 µm sandpaper. Then, the thickness of samples was reduced to 50-65 µm with 6 µm and 1 µm polishing pads. Following the thickness reduction, twin-jet was used to finalize the TEM sample preparation.

Figure 3-8: TEM, JEM-2100 transmission electron microscope.

3.5 Electrical Conductivity Analysis

The electrical conductivity analysis was performed in order to evaluate the solute atom levels in Al matrix of the experimental alloys on as cast and heat-treated conditions. The measurements were carried out at room temperature by using SIGMACOPE SMP-10 Electrical Conductivity System. Minimum ten readings were taken for each sample and the average results were indicated as milisiemens per metre (MS/m).

Figure 3-9: Portable Fisher Sigmacope Electrical Conductivity Measurement System

3.6 Evaluation of Mechanical Properties

3.6.1 Microhardness Measurements

The Vickers microhardness measurements were carried out with a NG-1000 CCD Vickers microhardness test machine with a load of 300 grams and a 15seconds dwelling time as it is specified in ASTM E-92. For each sample, at least 15 measurements were carried out and average microhardness results was determined with their standard deviations.

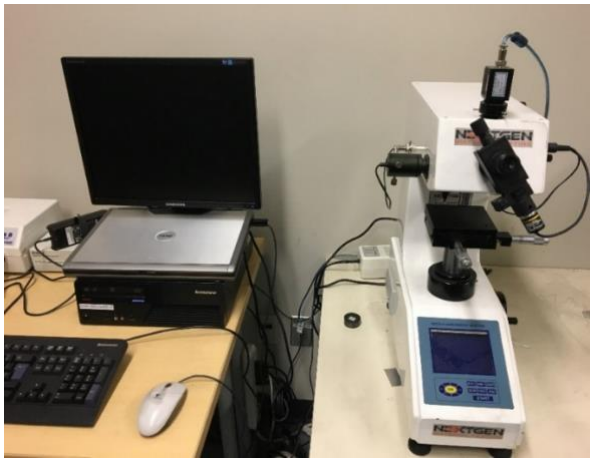

Figure 3-10: Vickers microhardness machine used for the hardness measurements

3.6.2 Evaluation of Tensile Properties

The tensile properties of the samples were evaluated using the Instron-8801 tensile tenting machine. For each sample, sub-size tensile test bars with 100mm in overage length and 25mm in gage length were machined from the cast plates according to ASTM-B557M. The tensile properties were reported as the average values of the ultimate tensile strength (UTS), yield strength (YS) at a 0.2% offset strain and fracture elongation (El) from four test bars and all the tensile tests were carried out at room temperature.

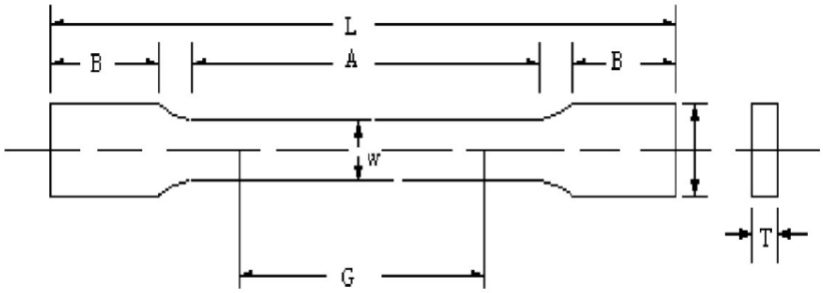

Figure 3-11: Schematic illustration of Tensile Test Specimen

Permanent Mold Castings;

G - Gage length: 25.0 ± 0.1 mm;

W - Width: 6 ± 0.1 mm;

T – Thickness: 3 ± 0.1 mm;

R – Radius of fillet, min: 6 mm;

L – Overall length, min: 100 mm;

A – Length of reduced section: 32 mm;

B – Length of grip section, min: 30 mm;

C – Width of grip section: 10 mm

HPVD Castings;

G - Gage length: 1.0 ± 0.003 inches;

W - Width: 0.250 ± 0.005 inches;

T – Thickness: 0.1 ± 0.05 inches;

R – Radius of fillet, min: 0.25 inches

L – Overall length, min: 4 inches;

A – Length of reduced section: 1 1/4 inches;

B – Length of grip section, min: 1 1/4 inches;

C – Width of grip section: 0.4 inches;

Figure 3-12: Instron-8801 tensile testing machine.

3.7 Differential Scanning Calorimetry

The differential scanning calorimetry (DSC) analyses were performed under the argon atmosphere using DSC 8000. 4 mm diameter disc samples with a mass about 30 mg prepared from the experimental alloys which were solution heat treated at 520^{o}C for 3h and immediately water quenched, then transferred to DSC machine with a 10^{o}C/min heating rate to 540^{o}C

Figure 3-13: Differential scanning calorimetry system (DSC 8000) used in thermal analysis.

CHAPTER 4

EFFECT OF ZR, V AND MO ADDITIONS ON MECHANICAL PROPERTIES AND MICROSTRUCTURE FEATURES OF PERMANENT MOLD CASTINGS

Chapter 4

EFFECT OF ZR, V AND MO ADDITIONS ON MECHANICAL PROPERTIES AND MICROSTRUCTURE OF PERMANENT MOLD CASTINGS

4.1 The Mechanical Properties of the Experimental Alloys

4.1.1 Hardness and Tensile Properties on As-Cast Condition

The mechanical properties of the experimental alloys were determined with Vickers micro-hardness measurements and tensile tests in the room temperature. *Figure 4-1* shows the hardness results of 10% Si containing alloys on as-cast condition. The average hardness of the Base 10 alloy is 74.6 HV while it is 85.1 HV in the HPD 101 alloy, 80 HV in HPD 102 alloy and 79.4 HV in HPD 103 alloy. On the as-cast condition, it is found that the increases of hardness for the experimental alloys are 14%, 7.5% and 7% for HPD 101, HPD 102 and HPD 103 alloys respectively, indicating that addition of trace elements has significant benefit on the hardness of AlSi10Mg alloy.

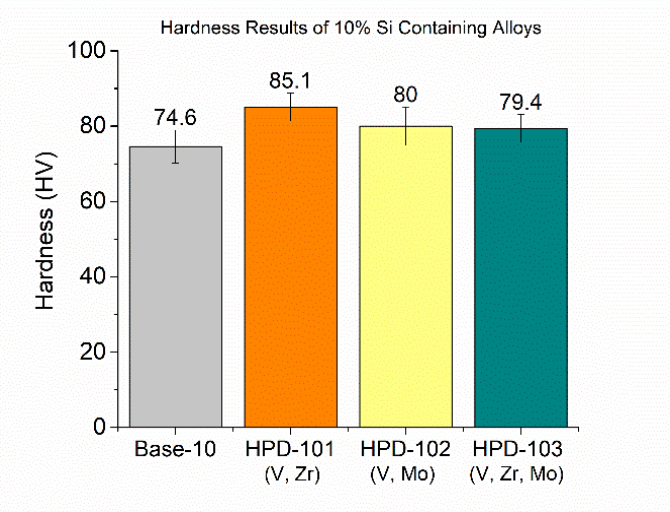

Figure 4-1: Hardness results of 10% Si containing alloys on as-cast condition

The hardness results of 8% Si containing experimental alloys are given in *Figure 4-2*. The average hardness of the experimental alloys is 72.3 HV, 75.1 HV, 80.1 HV and 78.3 HV in base, HPD 801, HPD 802 and HPD 803 alloys respectively. The measurements of the electrical conductivity (EC) show that the electron conductivity of HPD-101 and HPD-802 alloys are remarkably lower than that of the base alloys, confirming that the Zr and V present in the aluminum matrix as solute atoms. Addition to this, in comparison with 10% Si containing experimental alloys, reduction in the Si content of the alloys resulted a significant drop in hardness of HPD-802 and HPD-801 alloys while this reduction is limited in HPD 803 alloy. This limited reduction may be attributed to presence of similar level V, Zr, and Mo solute atoms in 8 and 10% Si containing alloys as can be seen in *Table 4-1*.

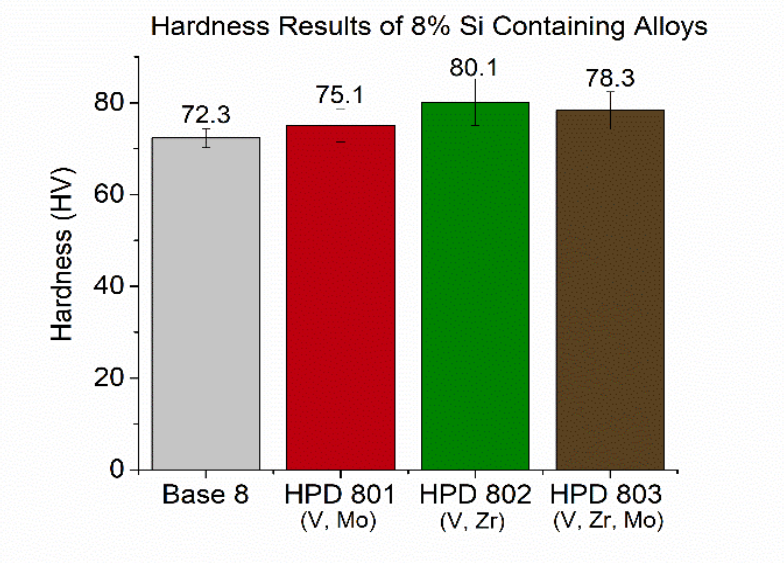

Figure 4-2: Hardness results of 8% Si containing alloys on as-cast condition

Table 4-1**:** Electrical conductivity of the 10% and 8% Si containing alloys on as-cast and solution heat treated conditions

	Electrical Conductivity (MS/m)
Alloy	**As-cast**
Base 8	20.13
HPD 801 (V,Mo)	16.3
HPD 802 (V,Zr)	17.5
HPD 803 (V,Zr,Mo)	16.5
Base 10	19.28
HPD 101 (V,Zr)	17.35
HPD 102 (V,Mo)	15.5
HPD 103 (V,Zr,Mo)	16.2

Figure 4-3 represents the tensile properties of 10% Si containing alloys on as-cast condition. The results indicate that the addition of trace elements (V, Zr, Mo) resulted in significantly higher tensile properties than those in the base alloy. For instance, the addition of V and Zr resulted a major increase in yield strength (YS), ultimate tensile strength (UTS) and elongation by 28%, 29% and 25% respectively.

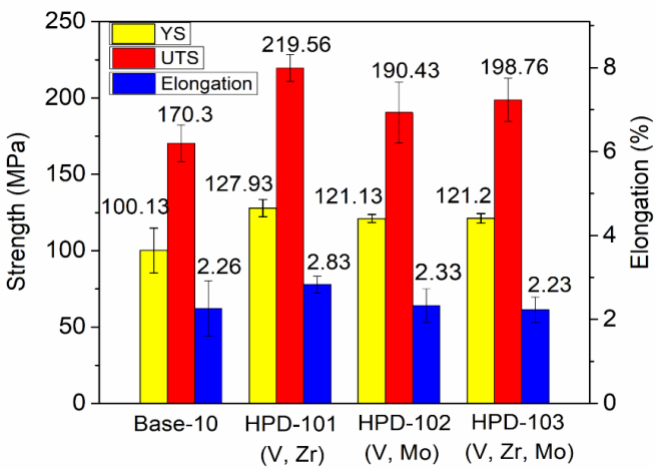

Figure 4-3: Tensile properties of 10% Si containing alloys on as-cast condition

On the other hand, in HPD 103 alloy, while the YS and UTS is considerable increasing, a negligible reduction in the elongation is observed after addition of V, Zr and Mo. *Table 4-2* shows the effect

of addition elements on the mechanical properties for 10% Si containing alloys on as-cast condition.

Table 4-2: The effect of addition elements on tensile properties of 10% Si containing alloys

Alloy	Improvement (%)		
	YS	UTS	Elongation
HPD 101 (V,Zr)	28	29	25
HPD 102 (V,Mo)	21	12	3
HPD 103 (V,Zr,Mo)	21	17	-1.5

Tensile properties of 8% Si containing alloys are given in *Figure 4-4*. The results indicate that all modified alloys show higher YS, UTS as well as elongation properties than those in the base alloy. This improvement in tensile properties might be attributed to: (1) the solid solution strengthening of V, Zr and Mo and (2) the microstructural modifications caused by addition elements which will be discussed in following parts for the selected alloys. Besides, it is seen that in comparison with 10% Si containing alloys, 8% Si containing alloys show significantly higher elongation properties, indicating that the reduction in Si content resulted in improved elongation for the experimental alloys. Although detailed explanation on improvement of mechanical properties is provided in microstructure investigation of permanent mold castings, it is still important to discuss a little on why the V, Zr and Mo have different effect on mechanical properties of the alloys. As can be seen from Table *4-1*, each combination of additions has different solubility in the aluminum matrix which would be a reason for different hardness values in each experimental alloy. In addition to that the addition of V, Zr and Mo metals results in formation of new intermetallic phases with different size and shape which may lead higher tensile properties in the alloy. Also, the additions may modify the Si particles and present intermetallic phases in the microstructure.

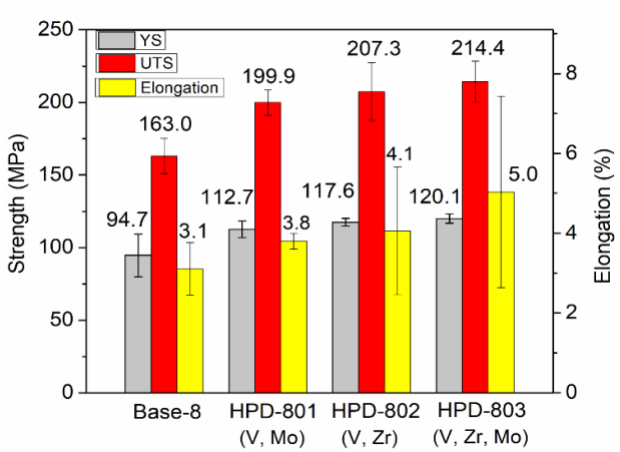

Figure 4-4: Tensile properties of 8% Si containing alloys on as-cast condition

Table 4-3 represents the effect of addition elements on tensile properties of 8%Si containing alloys on as cast condition. As can be seen, HPD-803 (V, Zr, Mo) alloy shows the highest YS, UTS and elongation in comparison with the other experimental alloys.

Table 4-3: Effect of addition elements on tensile properties of 8%Si containing alloys

Alloy	Improvement (%)		
	YS	UTS	Elongation
HPD 801 (V,Mo)	19	23	23
HPD 802 (V,Zr)	24	27	33
HPD 803 (V,Zr,Mo)	27	32	61

4.1.2 Optimization of Heat Treatment Parameters

In order to define the optimum T6 heat treatment condition, two solution temperatures (500°C and 540°C) with the same aging parameter (170°C x 4h) were selected for the investigation. The experimental alloys were exposed to solution heat treatment up to 8 hours and *Figure 4-5* shows the hardness evaluation of the 10% and 8% Si containing alloys as a function of the holding time at two temperatures.

The results show that in solution heat-treated condition at 500 °C, the hardness of the both 10% and 8% Si containing alloys increase with increasing holding time and reaches its maximum value after 8 hours. On the other hand, at 540 °C solution heat treatment temperature, the hardness

increases rapidly in the first two hours for all experimental alloys and then follows a plateau. As can be seen from the *Figure 4-5*c and *Figure 4-5*d, the alloys heat treated at 540 °C exhibit higher hardness values than those in heat treated at 500 °C. According to the hardness values for solution heat treated alloys at 500 °C and 540 °C, the optimum T6 heat treatment condition was defined as solution treatment at 540 °C for 2h and aging at 170 °C for 4h. Therefore, further investigation on heat treated mechanical properties and microstructural observations will be only focused on this optimum heat treatment parameters.

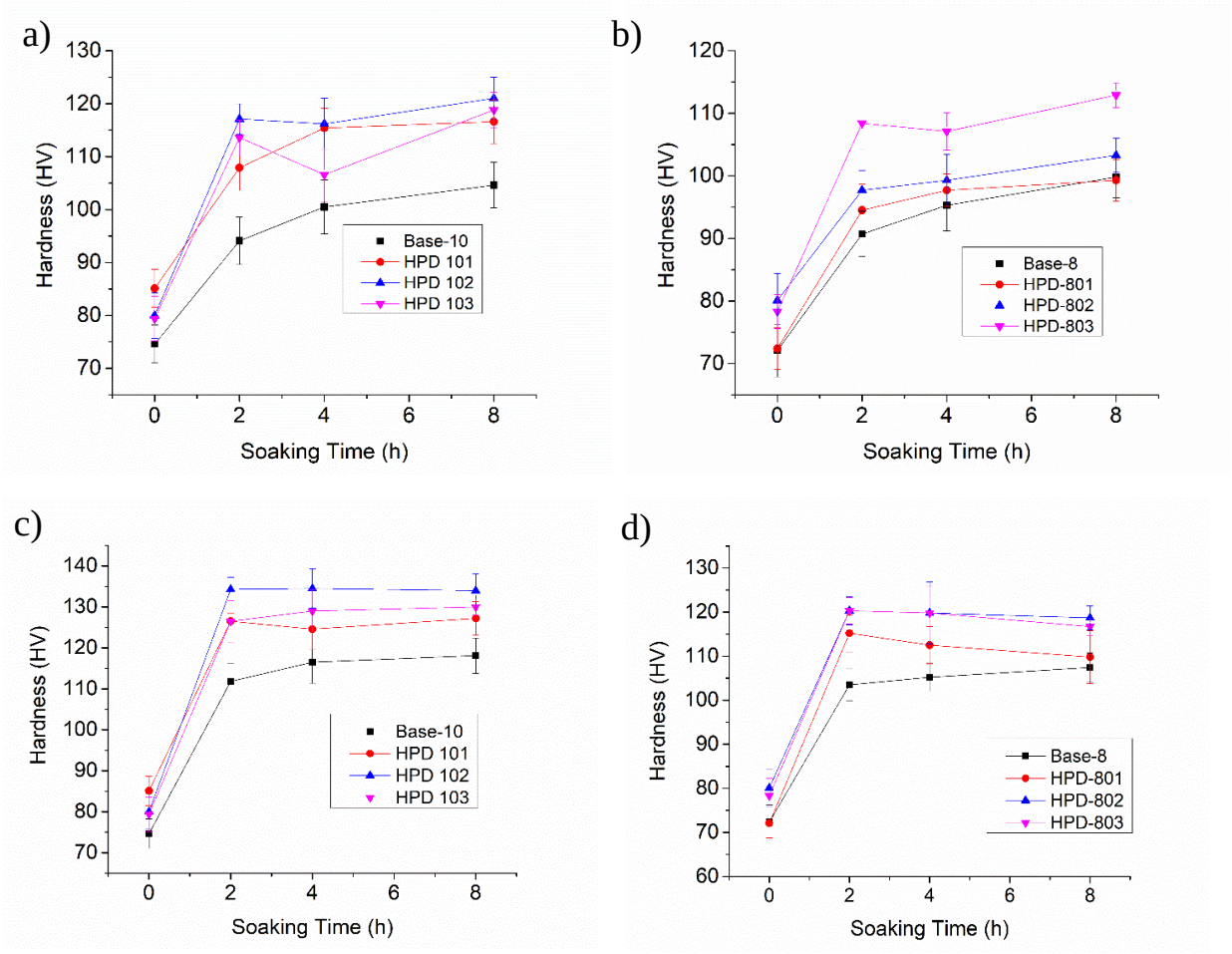

Figure 4-5: Evaluation of the hardness as function of holding times at the solution temperature 500°C (a,b) and at the solution temperature of 540°C (c,d)

4.1.3 The Mechanical Properties on T6 Condition

The hardness test results of 10% and 8% Si containing alloys are shown schematically in *Figure 4-6*, indicating that T6 (540 °C x 2h + WQ + 170 °C x 4h) heat treated hardness values are obviously higher than those on as-cast condition. The results also reveal that increasing Si content can provide higher hardness after solution heat treatment in optimized heat treatment conditions. For instance, both HPD-102 and HPD-801 alloys are modified with V and Mo elements and these alloys contain 10% and 8% Si respectively. After T6 heat treatment, the hardness of 10% Si containing alloy (HPD-102) reached 132.3 HV with an increase of 68% whereas the hardness of 8% Si containing alloy is 115.2 HV with improvement of 52%. It is also seen that similar tendency can be observed in other modified experimental alloys.

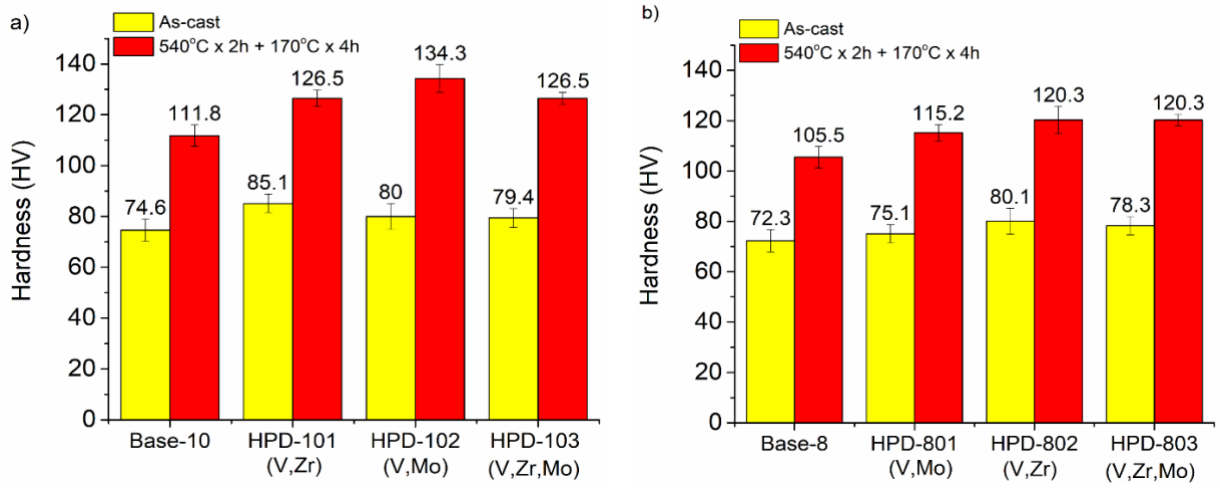

Figure 4-6: Hardness evaluation of the experimental alloys on as-cast and T6 heat treated conditions.

The electrical conductivity of the experimental alloys on T6 (540 °C x 2h + WQ + 170 °C x 4h) condition is given in *Table 4-4* in order to reveal the influence of additions on evaluation of the mechanical properties.

Table 4-4: Electrical conductivity of T6 heat treated experimental alloys

	Electrical Conductivity (MS/m)
Alloy	540 °C x 2h + 170 °C x 4h
Base 8	20.66
HPD 801 (V,Mo)	18.88
HPD 802 (V,Zr)	19.13
HPD 803 (V,Zr,Mo)	19.03
Base 10	20.07
HPD 101 (V,Zr)	19.32
HPD 102 (V,Mo)	18.64
HPD 103 (V,Zr,Mo)	18.55

Figure 4-7 illustrates the tensile properties of 10% Si containing alloys on T6 heat treated condition. The results reveal that in comparison with the Base-10 alloy, HPD-101, HPD-102 and HPD-103 alloys shows higher YS and UTS values after T6 solution heat treatment process, indicating that further improvement in YS and UTS can be achieved due to T6 heat treatment.

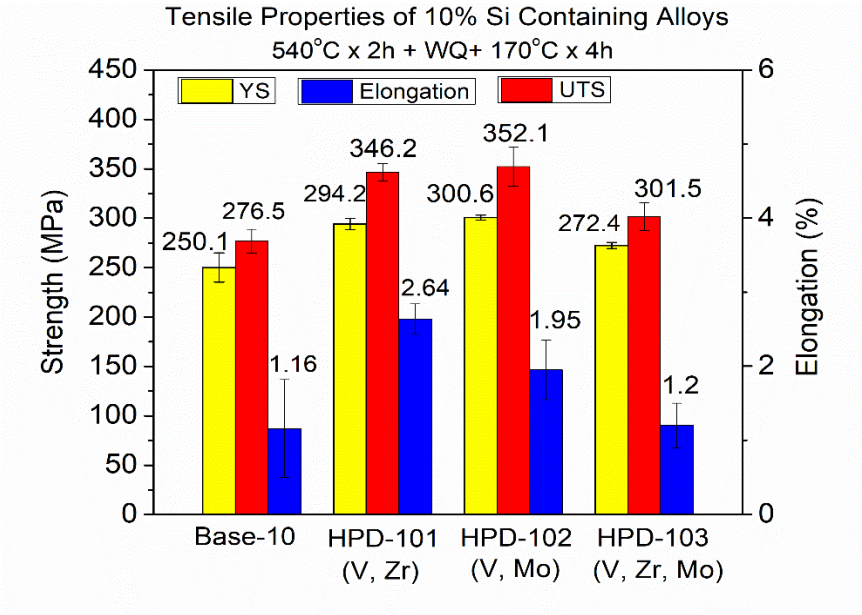

Figure 4-7**:** Tensile properties of 10% Si containing alloys on T6 (540 °C x 2h + 170 °C x 4h) condition

Although the alloy modified with V and Mo (HPD 102) reaches the highest YS (300.6 MPa) and UTS (352.1 MPa) values after T6 heat treatment, the elongation of the alloy significantly

dropped by 17% in comparison with as-cast condition. On the other hand, in HPD-101 (V, Zr) alloy, the elongation decreased by 6% (from 2.83% to 2.64%) after T6 heat treatment whereas YS (□ 294.2 MPa) and UTS (□ 346.3 MPa) increased by 130% and 58% respectively. In HPD-103 (V, Zr, Mo) alloy, the reduction in the elongation after heat treatment is more than 46% indicating that addition of Mo has a harmful effect on the elongation of the HPD-103 heat-treated alloy.

Tensile test results of 8% Si containing alloys after T6 heat treatment are given in *Figure 4-8*. In comparison with Base-8 alloy, all modified alloys exhibit remarkably higher YS, UTS and elongation results after solution heat treatment. On heat treated condition, although HPD 103 alloy (10 % Si containing alloy with addition of V, Zr, Mo) shows the lowest elongation property than other experimental alloys, HPD 803 exposes the highest elongation values among the experimental alloys which indicates that the reduction in Si content resulted a remarkable improvement on elongation values on as cast and heat-treated conditions.

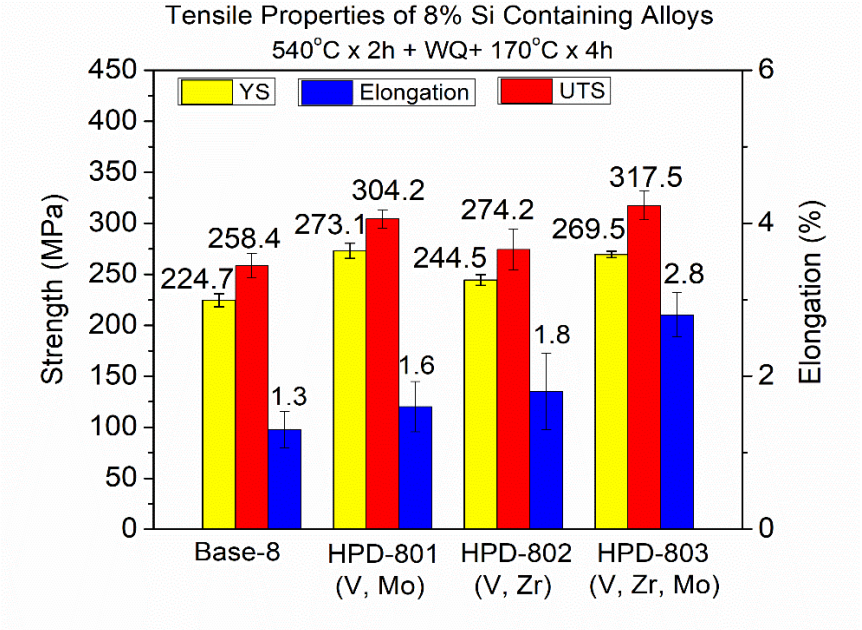

Figure 4-8: Tensile properties of 8% Si containing alloys on T6 (540 °C x 2h + 170 °C x 4h) treated condition.

4.2 Selection of the Promising Alloys

The selection of promising alloys was carried out in consideration of the mechanical properties of experimental alloys on as-cast and T6 heat treated conditions. In this regard, the experimental alloys were classified into two groups according to Si content. Then, their mechanical properties were compared with the other experimental alloys which are belongs to the same group.

4.2.1 Promising Alloy Selection for 10% Si Containing Alloys

The results indicate that the addition of V and Zr (HPD-101), V and Mo (HPD-102) and V, Zr, Mo (HPD-103) have beneficial effect on the hardness of the all experimental alloys on as-cast condition. However, the level of this beneficial influence depends on the combination of the addition elements. For instance, in HPD-101 (V, Zr) alloy, the improvement in hardness is 15% while it is 7% in HPD 102 (V, Mo) and 6% in HPD 103 (V, Zr, Mo) alloys on as-cast condition. Addition to the hardness data, tensile test results show that the combination of V and Zr additions can provide remarkably higher YS, UTS and elongation than those in V, Mo (HPD 102) and V, Zr, Mo (HPD-103) additions. It should also be pointed out that in comparison with the Base 10 alloy, there is no significant increase in elongation of HPD-102 (V, Mo) and HPD-103 (V, Zr, Mo) alloys whereas the addition of V and Zr leads to significant improvement in elongation of HPD 101 by 25% (in Table 4.3).

On heat treated condition, hardness, YS and UTS of the all experimental alloys significantly increased whereas different level of reduction was observed in elongation results of the alloys. Although HPD 102 (V, Mo) alloy displays the highest YS (300.6 MPa) and UTS (352.1 MPa) values among the 10% Si containing alloys, the elongation of the alloy was dramatically dropped following the T6 heat treatment. On the other hand, a slight reduction in elongation of HPD 101(V, Zr) alloy was observed while its YS (294.2) and UTS (346.3) almost as much high as HPD 102 alloy. As can be seen in *Figure 4-7*, the mechanical properties of HPD 103 (V, Zr, Mo) is not

significantly higher than those in Base 10 alloy. In addition to that elongation of the alloy decreased dramatically after T6 heat treatment process.

As a result, it is understood that addition of V and Zr has a greater influence on the mechanical properties of AlSi10Mg than all other addition combinations on both as cast and heat-treated conditions. Therefore, among the 10% Si containing alloys, HPD-101 was selected as promising alloys for the microstructure studies and high-pressure vacuum die casting investigation.

4.2.2 Promising Alloy Selection for 8% Si Containing Alloys

As seen in *Figure 4-2*, in comparison of the base-8 alloy on as-cast condition, a significant improvement in hardness was observed with the additions of V and Zr (HPD 802) and V, Zr, Mo (HPD 803) whereas there was a limited increase measured in HPD 801 (V, Mo) alloy. On the other hand, tensile test results indicate that all modified alloys exhibit relatively higher YS, UTS and elongation values than the base-8 alloy. It should also be pointed out that the addition of V, Zr and Mo (HPD 803) to Base-8 alloy resulted in a great improvement of the elongation while the YS and UTS of HPD 803 is still higher than other 8% Si containing alloys.

As seen in *Figure 4-6*-b, hardness of the experimental alloys significantly increased after solution heat treatment. It is measured that both HPD 802 (V, Zr) and HPD 803 (V, Zr, Mo) alloys display 120.3 HV with the increase of 50% and 53% respectively, whereas the hardness of HPD 801 (V, Mo) reached 115.2 HV. Besides, tensile results of heat-treated samples reveal that HPD 803 (V, Zr, Mo) alloy exhibits highest YS, UTS and elongation values in comparison with other 8% Si containing alloys. Although HPD 801 (V, Mo) alloy shows relatively higher YS and UTS values than HPD 802 (V, Zr), the elongation of HPD 802 (V, Zr) is 13% higher than those in HPD 801 (V, Mo).

Consequently, considering its mechanical properties on as cast and heat-treated conditions, HPD 803 (V, Zr, Mo) was selected as the promising alloy among the 8% Si containing alloys. Addition to that, in order to have better understanding on the effect of V and Zr elements on mechanical properties with different level Si content, HPD-802 (V, Zr) alloy was chosen for the further studies.

4.3 Microstructure Investigation of the Promising Alloys

4.3.1 Microstructure of 10% Si Containing Alloys

Figure 4-9 shows the typical microstructures of the Base10 and HPD 101 (V, Zr) alloys on as-cast condition. Microstructure observations showed that both Base10 and HPD-101 (V, Zr) alloys are consisted of dendrite-like aluminum grains, eutectic Si particles, primary Mg_2Si phases as well as different types of intermetallic phases. In Base-10 alloy, it is established that eutectic Si phase exists in the microstructure either in unmodified (plate-like) or modified (fiber-like) morphology, indicating that addition of Sr as microstructure modifier did not fully modify the eutectic silicon. On the other hand, the most of eutectic Si in the HPD-101 alloy were fully modified, indicating that Zr and V addition are favor to the modification of eutectic Si phase.

The chemical composition of the intermetallic phases was analyzed with EDS-SEM for both Base 10 and HPD-101 alloys. As seen in *Figure 4-9*a and *Figure 4-10*a, the long needle-like intermetallic phases were observed in Base 10 alloy. The EDS spectrums indicate that the needle-like intermetallic phases in base alloy is composed of Al, Fe, Si and Mn and refereed as $Al_{16}(FeMn)_4Si_3$ intermetallic phase [1]. In HPD-101 alloy, the microstructure observations reveal the presence of three distinct intermetallic phases with different morphologies (***Figure** 4-11*a) and the corresponding spectrums of intermetallic phases are shown in *Figure 4-11*b and *Figure 4-11*c. These intermetallic phases are; the block-like phase that contains Al, V, Si elements indicated as

V-rich intermetallic phases. The rod-like phase is composed of Al, Zr, Si and Ti, referred as $(AlSi)_3(ZrTi)$ in the literature [2]. In addition to the needle-like Fe-rich intermetallic phase, the Zr and V addition generated its own intermetallic phases although their amount is quite limited.

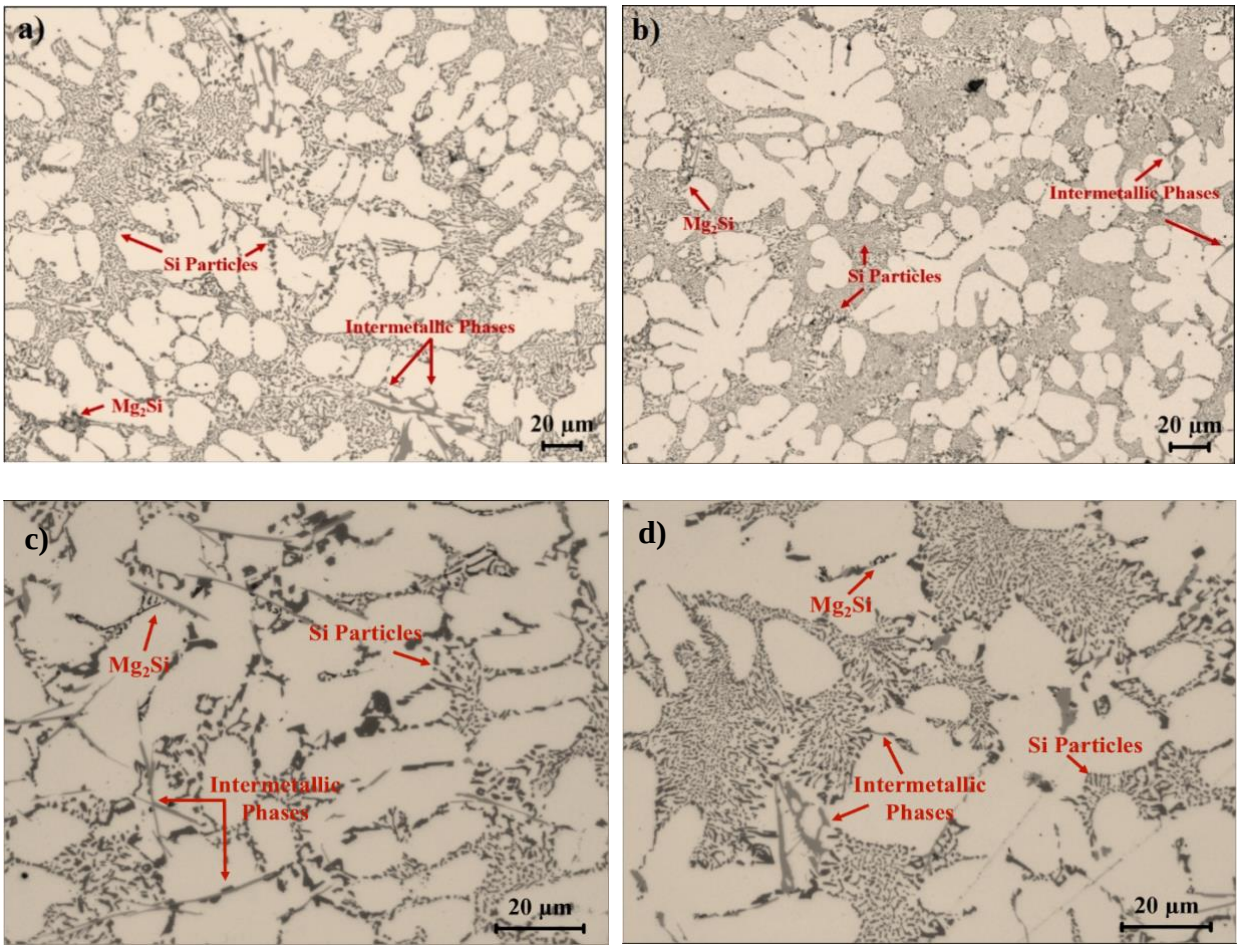

Figure 4-9**:** Optical microstructure images of the Base10 (a,c) and HPD 101 (b,d) alloys on as cast condition.

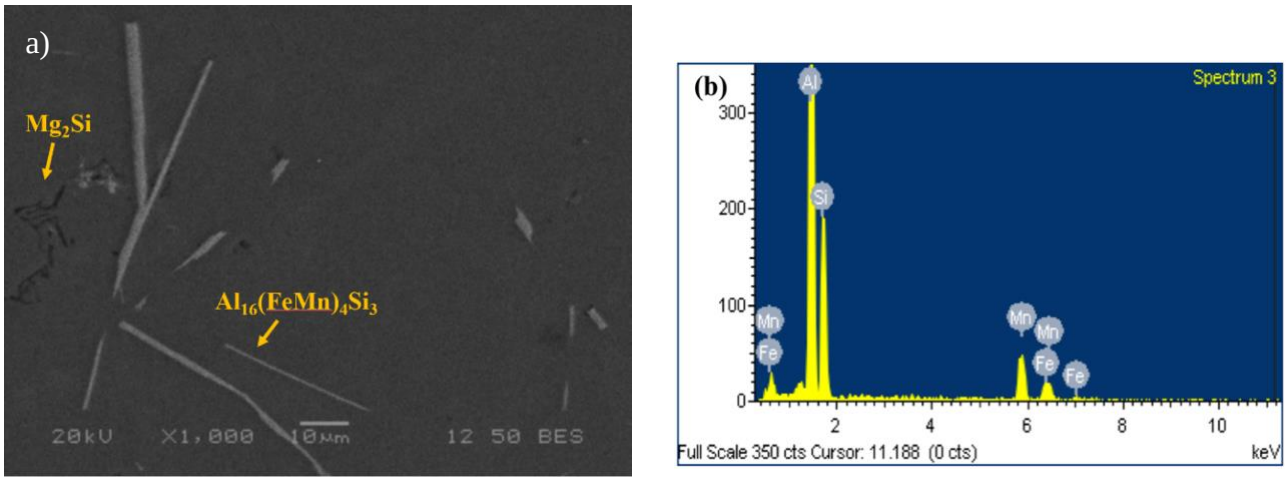

Figure 4-10**:** SEM backscattered electron image of the base alloy (a) and EDS spectrum of Fe-rich phase (b)

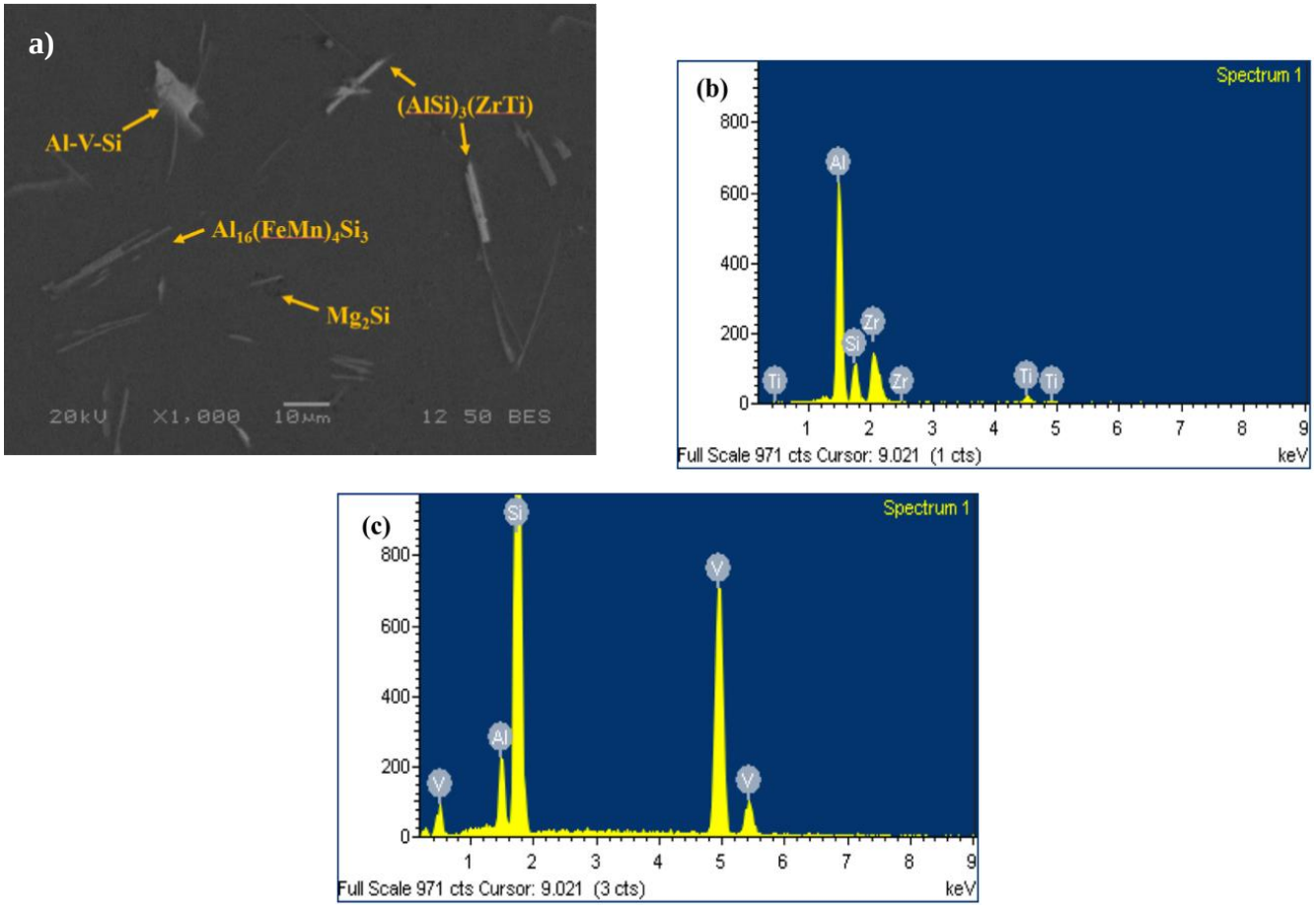

Figure 4-11**:** SEM backscattered electron image of HPD101 alloy (a), and EDS spectrum of Zr-rich intermetallic phase (b), and V-rich intermetallic phase (c)

Figure 4-12 and *Figure 4-13* represents the microstructural changes occurred after solution heat treatment (540°C for 2 hours plus 170°C for 4 hours) in both Base10 and HPD-101 alloys. As seen, the eutectic Si particles broke down into smaller fragments and became spheroidized in both alloys (*Figure 4-12*). Although most of the eutectic Si phase spheroidized after the T6 heat treatment, a small number of Si particles were observed as non-spheroidized in the heat-treated microstructure. According to Mohamed et.al [3], this uncompleted spheroidization may be explained with instability of the interface between two phases. It is mentioned that plate-like eutectics are more resistant to interfacial instabilities and spheroidization than the fibrous kind. Therefore, plate-like eutectic silicon particles in the as-cast microstructure did not completely spheroidized and tend to stay in the heat-treated microstructure as bigger fragments.

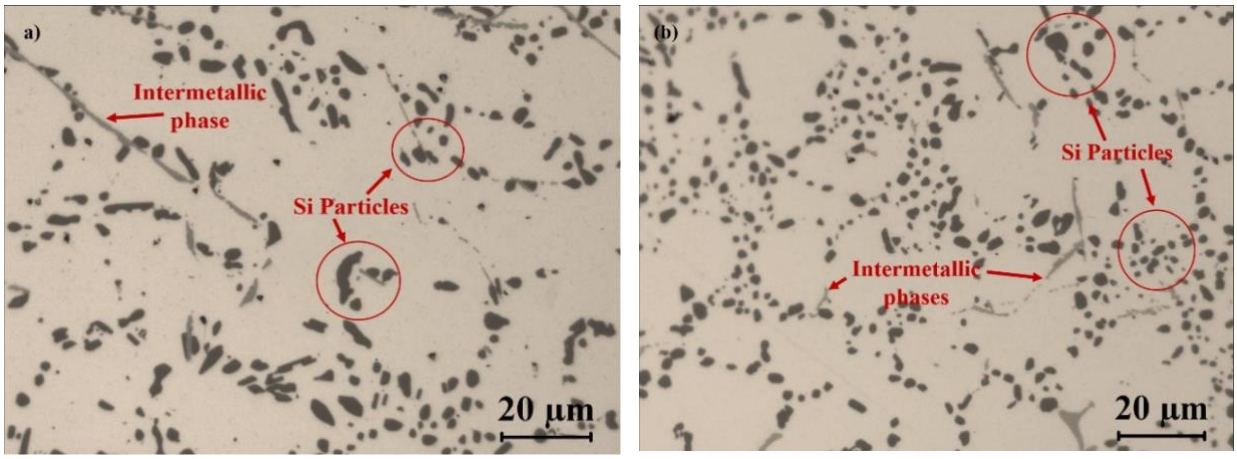

Figure 4-12**:** Optical images of the Base10 (a) and HPD101 (b) alloys on heat-treated condition

On the other hand, the needle-like intermetallic phase was observed in the base alloy whereas three different intermetallic phases were still in the HPD-101 structure (block-like V-rich intermetallic, rod-like Zr-rich intermetallic and needle-like intermetallic phases). (*Figure 4-13* and Table *4-5*)

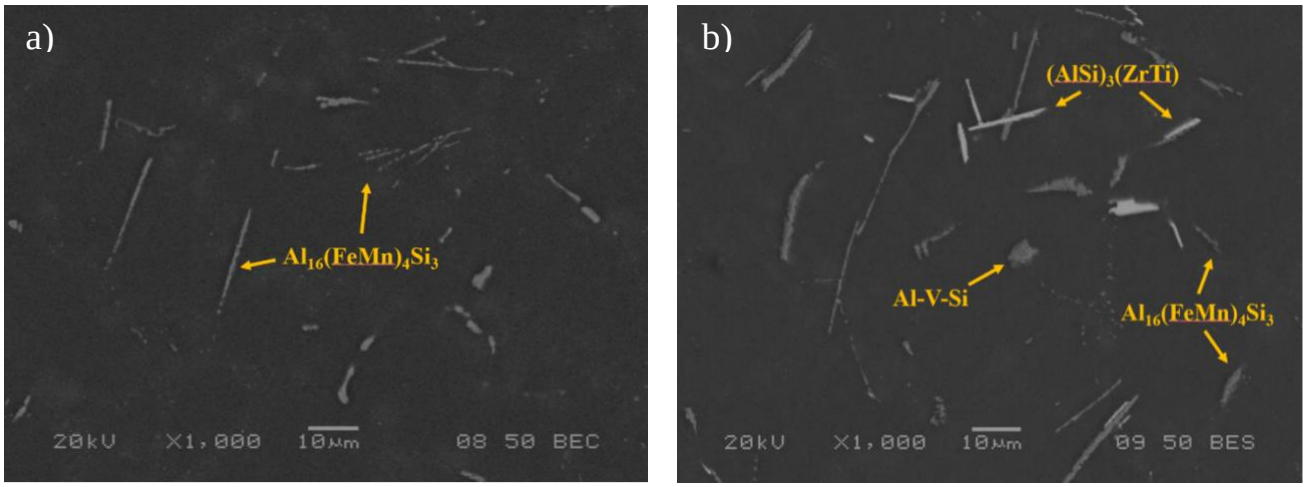

Figure 4-13: SEM backscattered electron images of the Base10 (a) and HPD101 (b) alloys.

Table 4-5: The main phases and their morphology identified using SEM/EDS in HPD101 alloy.

Calculated phase from SEM/ EDS	Response during T6 heat treatment	Phase morphology
α-aluminum	No change	Dendritic
Eutectic silicon	Partially dissolved/thermally modified	Fibrous/plate-like
Mg_2Si	Dissolved	Chinese script
$Al_{16}(FeMn)_4Si_3$	Partially dissolved	Needle-like
Al-Si-V	Partially dissolved	Block-like plate
$(AlSi)_3(ZrTi)$	Partially dissolved	Rod-like

In order to have a better understanding on the microstructural changes occurred after addition elements and also T6 heat treatment, Si particles and intermetallic phases were quantitatively analyzed. *Figure 4-14* represents the equivalent diameter of the Si particles in Base 10 and HPD-101 alloy on both as-cast and heat-treated conditions. It is seen that the equivalent diameter of Si particles is smaller than those in Base-10 alloy, indicating that the addition of V and Zr has beneficial effect on the Si modification (see *Figure 4-9*). Following the T6 heat treatment, the equivalent diameter of Si particles in both Base 10 and HPD 101 alloy became larger which is a remarkable sign to the coarsening of the Si particles. It is also observed that the morphology of eutectic Si was changed in heat-treated alloys. Thus, it can be concluded that the additions of V

and Zr elements plays a significant role to reduce the size of Si particles in the AlSi10Mg alloys and the solution heat treatment can further change the Si morphology and promote the spheroidization of Si particles.

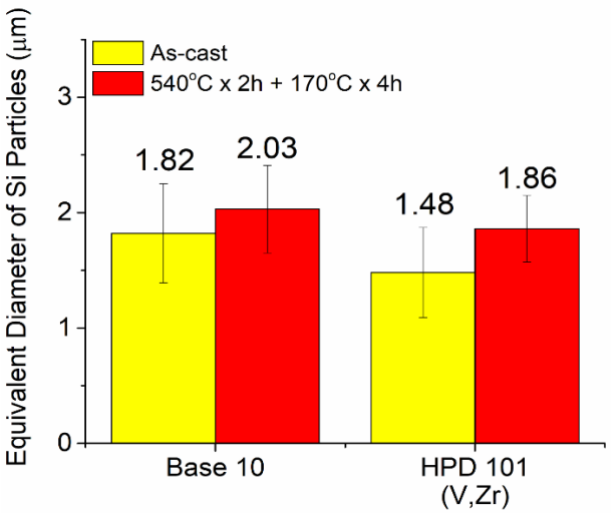

Figure 4-14**:** Equivalent Diameter of Si particles for Base-10 and HPD 101 alloy in both as-cast and heat-treated conditions

Figure 4-15 shows the volume fraction and aspect ratio of the intermetallic phases in two alloys on as cast and heat-treated conditions. The results indicated that the addition of V and Zr elements resulted slight increase in volume fraction of intermetallic phases on as-cast condition which is attributed to formation of V-rich and Zr-rich intermetallic phases. Following the solution heat treatment, volume fraction of intermetallic phases decreased in both Base-10 and HPD-101 alloy, most likely due to the fragmentation and partial dissolution of intermetallic phases (Table 4.4). It should also be pointed out that after heat treatment, volume fraction of intermetallic phases in the HPD-101 is even less than that in Base10 alloy, indicating that Zr and V additions has beneficial influence on the partial dissolution of intermetallic phases during solution heat treatment and resulting in more solute elements in the aluminum matrix.

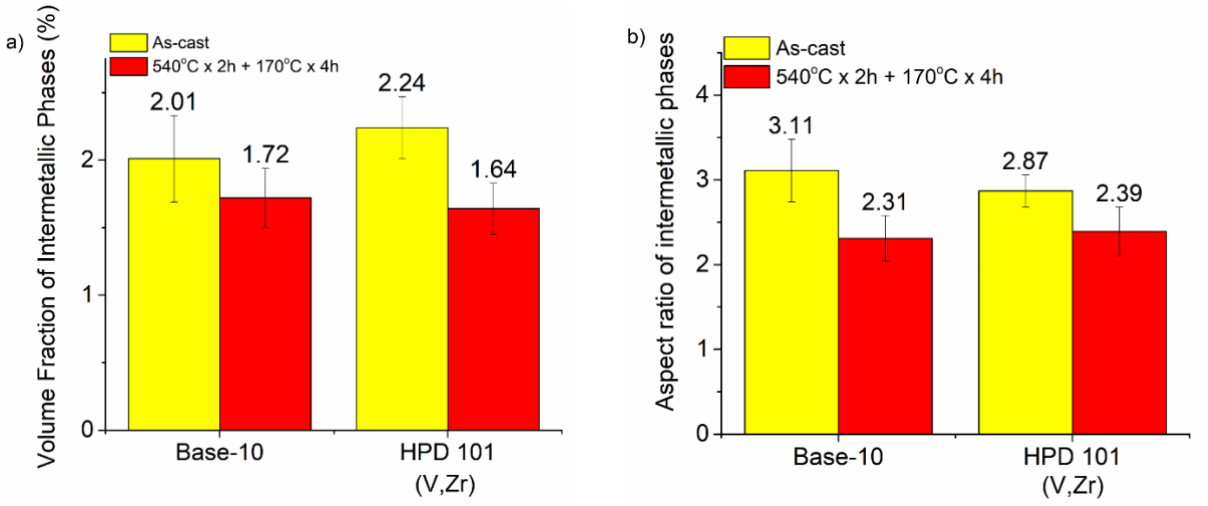

Figure 4-15: Volume Fraction (a) and aspect ratio (b) of the intermetallic phases in the Base10 and HPD 101 alloys on both as cast and heat-treated conditions

On the other hand, addition of V and Zr decreases the aspect ratio of intermetallic phases and further reduction can be achieved due to T6 heat treatment. This implies that Zr and V additions and solution heat treatment can modify morphology of the intermetallic phases in the Base10 alloy. Besides, *Figure 4-16* illustrates length of each intermetallic phases in Base-10 and HPD101 alloys on as-cast and heat-treated conditions. The results reveal that after the additions of V and Zr, the length of the Fe-rich phase became 20% shorter in HPD101 alloy, proving that the V and Zr additions can reduce the length of Fe-rich intermetallic phases in AlSi10Mg alloy.

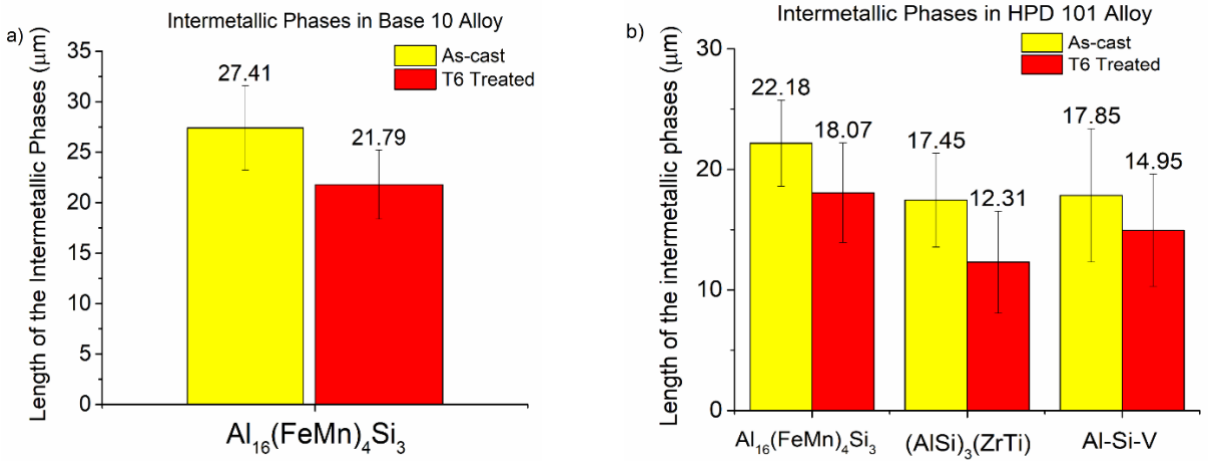

Figure 4-16: Length of the intermetallic phases in Base-10 (a) and HPD-101 (b) alloys.

As well known, the Al-Si alloys are designed to form dispersoids and precipitates which are generated during heat treatment to strength aluminum alloys. *Figure 4-17* shows the distribution of dispersoid zone and dispersoid free zone (DFZ) in 10% Si containing permanent mold casting alloys. In HPD-101 alloy, following the solution heat treatment at 540°C for 2h, considerable number of dispersoids was observed within aluminum grains while the dispersoid free zone formed in inter-dendritic regions. The qualitative analysis of Base-10 and HPD-101 etched microstructures reveals the influence of addition elements on the wideness of dispersoid zone and dispersoid free zone. As it is seen clearly, the dispersoid zone significantly increases due to addition of V, Zr while significant reduction was observed in dispersoid free zones. In addition to that *Figure 4-19* shows the number density (a) and the area fraction (b) of dispersoids in 10% Si containing alloys. The analysis revealed that the area fraction of dispersoids in HPD-101 alloys is higher than that in Base-10 alloy, proving the beneficial effect of V and Zr metals on the formation of higher amount dispersoids in the matrix.

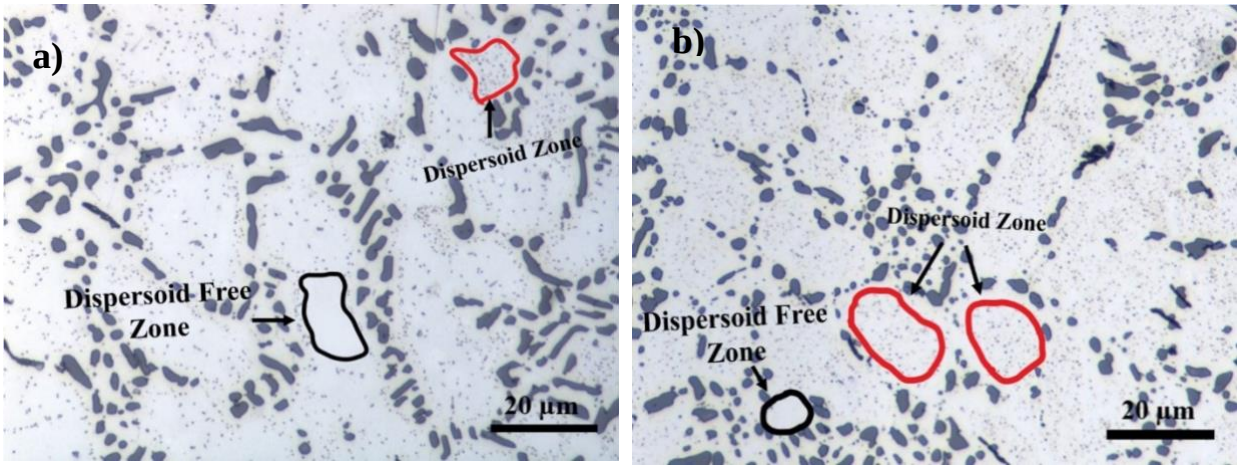

Figure 4-17**:** Dispersoid zone and dispersoid free zone in the solution heat treated Base-10 (a) and HPD-101 (b) microstructures.

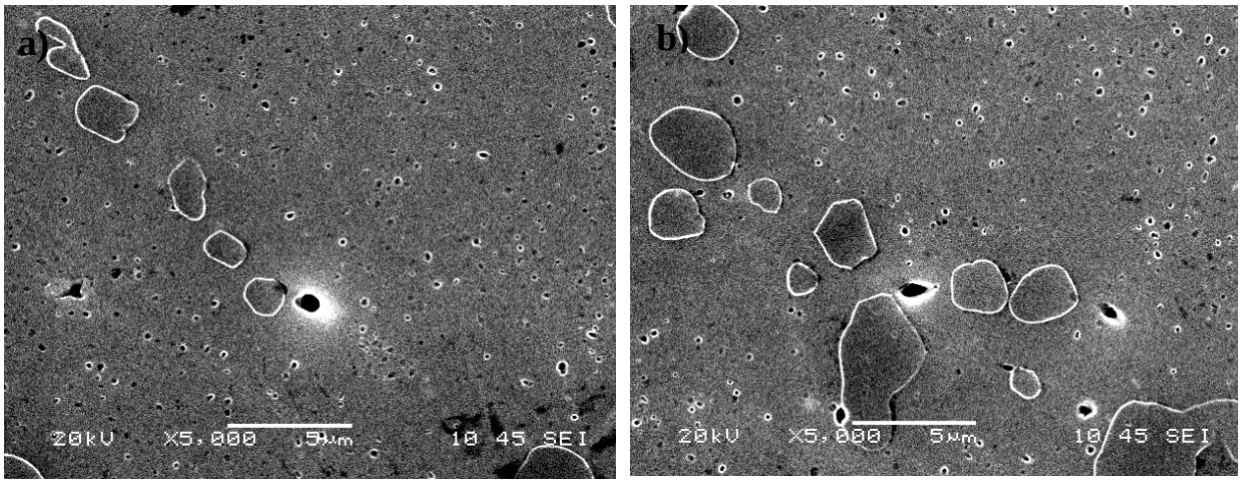

Figure 4-18: Secondary electron images of etched Base-10 (a) and HPD-101 alloys after solution heat treatment

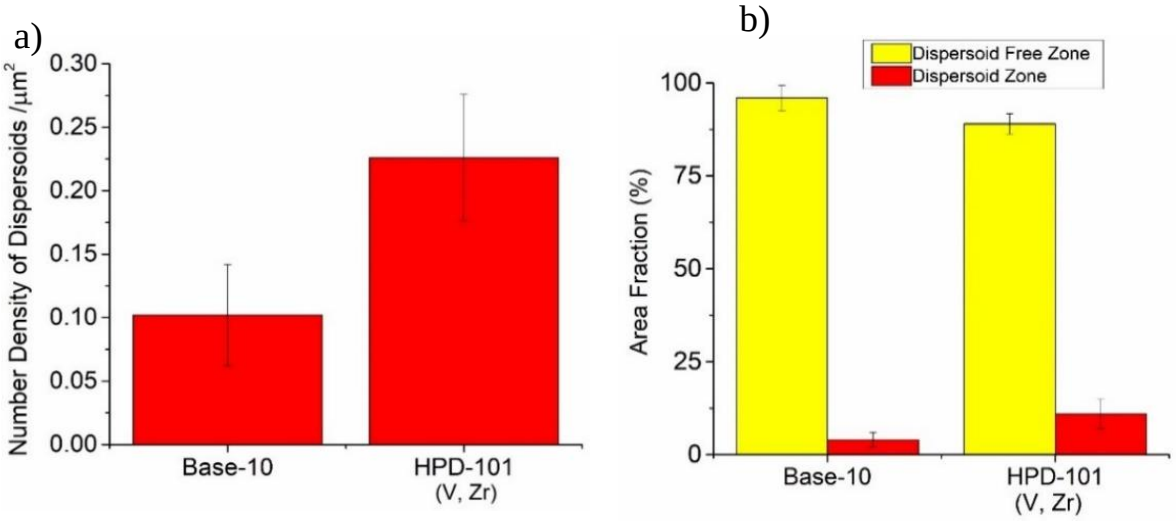

Figure 4-19: Number density of dispersoids (a) and area fraction of dispersoid zones (b)

TEM images of the Base-10 and HPD-101 (V, Zr) alloys are given in *Figure 4-20*. The EDX analysis reveals that α-Al(MnSi)Fe dispersoids formed in α-Al grain interiors of the base alloy at solution heat treatment stage. On the other hand, the additions of V and Zr elements in the modified alloy resulted in the formation of V and Zr-containing dispersoids. TEM-EDS analysis confirmed the presence of two distinct dispersoids in the microstructure of HPD-101; α-Al(MnVFe)Si and dispersoid which composed of Al-Si-Fe-Zr-Ti. According to Jovid et al. [4], the

presence of V and Zr transition elements can contribute higher amount of dispersoids in the microstructure. In addition to that the combination of V and Mn to form dispersoids in the α-Al grain interiors is highly beneficial due to the high partition tendency of V element during solidification. Therefore, a more uniform distribution of the precipitates can be obtained along the microstructure.

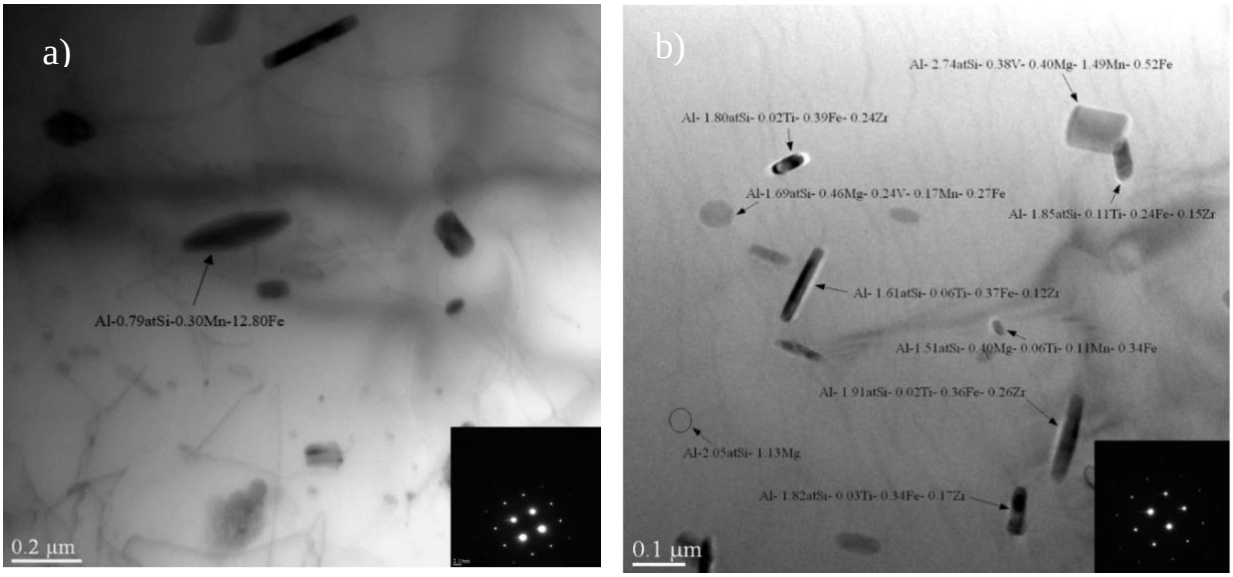

Figure 4-20: TEM images of Base-10 (a) and HPD-101 (b) alloys on solid- solution state.

Consequently, it is seen that the additions of V and Zr resulted significant changes in microstructure of AlSi10Mg alloy such as modification of eutectic Si particles, generating new distinct intermetallic phases, reduction in the length of Fe-rich intermetallic phases and modification in the size of the intermetallic phases. It is also well established that the solution heat treatment can further change the microstructure and provide the partial dissolution of intermetallic phases. Beside the microstructural changes, additions of V and Zr also influenced the mechanical properties of AlSi10Mg alloy. The results indicated that the modified alloy displayed remarkably higher mechanical properties than those in Base-10 alloy on both as-cast and heat-treated conditions. Improvement in mechanical properties can be attributed to: (1) reduction of the size of

intermetallic phases as well as refinement of eutectic Si particles; (2) solute solution strengthening of Zr and V; (3) the high supersaturation of solid solution due to the favourable partial dissolution of intermetallic phases during heat treatment; (4) reduction in the length and volume fraction of the intermetallic phases following the heat treatment; (5) the promotion of the dispersoids due to the presence of Zr and V solute atoms in the solid solution.

4.3.2 Microstructure of 8% Si Containing Alloys (Base-8, HPD 802, and HPD 803)

Typical microstructure images of AlSi8Mg, HPD-802 (V, Zr) and HPD-803 (V, Zr, Mo) alloys on as-cast condition are given in *Figure 4-21*. It is observed that the microstructure of base, HPD-802 and HPD-803 alloys are consisted of dendrite-like aluminum cells, eutectic Si particles, Mg_2Si phase and different types of intermetallic phases. The analysis of microstructure reveals that Mg_2Si is typically present in the Chinese-script morphology in all experimental alloys. As it is in 10% Si containing base alloy, addition of Sr into the Base-8 did not fully modify the eutectic Si phase and considerable amount of Si particles still observed as-plate-like. On the other hand, in HPD802 (V, Zr) and HPD803 (V, Zr, Mo) alloys, the Si particles mostly modified and showed the fiber-like morphology.

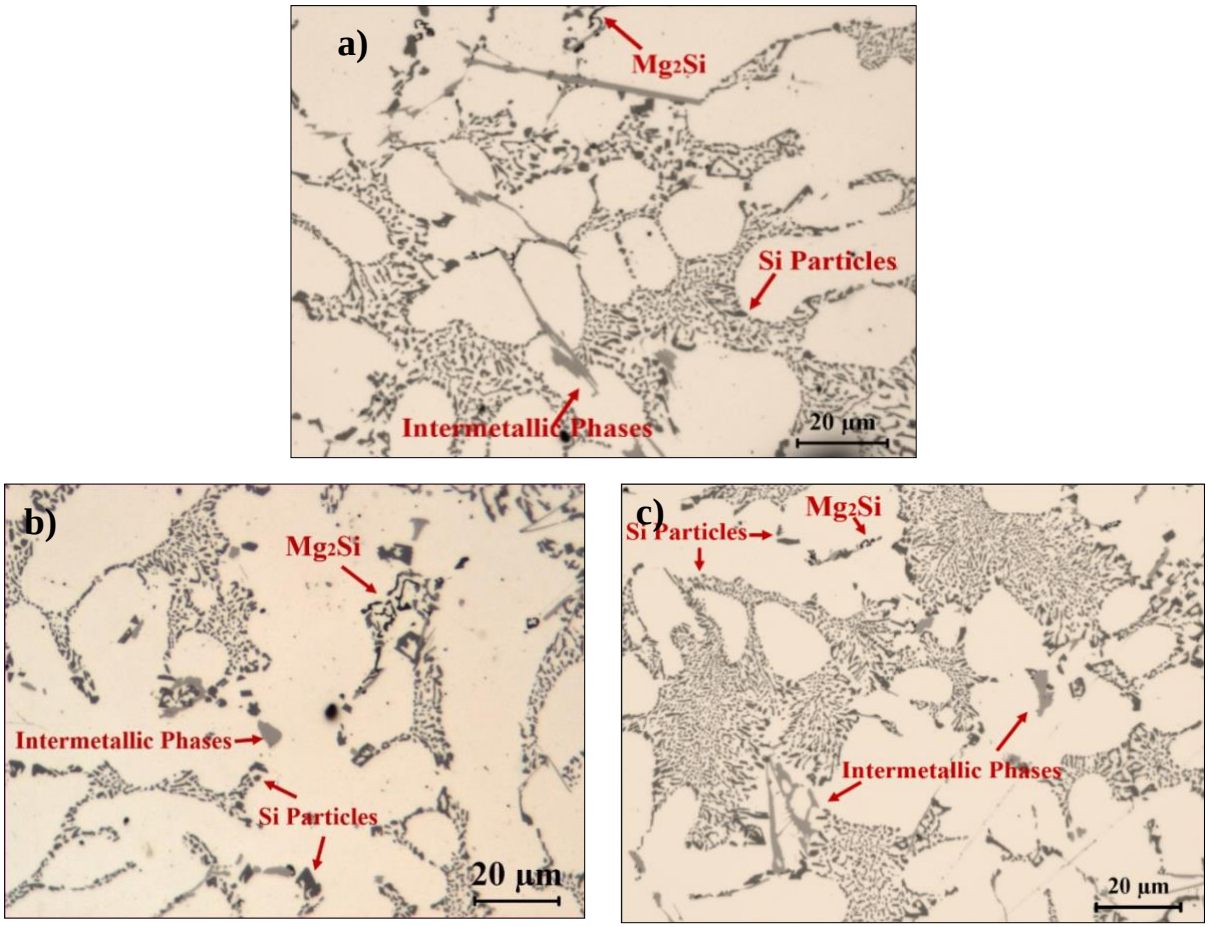

Figure 4-21: Optical microscope images of Base8 (a), HPD802 (b) and HPD803 (c) alloys respectively.

The microstructure investigation reveals that the additions of approximately 0.20 Zr and 0.30 V resulted in the formation of rod-like Al, Zr, Si and Ti containing intermetallic phase which referred as $(AlSi)_3(ZrTi)$, irregular shape intermetallic phase that is composed of Al, V and Si elements and needle-like Fe-rich intermetallic phase in HPD-802 alloy. On the other hand, three distinct intermetallic phases with different morphologies were found in HPD-803 alloy (V, Zr, Mo). These intermetallic phases were confirmed as Al, Si, Fe, Mn, Mo and V containing phase with blocky shape, the needle-like $Al_{16}(FeMn)_4Si_3$, phase and rod-like Zr-rich intermetallic phase. It is well established that, following the additions of V, Zr and Mo, needle-like $Al_{16}(FeMn)_4Si_3$ intermetallic phases disappeared as distinct from Base-8 and HPD-802 alloys. Instead, block-like

micro-sized intermetallic phase was observed in the HPD-803 microstructure. This implies that Mo addition suppressed the formation of needle-like $Al_{16}(FeMn)_4Si_3$ intermetallics and promoted the formation of blocky Al-Si-Fe-V-Mo intermetallic phases which resulted in a further improvement of the tensile properties in comparison to HPD-802 (V, Zr) alloy [5].

The SEM images of the three experimental alloys and the present phases in their microstructure were given in *Figure 4-22*, *Figure 4-23* and *Figure 4-24*.

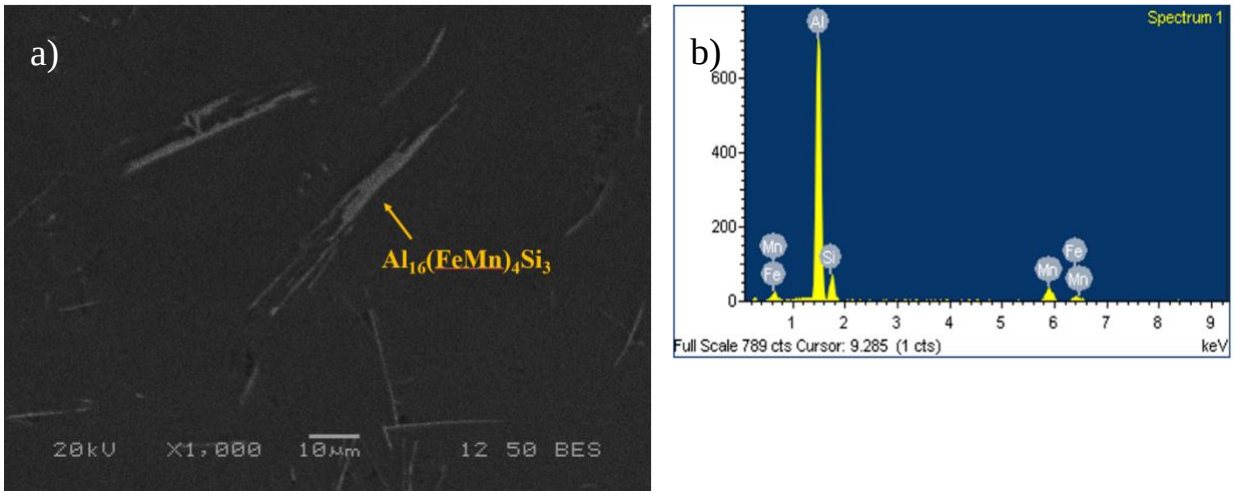

c)

Alloy	SEM-EDS	Phase Morphology
Base-8	α– aluminum	Dendritic
	Eutectic silicon	Fibrous/plate-like
	Mg_2Si	Chinese Script
	$Al_{16}(FeMn)_4Si_3$	Needle-like

Figure 4-22**:** SEM image (a), EDS spectrum (b) and present phases (c) in Base-8 alloy on as-cast condition

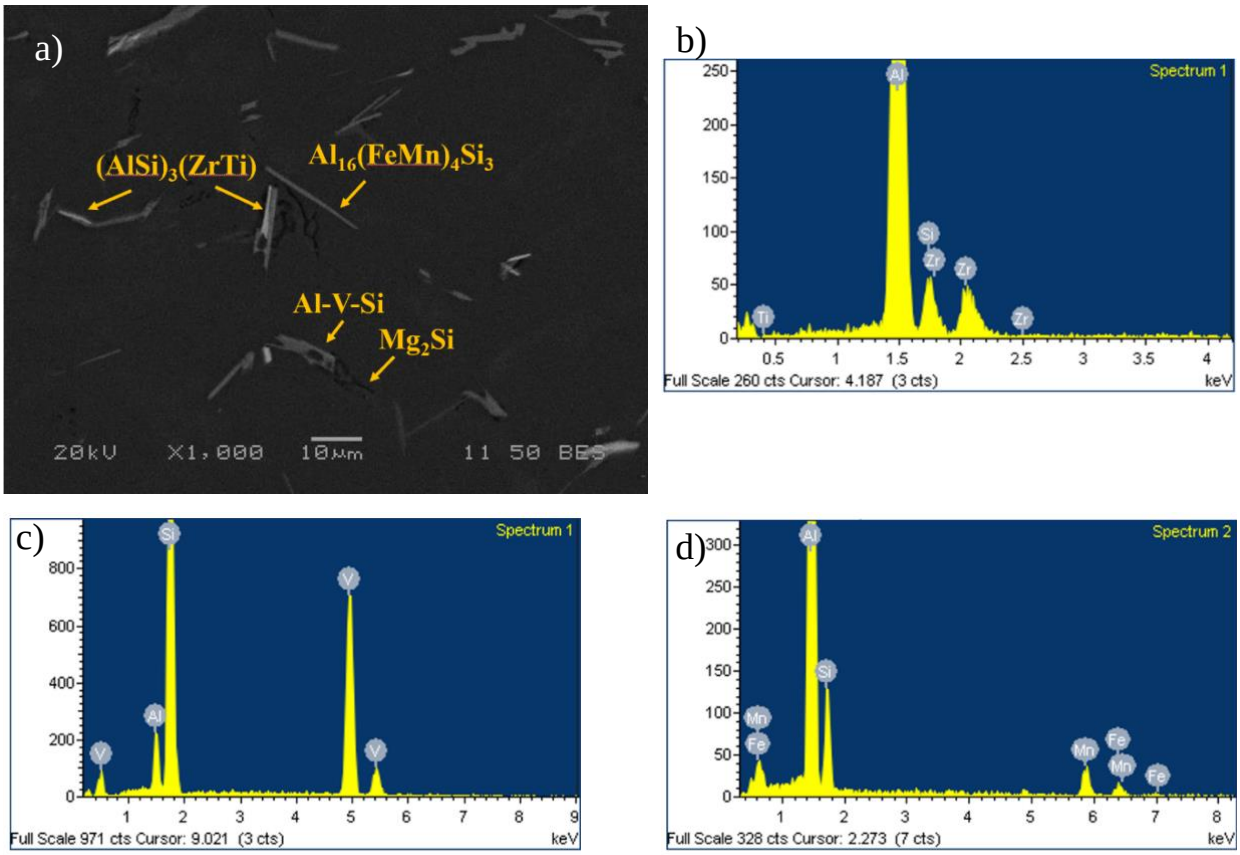

e)

Alloy	SEM-EDS	Phase Morphology
HPD-802	α– aluminum	Dendritic
	Eutectic silicon	Fibrous/plate-like
	Mg_2Si	Chinese Script
	$Al_{16}(FeMn)_4Si_3$	Needle-like
	AlSiV	Irregular
	$(AlSi)_3(ZrTi)$	Rod-like

Figure 4-23: SEM image (a), EDS spectrums (b,c,d) and present phases (e) in HPD-802 alloy on as-cast condition.

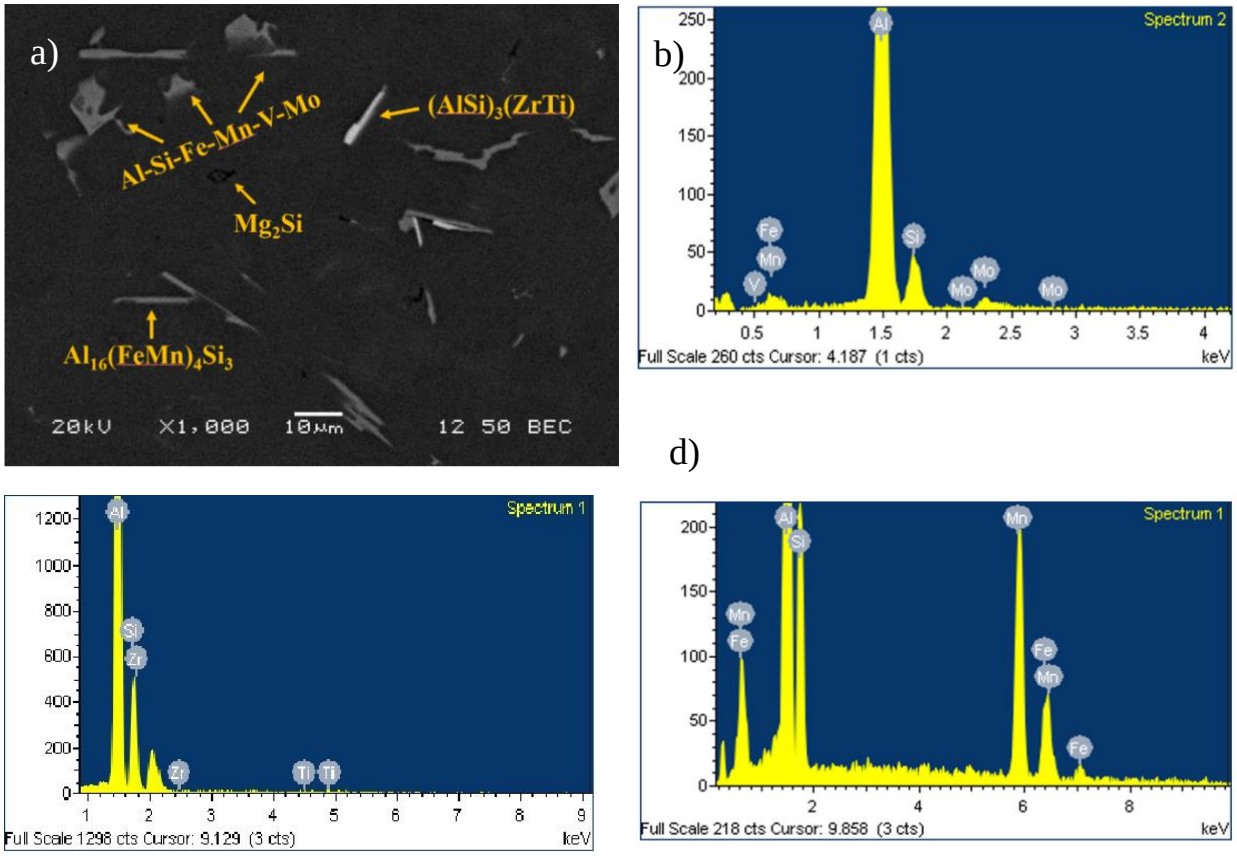

e)

Alloy	SEM-EDS	Phase Morphology
HPD-803	α– aluminum	Dendritic
	Eutectic silicon	Fibrous/plate-like
	Mg_2Si	Chinese Script
	Al-Si-Fe-Mn-V-Mo	Block-like
	$(AlSi)_3(ZrTi)$	Rod-like
	$Al_{16}(FeMn)_4Si_3$	Needle-like

Figure 4-24: SEM image, EDS spectrum and present phases in HPD-803 alloy on as-cast condition

The optical and SEM images of T6 treated (540°C for 2 hours plus 170°C for 4 hours) experimental alloys are given in *Figure 4-25*. After the heat treatment, most of the eutectic Si particles became spheroidized in the alloys. Addition to that Chinese-script Mg_2Si phase could not detected in the heat-treated microstructures, indicating that Mg_2Si phase completely dissolved in

the all experimental alloys. However, other intermetallic phases are still in present with smaller size compared to as-cast conditions which is attributed high thermal stability of these intermetallic phases.

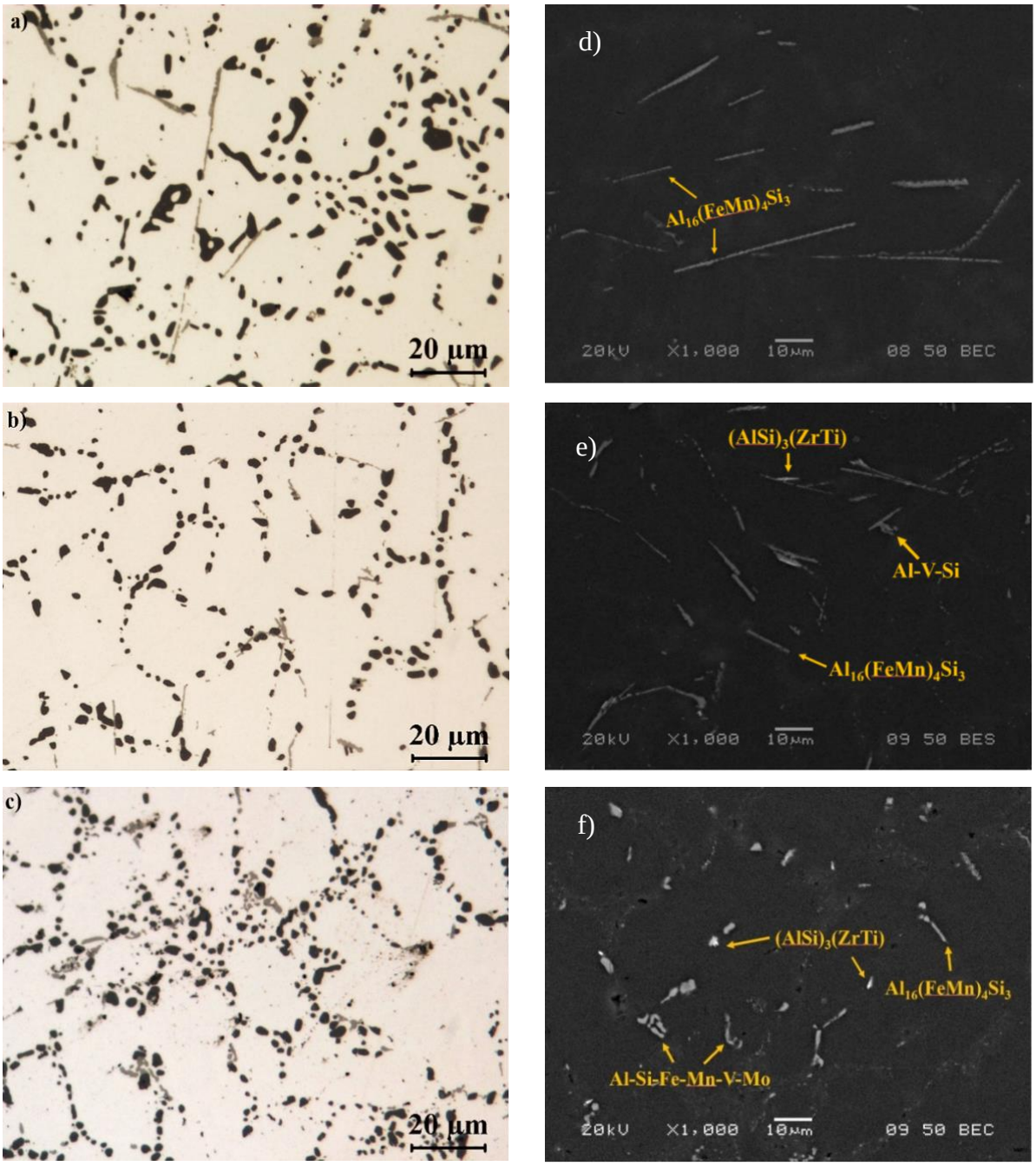

Figure 4-25: Optical images and SEM micrographs of Base8 (a, d), HPD802 (b, e) and HPD803 (c, f) on heat-treated condition (540 °C x 2h + 170 °C x 4h).

Quantitative image analysis of Si particles and intermetallic phases was performed to reveal the effect of V, Zr and Mo (HPD-802 and HPD-803 alloys) additions on size and phase morphologies on as-cast and T6 heat-treated conditions. *Figure 4-26* represents the equivalent diameter of Si particles for 8% Si containing alloys. As it is also confirmed in 10% Si containing alloys, additions of V and Zr elements (HPD-802) resulted in a remarkable reduction of the size of Si particles compared to Base8 alloy. Following the T6 heat treatment, the morphology of Si particles in both Base8 and HPD-802 alloys have changed and Si particles became larger which are attributed to the spheroidization and the coarsening of Si particles. Addition to that the results showed that in comparison with the Base8 alloy, the coarsening of Si particles in HPD-802 (V, Zr) alloy was quite limited, indicating the high resistivity of V and Zr elements on the coarsening.

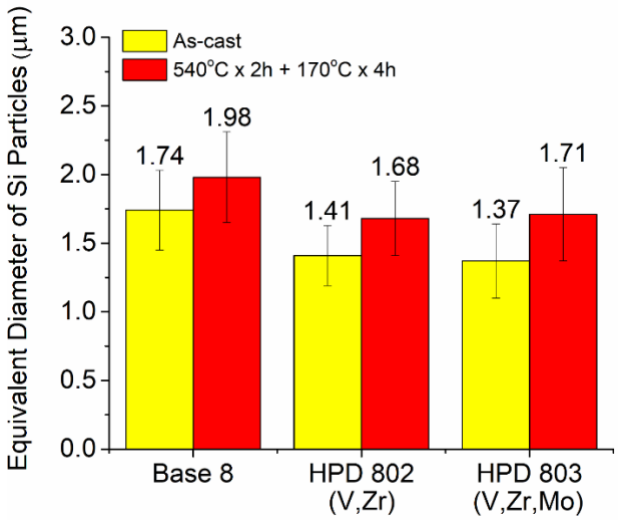

Figure 4-26: Equivalent diameter of Si particles on as cast and heat-treated conditions for 8% Si containing alloys

On the other hand, the additions of V, Zr and Mo (HPD-803) to AlSi8Mg alloy significantly reduced the size of eutectic Si particles and changed its morphology in comparison with Base-8 alloy. However, it is reported that the additions (V, Zr, Mo) did not provide further modifications on the morphology and size of Si particles when compared to HPD-802 alloy. On heat treated

condition, it is well established that the size of Si particles in HPD-803 (V, Zr, Mo) alloy was very similar that in HPD802 (V, Zr) alloy, indicating that the additions of V, Zr and Mo elements have no further influence on coarsening of Si particles after solution heat treatment.

Figure 4-27 illustrates the volume fraction, aspect ratio and the length of intermetallic phases in the experimental alloys. As seen in *Figure 4-27*a, the additions of V, Zr (HPD-802) and V, Zr and Mo elements (HPD-803) slightly increase the volume fraction of intermetallic phases on as-cast condition which is attributed to formation of V-rich, Zr-rich and Mo-rich intermetallic phases. Following the solution heat treatment, the volume fraction of the intermetallic phases in all experimental alloys becomes less than those on as-cast condition, most likely due to the fragmentation and partial dissolution of intermetallic phases. It should be noted that after T6 heat treatment, the volume fraction of intermetallic phases in HPD803 alloy is even less than those in Base and HPD802 (V, Zr) alloys. This implies that the addition of Mo element to HPD-802 alloy can promote the partial dissolution of intermetallic phases during heat treatment, resulting in more solute elements in the aluminum matrix.

The aspect ratio of the intermetallic phases is given in *Figure 4-27*b. In HPD-802 alloy, additions of V and Zr elements resulted in reduction of the aspect ratio of intermetallic phases as it was also observed in 10%Si containing alloys. Following the heat treatment, the reduction in aspect ratio of the intermetallic phases was further increased which was attributed to partial dissolution of intermetallic phases. On the other hand, the aspect ratio of intermetallic phases in as-cast HPD-803 alloy is relatively bigger than that in HPD-802 alloys. This increment may be explained by the formation of large, irregular Al-Si-Mn-Fe-V-Mo intermetallic phases. After the solution heat treatment, the aspect ratio of intermetallic phases in HPD803 dramatically decreased due to the spheroidization and partially dissolution of the intermetallic phases.

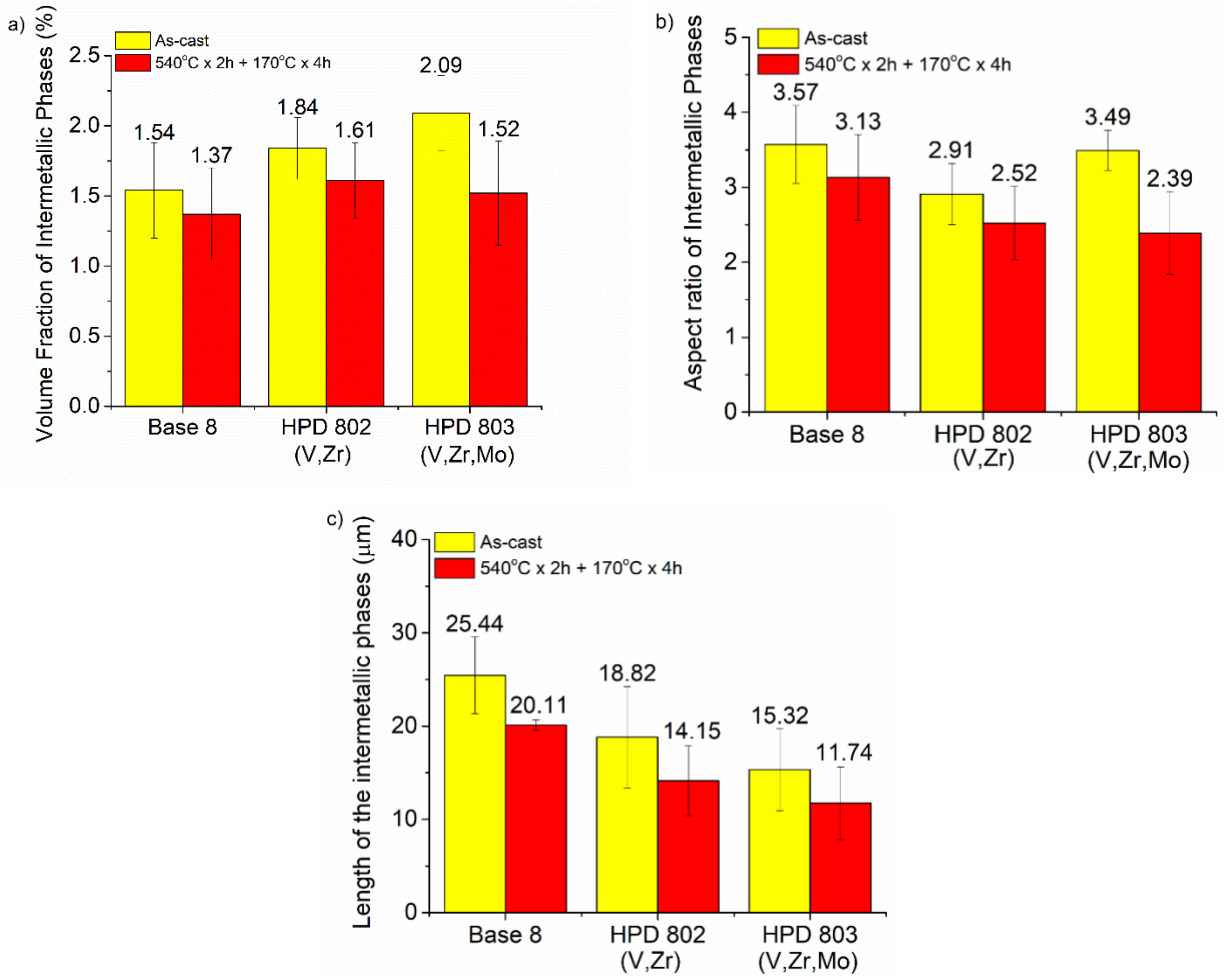

Figure 4-27: Volume fraction (a), aspect ratio (b) and length of the intermetallic phases (c) in the experimental alloys on as cast and heat-treated conditions

*Figure 4-27*c indicates that the additions of V, Zr (HPD-802) and V, Zr and Mo (HPD-803) into Base-8 alloy can reduce the length of the intermetallic phases on as-cast condition. Moreover, further modification can be achieved via solution heat treatment at 540°C for 2h + 170°C for 4h.

The distribution of dispersoid zone and dispersoid free zone (DFZ) in 8% Si containing experimental alloys are given in *Figure 4-28*. Following the solution heat treatment at 540°C for 2h, significant number of dispersoids were precipitated within aluminum grains. The quantitative analysis of dispersoids indicated that the addition of V and Zr (HPD-802 alloy) metals to Base-8

leads significant improvement in the area fraction of dispersoid zone, while dispersoid free zones decrease in comparison with Base-8 alloy. It is also observed that area fraction of dispersoid zone can further increase via addition of V, Zr and Mo elements which proves the beneficial influence of Mo addition on the formation of higher amount dispersoids. This idea can also be supported with another study. Farkoosh et al. [6], indicated that the presence of Mo in Al-Si alloys may lead the formation of a large amount of metallurgically stable dispersoids in the microstructure, resulting in a significant increase in the mechanical properties of the alloy.

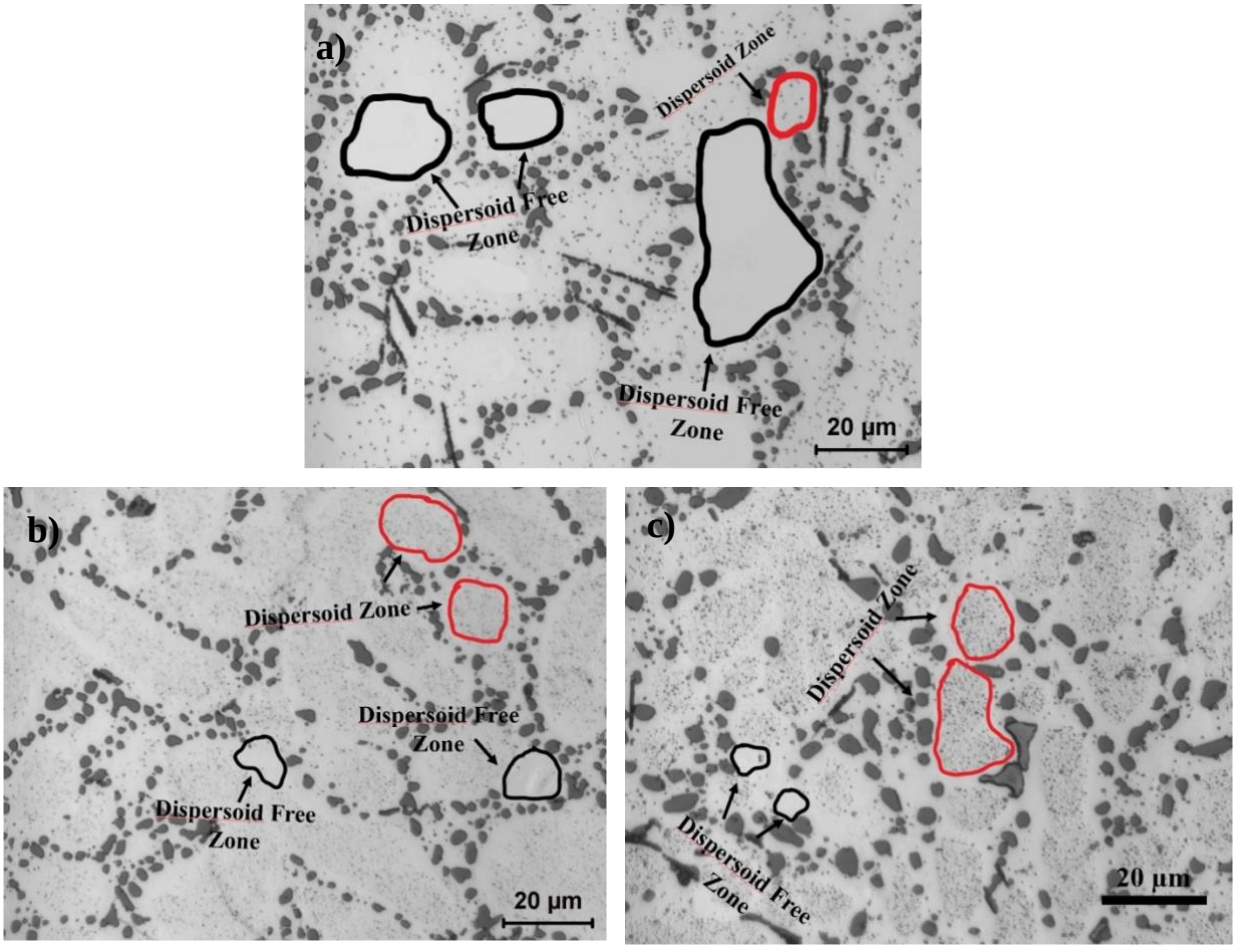

Figure 4-28: Dispersoid zone and dispersoid free zone in the solution heat treated Base-8 (a), HPD-802 (b) and HPD-803 (c) microstructures

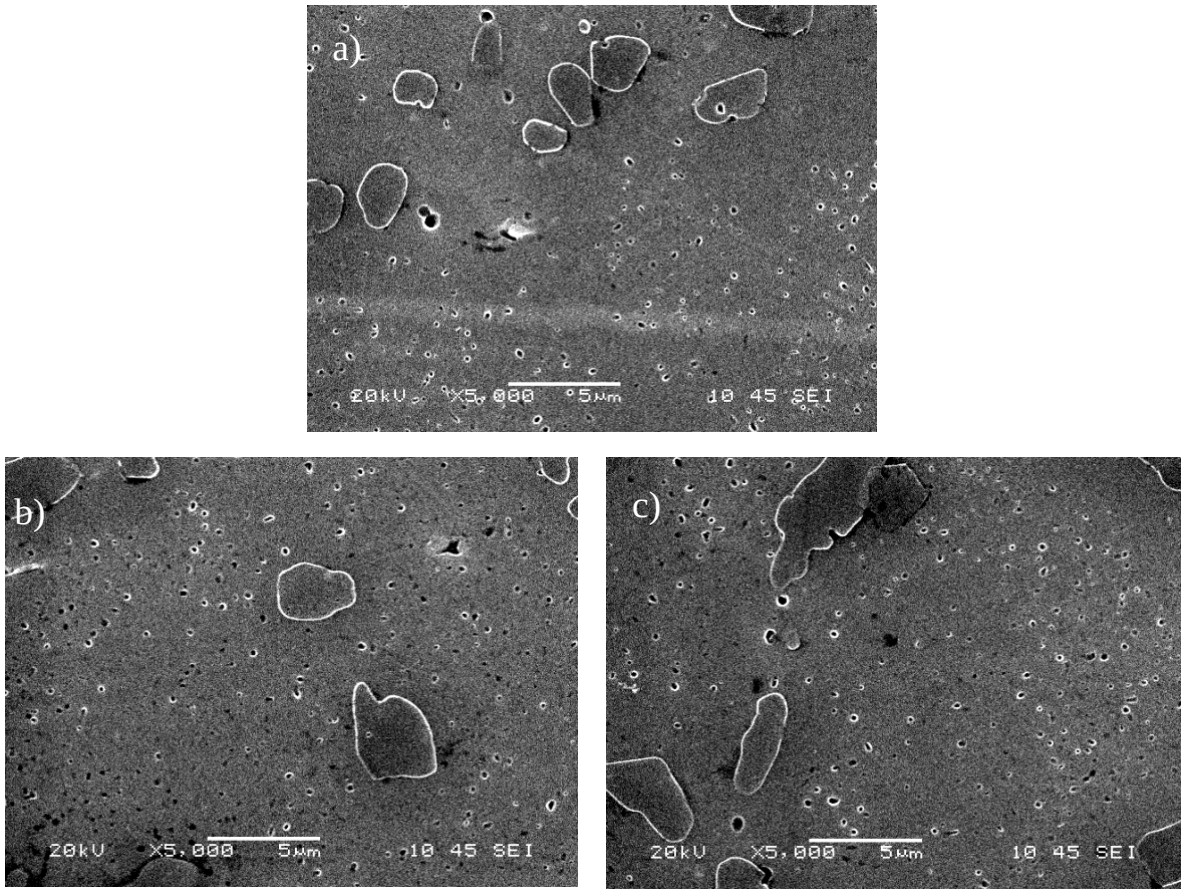

Figure 4-29**:**Secondary electron images of etched Base-8 (a), HPD-802 (b) and HPD-803 (c) alloys after solution heat treatment

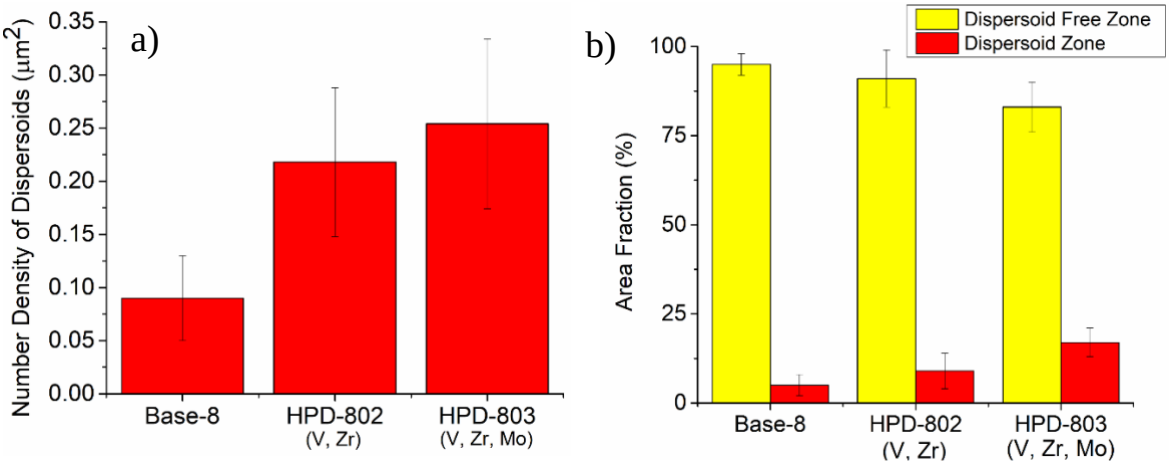

Figure 4-30: Number density of dispersoids and area fraction of dispersoid zones in Base-8, HPD-802 and HPD-803 alloys.

In brief, microstructure analysis of the 8% Si containing experimental alloys reveals that the additions of V, Zr and V, Zr (HPD-802) and V, Zr, Mo (HPD-803) can modify the eutectic Si particles, generate new distinct intermetallic phases and reduce the length of the intermetallic phases. It is also obtained that further modifications on microstructure can be achieved by solution heat treatment. In addition to the microstructural changes, transition elements can also influence the mechanical properties of AlSi8Mg alloys. The results showed that the modified alloys displayed significantly higher mechanical properties than those in unmodified alloy on both as cast and heat-treated conditions. Improvement in mechanical properties of 8% Si containing alloys can be attributed to: (1) reduction of the size of intermetallic phases and refinement of eutectic Si particles; (2) solute solution strengthening of Zr, V and Mo; (3) the high supersaturation of solid solution due to the beneficial partial dissolution of intermetallic phases during heat treatment; (4) reduction in the length and volume fraction of the intermetallic phases following the heat treatment; (5) the promotion of the dispersoids and precipitations due to the presence of Zr, V and Mo solute atoms in the solid solution.

4.4 Summary

In this chapter, mechanical properties and microstructural features of permanent mold casting alloys are discussed. In general view, it is well established that the presence of higher silicon content results in higher hardness, yield strength and ultimate tensile strength while it significantly reduces the elongation of the Al-Si alloy. Following the additions of transition elements (V, Zr) and (V, Zr, Mo) into the base alloy, a noticeable increase in mechanical properties was reported whereas a significant reduction observed in electrical conductivity. For instance, in all 10% Si containing alloys, at least 20% higher yield strength values were reported while a remarkable improvement was also obtained in ultimate tensile strength. It is well established that

among 10% Si containing alloys, the addition of V, Zr (HPD-101) into Base-10 alloy gives the best response in terms of mechanical properties improvement. Following the V and Zr additions, hardness, yield strength, ultimate tensile strength and elongation of the Base-10 alloy improved by 14%, 28%, 29% and 25% respectively on as cast condition. In as cast 8% Si containing alloys, the additions of transition elements resulted much higher elongation values when compared to 10% Si containing alloys. Three different combinations of V, Zr and Mo additions resulted at least 20% higher yield strength and ultimate tensile strength while even higher improvements were obtained in elongation values. It is determined that among 8% Si containing alloys, higher mechanical properties on as cast condition were achieved with the addition combinations of V, Zr (HPD-802) and V, Zr, Mo (HPD-803). In HPD-802, yield strength, ultimate tensile strength and elongation were increased by 24%, 27% and 33% respectively, where as they were obtained 27%, 32% and 61% higher in HPD-803 alloy respectively.

In order to evaluate precipitation potential of the experimental alloys, several heat treatments were carried out and the hardness results were studied extensively. The heat-treated hardness and tensile results indicated that the mechanical properties of the experimental alloys can be further improved via solution heat treatment. It was determined that increasing solution heat treatment temperature (from 500°C to 540°C) results in higher hardness values for all experimental alloys. It is also found longer soaking times result in higher hardness results for the alloys which were heat treated at 500°C while no significant improvement in hardness reported for T6 treated alloys at 540°C. According to hardness results of T6 treated alloys, the heat treatment parameters were optimized as 540°C for 2 hours plus 170°C for 4 hours due to its higher hardness results and short soaking times.

The microstructure investigation of experimental alloys revealed that the addition of V, Zr and Mo metals lead the modification of eutectic Si particles, Fe-rich intermetallic phases and the formation of new intermetallics on as cast condition. For example, following the addition of V and Zr into Base-10 alloy, equivalent diameter of Si particles and length of the Fe-rich intermetallic phases were decreased from 1.82 µm to 1.48 µm and 27.41 µm to 22.18 µm respectively. Besides, V and Zr additions generate their own intermetallic phases, $(AlSi)_3(ZrTi)$ and Al-Si-V, thus increased the volume fraction of intermetallic phases from 2.01% to 2.24%. On the other hand, in HPD-803 alloy (V, Zr, Mo), equivalent diameter of Si particles was obtained 20% less than that in Base-8 alloy, indicating the beneficial influence of V, Zr, Mo additions on Si modifications. Moreover, volume fraction of intermetallic phases in Base-8 alloy was increased from 1.59% to 2.09% due to newly generated intermetallic phases in HPD-803 alloy $(AlSi)_3(ZrTi)$ and Al-Si-Fe-Mn-V-Mo). It is also seen that solution heat treatment can induce a reduction in the size and volume fraction of intermetallic phases via dissolution of the intermetallic phases and results spherodizition of the eutectic Si particles.

The quantitative analysis of dispersoids and mechanical properties of T6 heat treated alloys show that V, Zr and Mo additions can greatly promote the formation of dispersoids and thereby further increase the mechanical properties of the alloys. The results reveal that the number density of dispersoids / μm^2 was significantly increased from 0.10 to 0.24 to with the additions of V and Zr into Base-10 alloy. On the other hand, in 8% Si containing alloys, the additions of V and Zr (HPD-802) resulted an improvement in number density of dispersoids / μm^2 from 0.09 to 0.21 while even further improvement was obtained with the combination of V, Zr and Mo additions in HPD-803 alloy (from 0.09 to 0.26).

As a second step of this study, six alloys with different compositions were suggested for the investigation of high-pressure vacuum die casting alloys. Table *4-6* shows the recommended alloys for next step.

Table 4-6: The suggested alloys for high pressure vacuum die casting investigation.

10% Si Containing Alloys	8% Si Containing Alloys
Aural^{TM}-3 (Base)	8-I (Base)
10-I (0.15 Zr- 0.15 V)	8-II (0.15V – 0.15 Zr)
10-II (0.25 Zr – 0.25 V)	8-III (0.15V – 0.15 Zr – 0.15 Mo)

REFERENCES

[1] N.A.Belov, D.G. Eskin, A.A. Aksenov, Multicomponent Phase Diagrams: Applications for Commercial Aluminum Alloys. (2005) 15-19.

[2] J. Rakhmonov, G. Timelli, F. Bonollo, Characterization of the solidification path and microstructure of secondary Al-7Si-3Cu-0.3Mg alloy with Zr, V and Ni additions, Mater. Charact.,128 (2017) 100-108.

[3] A.M. Mohamed, A.M. Samuel, F.H. Samuel, H.W. Doty, Influence of additives on the microstructure and tensile properties of near-eutectic Al-10.8%Si cast alloy, Mater. Des. 30 (2009), 3943-3957.

[4] J. Rakhmonov, G. Timelli, A. Fabrizi, F. Bonollo, Effect of V and Zr microalloying and heat treatment on microstructure and mechanical properties of secondary Al-7Si-3Cu-0.3Mg alloy, International Journal of Materials Research

[5] A.R. Farkoosh, X. Grant-Chen, M. Pekguleryuz, Dispersoid strengthening of a high temperature Al–Si–Cu–Mg alloy via Mo addition, Mater. Sci. Eng.: A 620 (2015) 181–189.

[6] A.R. Farkoosh, X. Grant-Chen, M. Pekguleryuz, Interaction between molybdenum and manganese to form effective dispersoids in an Al-Si-Cu-Mg alloy and their influence on creep resistance, Mater. Sci. Eng.: A 627 (2015) 127- 138

CHAPTER 5

EFFECT OF ZR, V AND MO ADDITIONS ON MECHANICAL PROPERTIES AND MICROSTRUCTURE FEATURES OF HIGH-PRESSURE VACUUM DIE CASTINGS

Chapter 5

EFFECT OF V, ZR AND MO ON MICROSTRUCTURE AND MECHANICAL PROPERTIES OF HPVD CASTINGS

The selection process of the promising alloys for high pressure vacuum die casting applications was extensively studied and discussed in Chapter 4. In this chapter, microstructure features and mechanical properties of the selected and produced HPVD castings will be investigated. As it is mentioned earlier, the experimental alloys were classified into two groups according to their Si content and each of them contains different level of V, Zr or V, Zr and Mo additions.

5.1 The Mechanical Properties of HPVD Castings

5.1.1 The Hardness Evaluation of HPVD Castings on As Cast Condition

The hardness results of the HPVDC alloys in as-cast condition are given in *Figure 5-1*. The average hardness values for 10% Si containing alloys were obtained as 91.6 HV, 99.2 HV and 95.3 HV in Aural^{TM}-3, 10-I (V, Zr) and 10-II (V, Zr) alloys respectively. This indicates that the additions of V and Zr resulted in 8% increase in hardness of 10-I whereas 4% increase was obtained in 10-II alloy on as-cast condition. Although 10-II alloy contains higher amount of V and Zr additions than 10-I alloy, the hardness improvement in 10-II alloys is less than that in 10-I alloy. It is believed that higher Si and Mg content in 10-I alloy resulted in such a difference as it is given in *Table 3-2*.

On the other hand, the hardness of 8-I (Base) alloy was measured as 78.3 HV, while it is 81.1 HV in 8-II (V,Zr) and 84.3 HV in 8-III (V, Zr, Mo) respectively. The results indicated that hardness of base alloy increased 3.5% with addition of V and Zr whereas 8% hardness improvement observed in 8-III (V, Zr, Mo) alloy.

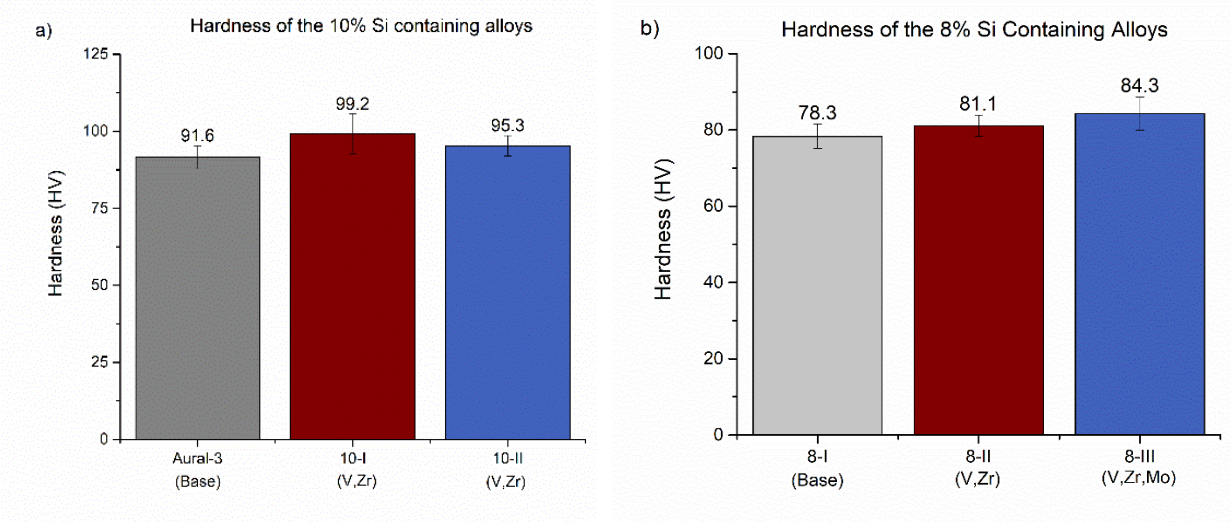

Figure 5-1**:** Hardness of the 10% (a) and 8% (b) Si containing alloys on as-cast condition

In order to evaluate the solid solution level, electrical conductivity of the alloys was measured and illustrated in Table *5-1*. It is established that the electrical conductivity of the modified alloys is remarkably lower than that of the base alloys, confirming that most of V, Zr and Mo additions present in the aluminum matrix as solute atoms.

Table 5-1: Electrical conductivity variation of the HPVD castings

Alloys (10% Si)	**Electrical Conductivity (MS/m)**	**Std. Dev**	**Alloys (8% Si)**	**Electrical Conductivity (MS/m)**	**Std. Dev**
Aural-3 (Base)	16.54	0.04	8-I (Base)	18.73	0.06
10-I (V, Zr)	14.49	0.05	8-II (V, Zr)	16.79	0.05
10-II (V, Zr)	14.35	0.03	8-III (V, Zr, Mo)	16.59	0.02

5.1.2 The Tensile Properties of HPVD Castings on As-cast Condition

The tensile properties of 10% and 8% Si containing high pressure vacuum die castings are illustrated in *Figure 5-2*. In Aural^{TM}-3 alloy, yield strength and ultimate tensile strength are found to be □ 155.7 MPa and □ 283.7 MPa whereas the elongation was obtained as □ 5.6%. The results show that for both 10-I and 10-II alloys, additions of V and Zr metals resulted in a slight improvement in yield strength and ultimate tensile strength, while a small drop was observed in

elongation results. For instance, yield strength and ultimate tensile strength values of 10-I alloy are found to be 164.6 MPa and 307.7 MPa respectively, indicating that yield strength and ultimate tensile strength values in 10-I alloy are higher than those in base alloy by 5.7% and 8.5% respectively. Meanwhile, in comparison with Aural^{TM}-3, 10-II alloy shows 4.6% higher yield strength (162.6 MPa) and 4.8% higher ultimate tensile strength (297.4 MPa). Although 10-II alloy contains higher amount of V and Zr addition than 10-I alloy, the improvement in yield and ultimate tensile strengths are less than that in 10-I alloy. Such a difference might be explained by higher content of Si and Mg elements in 10-I alloy (*Table 3-2*). It is reported that elongation of the 10-I alloy did not change by the additions of V and Zr. However, with increasing content of these elements, elongation of the 10-II alloy was found to be significantly lower than those in both base and 10-I alloy.

On the other hand, in 8% Si containing alloys, a significant improvement in tensile properties are obtained due to addition of V, Zr and Mo metals. As seen in Figure *5-2*b, yield strength of 8-I alloy was measured as 123.6 MPa whereas it determined as 139 MPa in 8-II (V, Zr) and 141.8 MPa in 8-III alloy. This implies that additions of V, Zr and V, Zr and Mo metals into 8-I (base) alloy resulted in 12.5 % and 14.5 % improvement in yield strength of 8-II and 8-III alloys respectively. In addition to that, ultimate tensile strengths of modified alloys were also obtained slightly higher than that in base alloy. It is also established that, following V and Zr additions, the elongation of 8-II alloy was obtained 11.6 % lower than that in 8-I (base) alloy. On the other hand, 5.8 % improvement in the elongation of 8-III alloy was observed via additions of V, Zr and Mo. This proves that the addition of V, Zr and Mo metals has beneficial influence on the elongation of AlSi8Mg high pressure vacuum die castings.

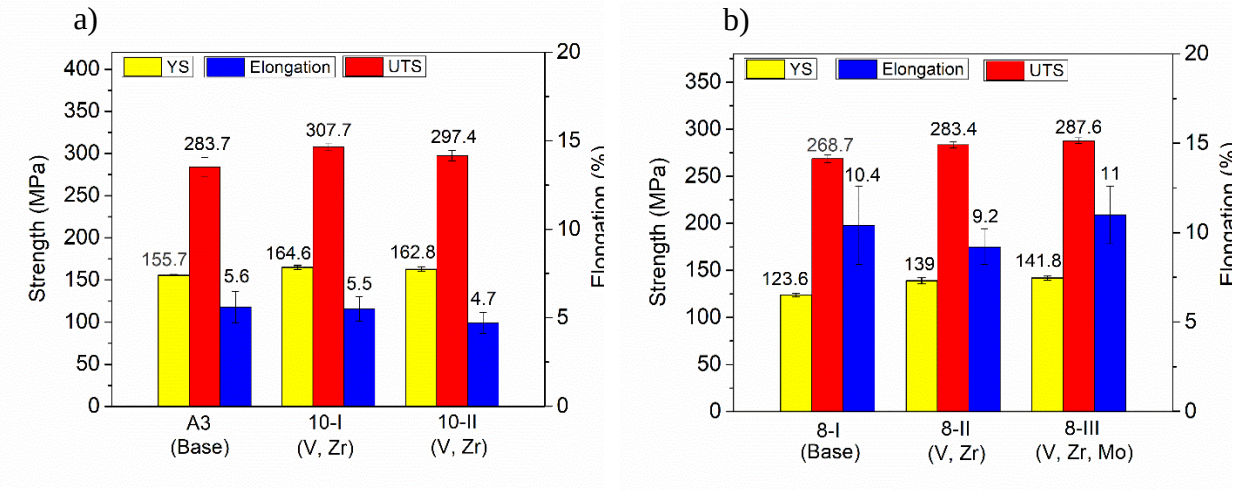

Figure 5-2**:** The tensile properties of 10 % (a) and 8 % (b) Si containing HPVD castings on as-cast condition.

5.2 Optimization of the Heat Treatment Parameters

Recently, considerable amount of studies was performed to meet alloy requirements and further increase in mechanical properties of high pressure die castings. In this regard, using a vacuum assistant system during casting process has brought new insight in high pressure die casting technologies. The presence of vacuum assistant allowed to perform T5 and T6 heat treatments, without the risk of blistering. Mainly, T5 temper used for the castings which are artificially aged at temperatures between 170°C and 210°C. Due to precipitation hardening, higher mechanical properties can be achieved by T5 heat treatment applications. Also, low heat treatment temperatures inhibit to formation of distortion and blistering which have harmful influence on the mechanical properties of alloys. On the other hand, in T6 temper, the alloys are subjected to solution heat treatment at high temperatures (500-540°C), then it is followed by an artificial aging treatment. Due to very high treatment temperatures, highest strength and good ductility can be achievable in T6 tempers.

As known well, due to its shorter process duration and lower capital investment requirements, T5 treatment is more cost effective than T6 temper. However, the downside of T5 temper is that hardness, yield strength and ultimate tensile strength of T5 heat treated castings are lower than those in T6 heat treated castings. Hence, optimization of heat treatment parameters is required to meet expected mechanical properties for new designed alloys. In order to do that, the response of the experimental alloys for various heat treatment applications should be carefully analyzed. In this study, an extensive heat treatment plan is designed and carried out for the high-pressure vacuum die casting alloys. The experimental alloys were exposed to T5 and T6 tempers and then, heat treatment parameters were determined according to hardness values of heat-treated alloys. As explained in experimental procedure (Chapter 3), T5 heat treatment temperatures were selected as 170°C and 210°C with various soaking times whereas T6 heat treatment temperatures were chosen as 500°C, 520°C and 540°C. For T6 tempers, solution heat treatment was carried out from 1 h to 24 hours. Then, it is followed by water quench and artificial aging at 170°C for 4 hours.

5.2.1 Hardness Evaluation of T5 Heat Treated Alloys

*Figure **5-3*** shows the hardness evaluation of the high-pressure vacuum die casting alloys in T5 conditions which performed at 170°C and 210°C for different soaking times. For T5 heat treated samples at 170°C, it was observed that as the time increase, a continuous increase in hardness of the alloys is seen until the soaking time reaches four hours. After four hours, the hardness values followed a plateau. On the other hand, hardness of the T5 heat treated alloys at 210°C reaches peak hardness values in one hour. After achieving peak values, the hardness decreases with further increase of ageing time. It is interesting to note that generally, T5 treated experimental alloys at 170°C reaches their peak hardness values between four to six hours while the peak values are observed in an hour for T5 treated alloys at 210°C. In addition, the peak

hardness values at 170°C is higher than those in 210°C. For example, the peak hardness of 8-II (V, Zr) alloy at 170°C reported as 106.9 HV while it was observed as 95.6 HV at 210°C. According to Kasprzak et al., [1] the peak hardness reduction with increasing ageing temperatures is a result of reduction in the supersaturation of the metal matrix. Due to supersaturation reduction, the precipitates continue to grow. This process results in dissolution of small precipitates and presence of larger ones. During precipitate growth, coherency strain increases until interfacial bond strength is exceeded and eventually this results a rapid hardness reduction as it is reported in *Figure **5-3***.

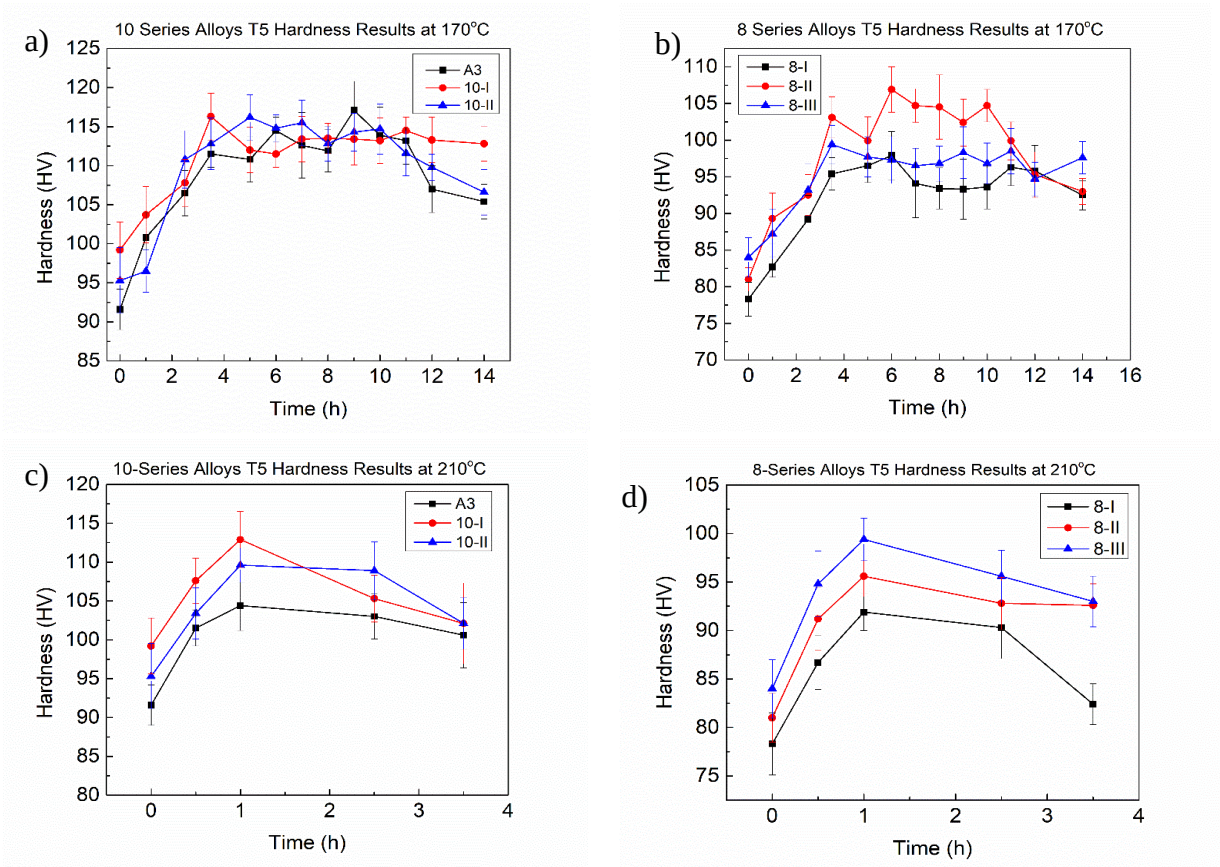

Figure 5-3: The hardness evaluation of the experimental alloys at 170°C (a,b) and 210°C (c,d) heat treated conditions

The general tendency of hardness evaluation of T5 heat treated HPVD castings is discussed above. However, it is also important to mention the T5 heat treatment response of each alloys. In Aural^{TM}-3 alloy, the peak hardness at 170°C was observed as 117.1 HV in 9 hours, whereas it was

obtained as 104.4 at 210°C in 1h. For both 10-I and 10-II alloys, the highest hardness value at 170°C was confirmed as 116.2 in 3.5h and 5h respectively. On the other hand, the peak hardness of T5 heat treated 10-I and 10-II alloys at 210°C were measured as 112.9 HV and 109.6 HV respectively and for both alloys, the soaking time for highest hardness achieved is 1h.

Among 8% Si containing alloys, 8-I (Base) and 8-II (V, Zr) reached their highest hardness values in 6 hours on condition of T5 heat treatment at 170°C and their hardness is obtained as 97.9 HV and 106.6 HV respectively. On the other hand, the peak hardness of T5 heat treated 8-III (V, Zr, Mo) at 170°C was obtained as 98.5 HV while soaking time reached 11 hours. For T5 heat treated alloys at 210°C, the peak hardness values are determined as 91.9 HV, 95.6 HV and 99.4 HV for 8-I, 8-II and 8-III respectively and the soaking time is 1 hour for all alloys.

5.2.2 Tensile Properties of T5 Heat Treated Alloys

As known well, tensile properties are one of the most important factors to define and understand the mechanical behavior of an alloy. Therefore, performing tensile tests and interpreting the results is crucial to evaluate and analyze the mechanical properties. Although a large amount of hardness measurements was carried out in this study, it is not realistic to perform tensile tests for each condition. For this reason, only one condition from each T5 heat treatment temperatures was selected (170°C and 210°C) and tensile tests were performed only for these two conditions (170°C x 4 h and 210°C x 1 h).

Figure 5-4 represents the tensile properties of 10 % Si (a, c) and 8 % Si (b, d) containing HPVD castings on T5 heat treated conditions.

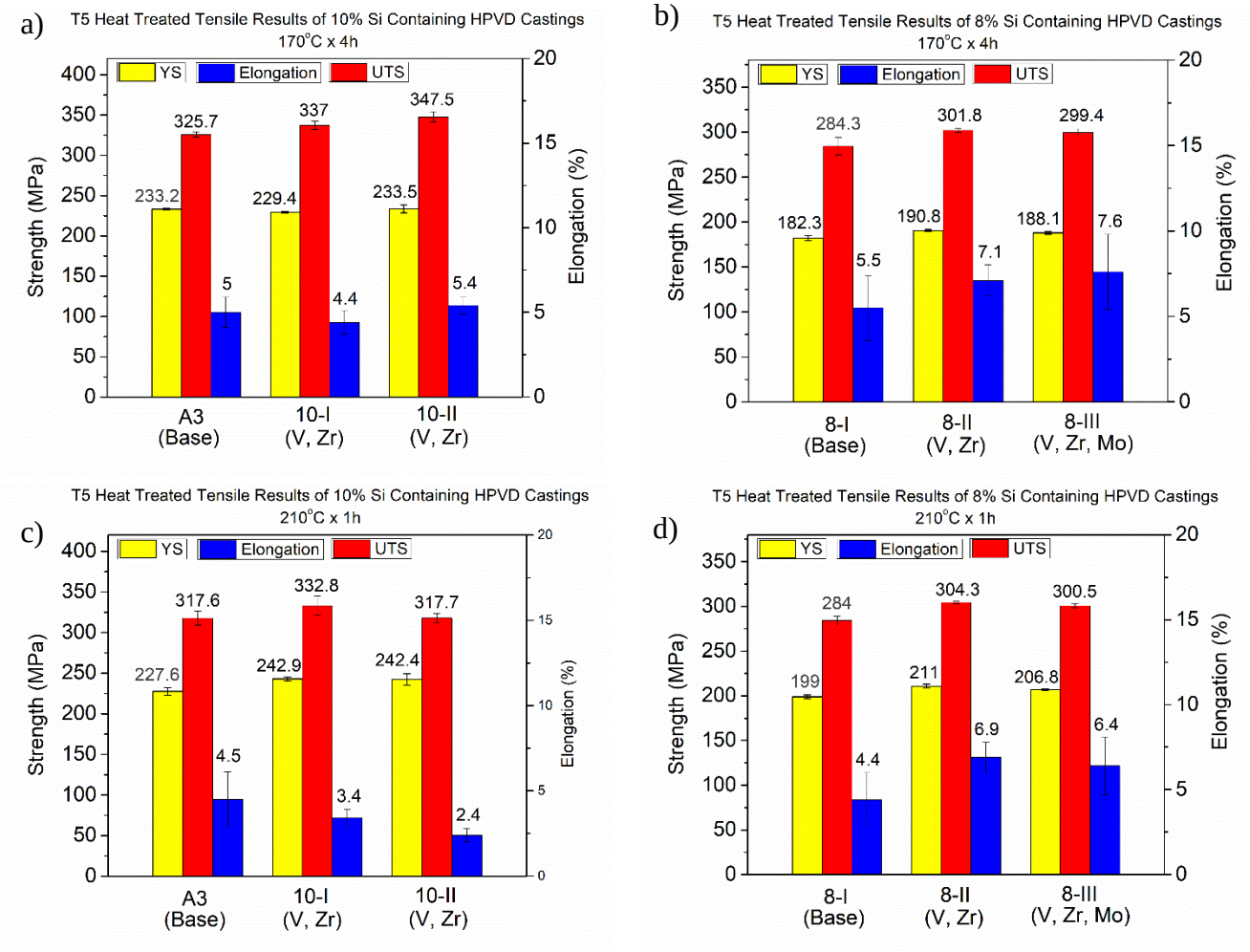

Figure 5-4: Tensile properties of HPVD castings on 170°C x 4h (a,c) and 210°C x 1h (b,d) conditions

As seen in Figure *5-4*a and Figure *5-4*b, no significant difference in yield strength of base and modified alloys was observed on T5 treated condition at 170°C x 4h. On the other hand, in comparison with the base alloys, a slight improvement in ultimate tensile strength of both 10 % and 8 % Si containing modified alloys was determined on 170°C x 4h condition. Although, a significant difference in elongation of base and modified alloys was not reported in 10% Si containing alloys, a remarkable difference was observed in 8% Si containing alloys. The results show that additions of V and Zr (8-II) and V, Zr and Mo metals (8-III) into the base alloy can provide respectively 30 % and 40 % higher elongation values on 170°C x 4h condition. This implies that on 170°C x 4h condition, elongation of AlSi8Mg alloy can be improved via additions

of V, Zr and Mo metals. The results also show that an increase in heat treatment temperature from 170℃ to 210 ℃ resulted in a slight increase in yield strength of the alloys. In addition to that no significant change was observed in ultimate tensile strength of the alloys which heat treated at 210 ℃ for 1 hour. On the other hand, elongation of the all experimental alloys significantly dropped with increasing heat treatment temperature. For instance, elongation of 10-II alloy was measured as 5.4 % on 170 ℃ x 4 hours condition whereas it is obtained as 2.4 % following the heat treatment at 210 ℃ for 1 hour.

5.2.3 Hardness Evaluation of T6 Heat Treated Alloys

It is well known that elevated heat treatment temperatures are required to obtain very small size precipitates which can significantly increase the hardness of the alloy. Thus, several T6 heat treatment process are applied to the high-pressure vacuum die casting alloys to find the optimum T6 heat treatment parameters. *Figure 5-5* represents the hardness evaluation of the alloys in T6 heat treated conditions. It is well established that, in 10% Si containing alloys, increasing solution heat treatment temperatures can provide higher hardness values for the experimental alloys. For instance, the maximum hardness achieved due to the T6 heat treatment at 540°C is 144.9 HV for 10-II (V, Zr) alloy while it is 130.7 HV at 520°C and 119.5 HV at 500°C for the same alloy. A similar tendency was also observed in 8% Si containing alloys. For 8-III (V, Zr, Mo) solution heat treated alloy, the highest hardness at 540°C was measured as 121.3 HV whereas it is observed as 112.7 at 520°C and 106.4 HV at 500°C. Such a significant difference might be explained by partial dissolution of intermetallic phases at higher temperatures, the promotion of higher amount V, Zr, Mo precipitates due to higher solution heat treatment temperatures and microstructural changes occurred during solution heat treatment which will be discussed in microstructure analysis of HPVDC alloys. Detailed analysis of the results revealed that the hardness values of 10% Si

containing alloys are significantly higher than those in 8% Si containing alloys in all T6 heat treatment conditions (500°C, 520°C and 540°C + WQ + 170°C x 4h), indicating that higher amount of Si content provides higher hardness values for the experimental alloys.

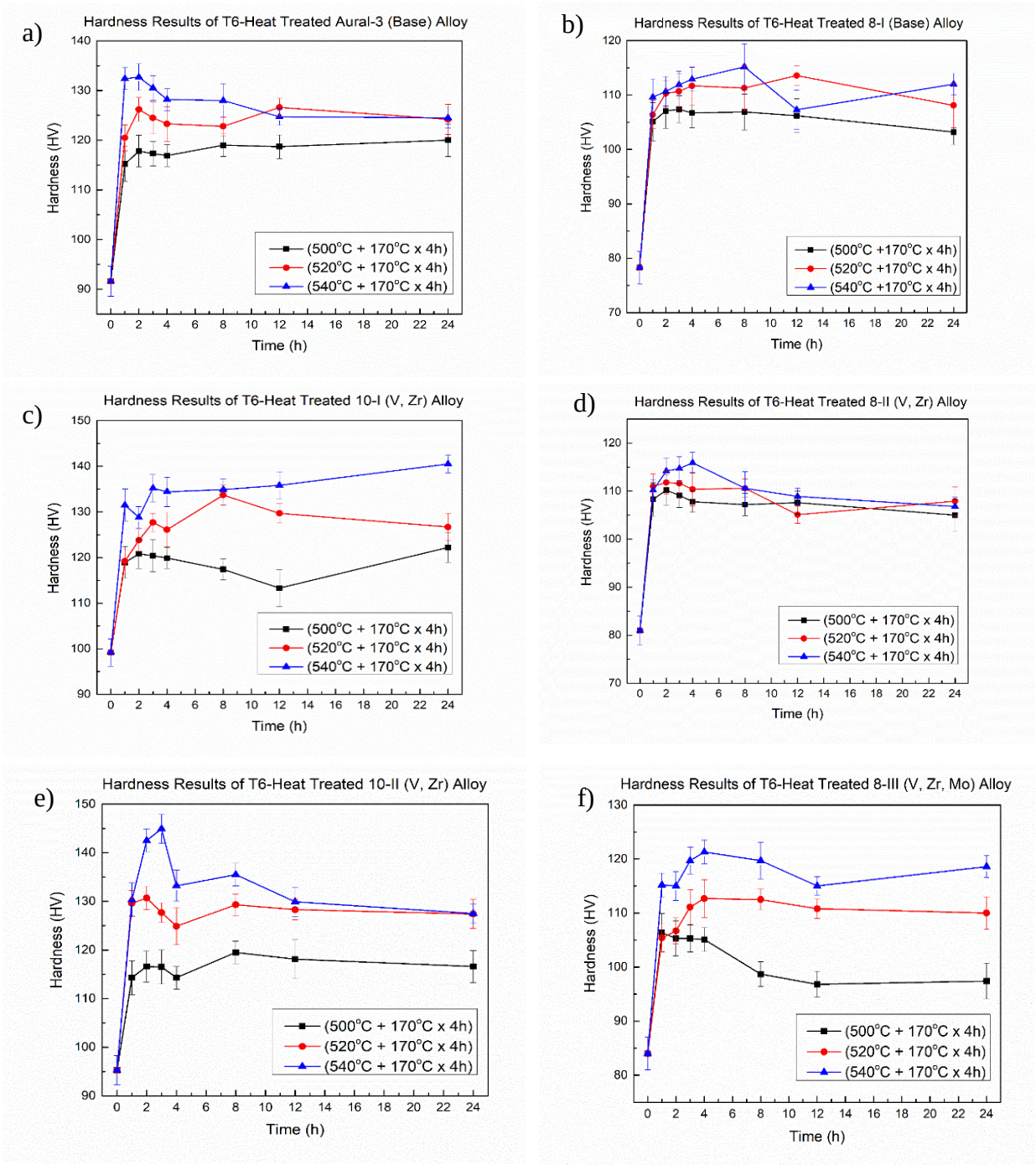

Figure 5-5*:* Hardness evaluation of 10 % Si (a, c, e) and 8 % Si (b, d, f) containing alloys on T6 heat treated conditions

Following the solution heat treatment at 500°C, no significant enhancement in hardness was observed in modified 10-I (V, Zr) and 10-II (V, Zr) alloys in comparison to Aural^{TM}-3 (Base). However, it is clearly seen that the further improvement in hardness for all alloys can be obtained with increasing heat treatment temperatures. For instance, in 10-I (V, Zr) alloy, the hardness was measured as 120.8 HV in condition of 500°C x 3h + WQ + 170°C x 4h while it is observed as 127.7 and 135.2 HV in conditions of 520°C x 3h + WQ + 170°C and 540°C x 3h + WQ + 170°C respectively. Therefore, it can be concluded that additions of V and Zr has beneficial effect on hardness of the alloys in T6 heat treated conditions, and further hardness improvement can be achieved via higher solution heat treatment temperatures. On the other hand, in 8% Si containing alloys, a significant difference between hardness values was not observed after the heat treatments at 500°C and 520°C. When the solution heat treatment temperature increases to 540°C, the difference between hardness of the base and modified alloys becomes more visible.

As it is described earlier, T6 temper is being evaluated as a high temperature solution treatment. Therefore, it is necessary to briefly discuss the aspect of casting porosity. In the industrial practice, porosity has a great impact on the casting suitability for the following heat treatment processing. The presence of porosity results in the formation of blisters due to expansion of gas trapped inside the pores during solution heat treatment. Generally, blistering occurs if the gas pressure inside the pore cavity is high enough to deform the thin metal layer surrounding the pore. In this regard, many studies suggest that the optimizing heat treatment parameters should not only focus on hardness evaluation but should also focus on the minimizing the blistering effect. Therefore, although the highest hardness values are achieved via solution heat treatment at 540°C x 3h + WQ + 170°C, the evaluation of tensile properties were studied only for following conditions; 500°C x 1h /3h + WQ + 170°C x 4 h and 520°C x 1h / 3h + WQ + 170°C x 4h).

Table 5-2: Electrical conductivity of HPVD castings at peak hardness values

Alloys (10% Si)	Electrical Conductivity (MS/m)	Std. Dev	Alloys (8% Si)	Electrical Conductivity (MS/m)	Std. Dev
Aural-3 (Base)	20.35	0.05	8-I (Base)	22.23	0.05
10-I (V, Zr)	18.80	0.06	8-II (V, Zr)	20.71	0.08
10-II (V, Zr)	18.71	0.03	8-III (V, Zr, Mo)	20.32	0.04

5.2.4 Tensile Properties of T6 Heat Treated Alloys

In order to evaluate the tensile properties of T6 heat treated alloys, two different heat treatment temperatures (500°C and 520°C) and holding times (1 hour and 3 hours) are selected. As it is mentioned earlier, no tensile tests were performed for T6 heat treated alloys at 540°C temperature due to possible blister presence.

Tensile properties of 10 % (a, c) and 8 % Si (b, d) containing HPVD castings on T6 heat treated condition at 500°C were given in Figure *5-6*. Generally, the results show that no significant change in yield and ultimate tensile strength were observed with increasing holding time in all experimental alloys. Due to lower content of Si, the elongation values of 8 % Si containing alloys are remarkably higher than those in 10% Si containing alloys on both 1 hour and 3 hours T6 heat treated conditions. However, it should be noted that increasing soaking time resulted a significant reduction in elongation of the 10 % Si containing alloys whereas no considerable drop was observed in 8 % Si containing alloys. For instance, elongation of 8-III alloy remained same with increasing soaking time while 23 % reduction was observed in 10-II alloy.

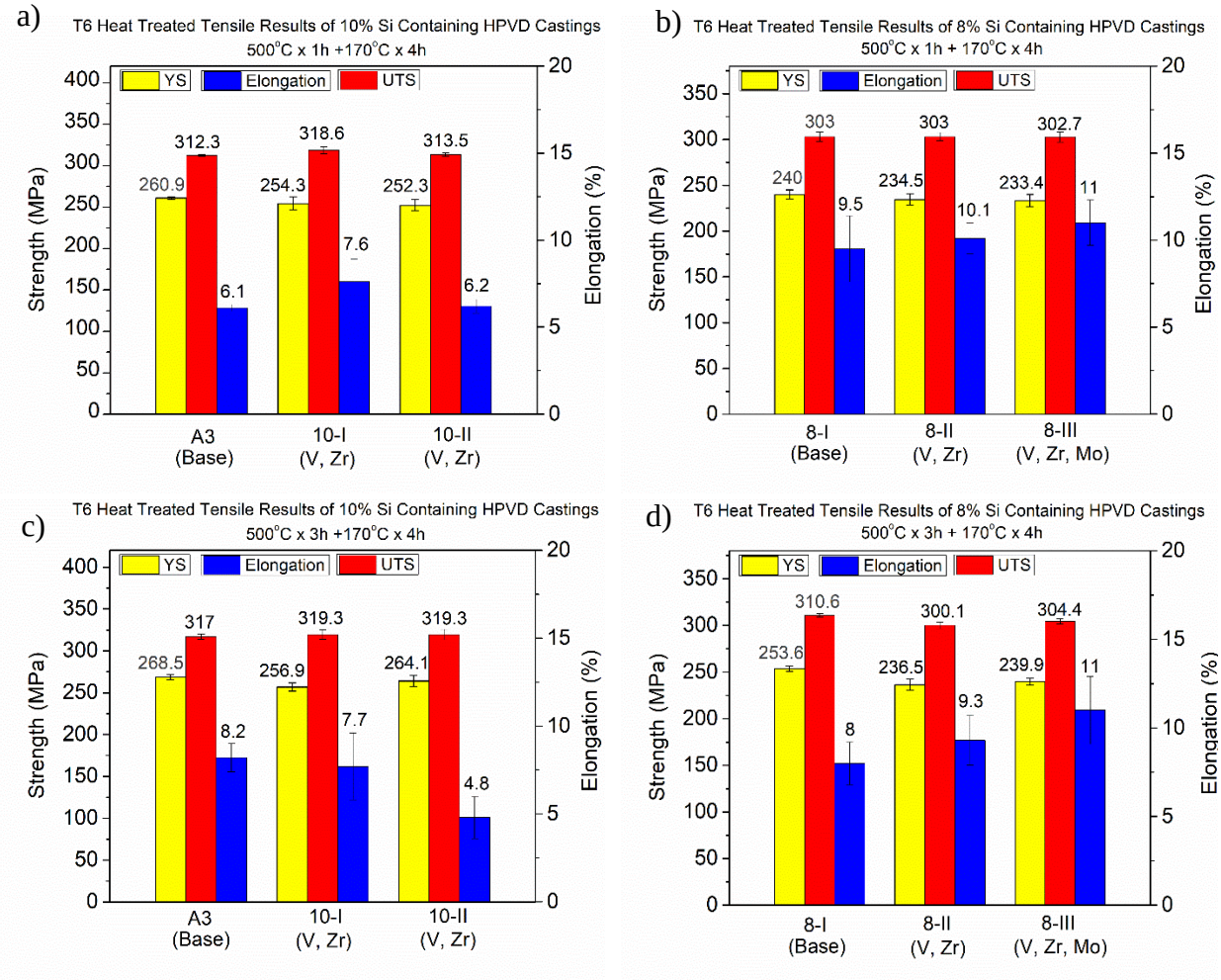

Figure 5-6: Tensile properties of HPVD castings on T6 heat treated condition at 500°C.

Figure *5-7* represents the tensile properties of T6 heat treated alloys at 520°C. The comparison of T6 heat treated tensile results at 500°C and 520°C reveal that yield strength and ultimate tensile strength of the experimental alloys can be improved by increasing heat treatment temperature (Figure *5-6* and Figure *5-7*). It is also established that increasing soaking time has no harmful impact on elongation values of the T6 heat treated alloys at 520°C, while longer soaking times can contribute a slight increase in the yield and ultimate tensile strength.

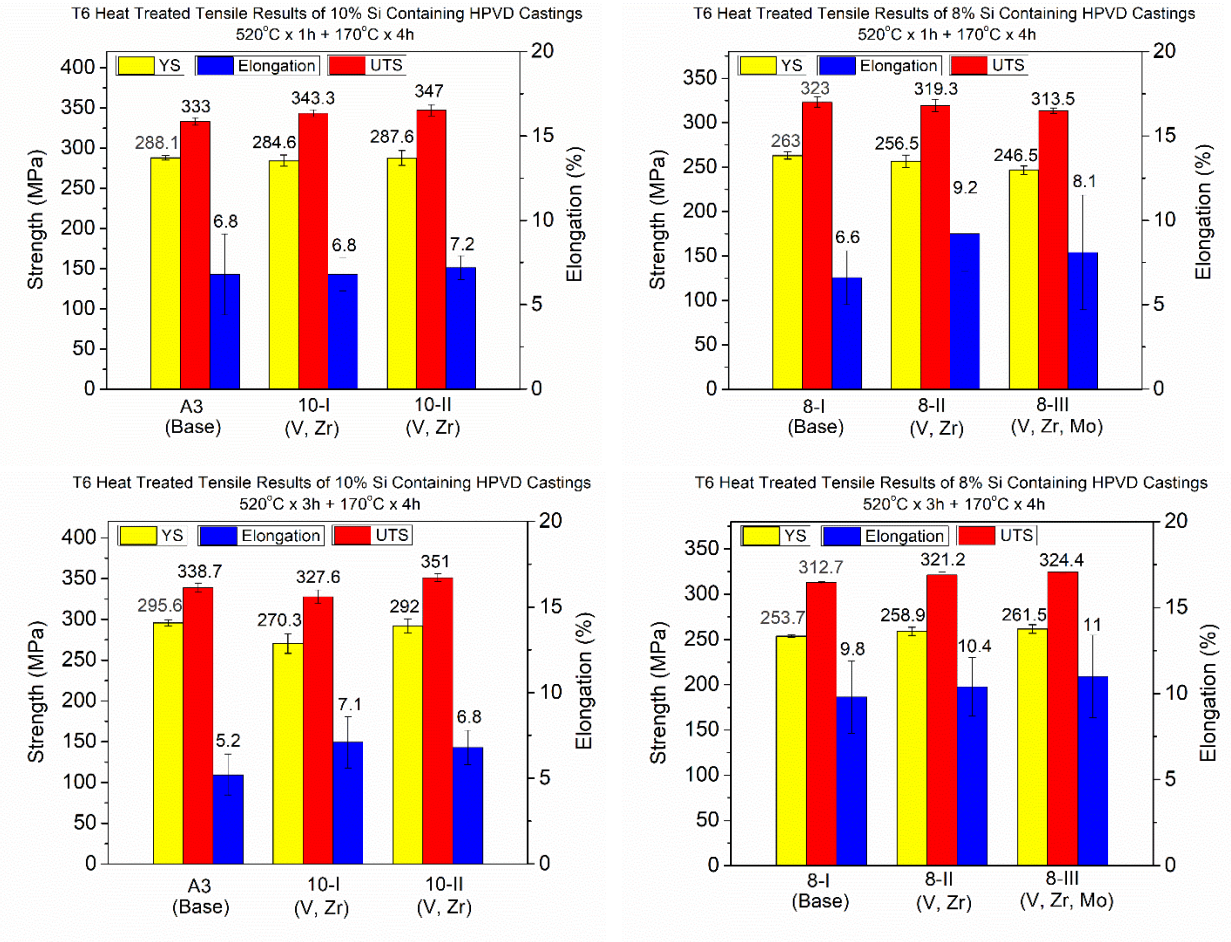

Figure 5-7**:** Tensile properties of HPVD castings on T6 heat treated condition at 520°C.

5.3 Microstructure Investigation of HPVDC Alloys

The detailed analysis on the mechanical properties of the experimental alloys suggest that the addition of trace elements such as V, Zr and Mo and also various heat treatment applications can contribute in improvement of hardness, yield strength, ultimate tensile strength and elongation of the alloys. In this chapter, an effort was made on to explain the microstructural features of the experimental alloys in both as-cast and T6 heat treated conditions as well as to find out possible reasons for the improvement in mechanical properties of the experimental alloys. Among 10% Si containing alloys, Aural^{TM}-3 (Base) and 10-II (V, Zr) were selected for microstructural analysis while 8-I (Base), 8-II (V, Zr) and 8-III (V, Zr, Mo) were chosen from 8% Si containing alloys.

A comprehensive microstructural analysis was performed for the heat-treated alloys however only optimum (520℃ x 3h + WQ + 170℃x 4h) heat treatment conditions for T6 temper will be discussed in the following sections.

5.3.1 Microstructure Analysis of 10%Si Containing Alloys on As-Cast Condition

Figure 5-8 shows the optical microscopic images of Aural^{TM}-3 and 10-II (V, Zr) alloys with X200 and X500 magnifications on as-cast condition. The microstructure investigations reveal that both Aural^{TM}-3 (Figure *5-8*a) and 10-II (Figure *5-8*b) alloys are consisted of rosette-like aluminum grains, eutectic Si particles, primary Mg_2Si phases and different types of intermetallic phases.

In order to analyze the chemical composition of intermetallic phases, backscattered SEM images were taken and EDS study was performed for the experimental alloys. In Aural^{TM}-3 alloy, the presence of Chinese script Mg_2Si and block like α-Al(Fe,Mn)Si intermetallic phases was confirmed. These Fe-rich compounds are referred to be $Al_{15}(FeMn)_3Si_2$ [2]. On the other hand, in 10-II alloy, flaky-like Zr-rich intermetallic compounds are observed and identified as $(AlSi)_3(ZrTi)$. In addition to that irregular shape Al-Si-Fe-V-Mn intemetallics and chinese script Mg_2Si were found in 10-II (V, Zr) alloy.

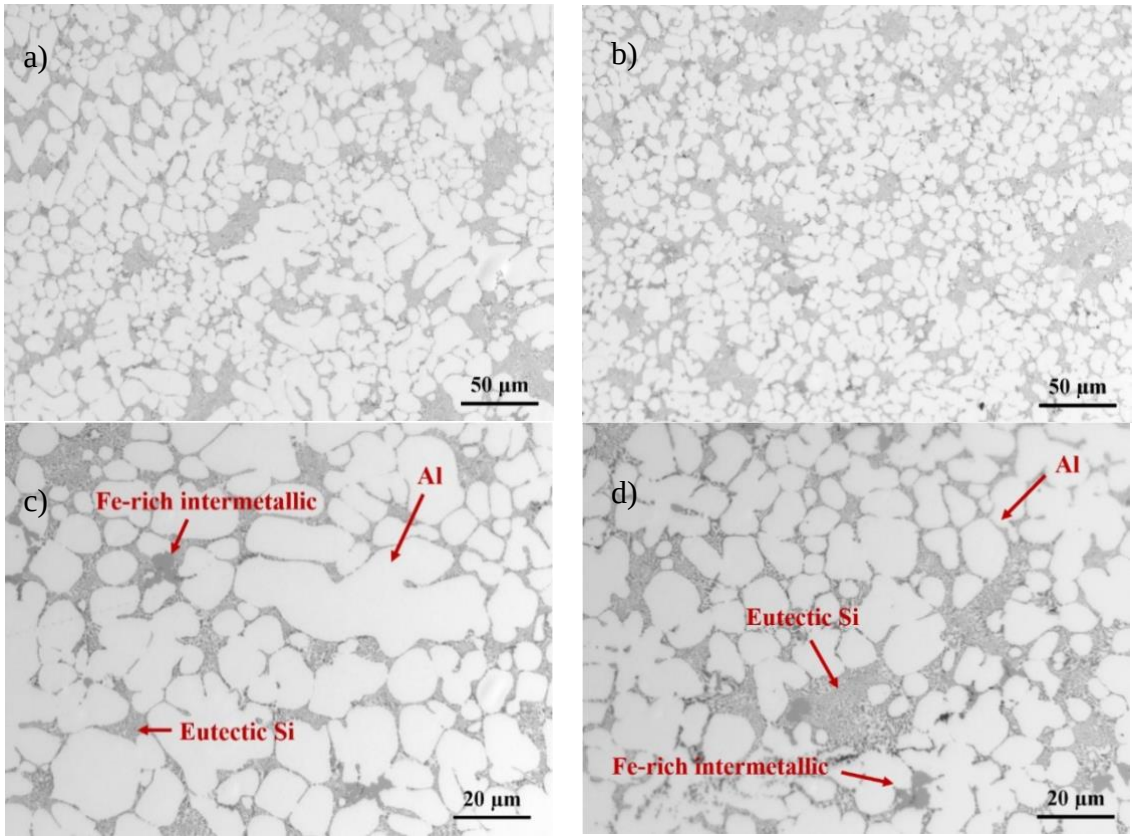

Figure 5-8: Optical microscopic images of Aural-3 (a,c) and 10-II (b,d) alloys at the center of samples on as-cast condition

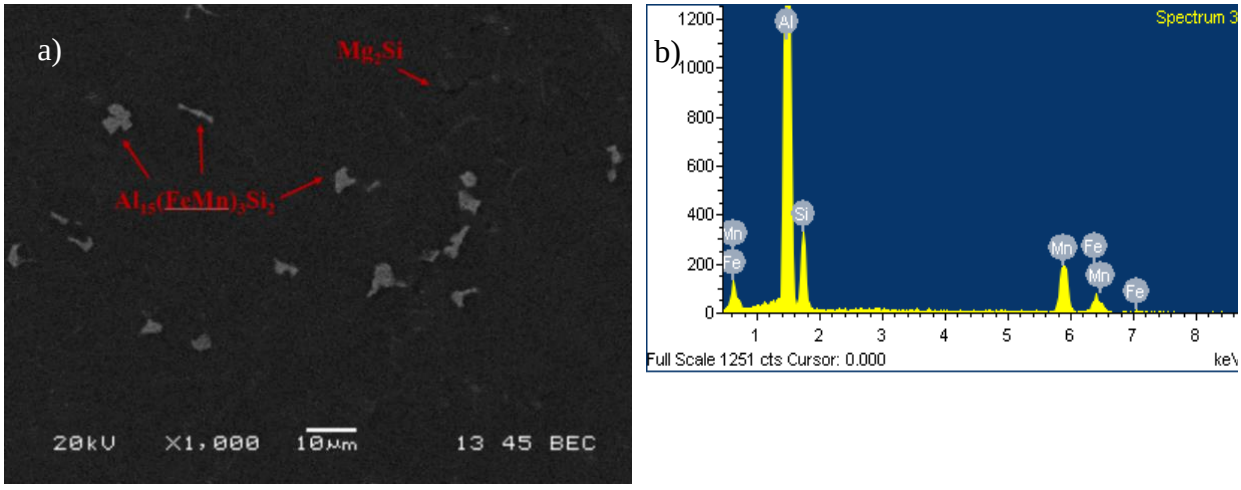

Figure 5-9: SEM backscattered image of Aural^{TM}-3 (a) and EDS spectrum of Fe-rich phase (b)

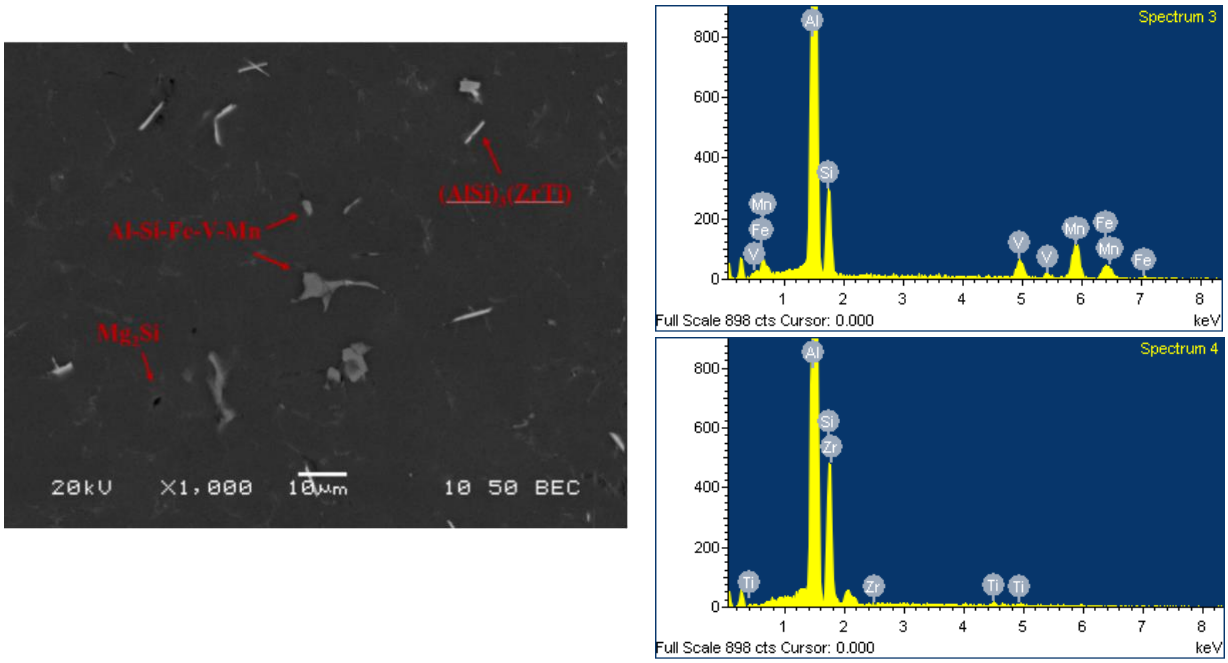

Figure 5-10**:** Backscattered SEM image of 10-II (a) and EDS spectrums (b,c)

It is established that following the addition V and Zr, considerable amount of these elements remains in α-Al solid solution (Table *5-1*) and their excess amounts tended to form the insoluble interdendritic V and Zr containing intermetallic phases (Figure *5-10*).

EBSD mapping was performed to measure the average grain diameters in base and modified alloys as well as to reveal the effect of V and Zr additions on grain size of the experimental alloys. *Figure 5-11* shows the EBSD mappings of the experimental alloys and the numerical data related to EBSD mappings are listed in Table *5-3*. The average grain diameter in Aural^{TM}-3 was reported as □ 87.7 µm (± 33.4) while it was found □ 43.1 µm (± 17.2) in 10-II (V, Zr) alloy, stating 51% reduction in the average grain diameter. This result reveals that additions of V and Zr resulted in a significant reduction in average grain diameter in 10-II alloy.

Table 5-3: The average grain diameter of 10% Si containing alloys

Alloy	Average Grain Diameter (µm)	Standard Deviation
Aural™-3	87.7	33.4
10-II (V, Zr)	43.1	17.0

Figure 5-11: EBSD mappings of Aural™-3 (a) and 10-II (b) alloys on as-cast condition

5.3.2 Microstructure Analysis of 10% Si Containing Alloys on T6 Heat-Treated Condition

Figure *5-12* represents the typical solution heat treated (520°C for 3 hours plus 170°C for 4 hours) microstructures of Aural™-3 (Base) and 10-II (V, Zr) alloys. Qualitative comparison of as-cast and T6 heat-treated microstructures reveals how applying heat treatment changed the size and morphology of eutectic Si particles. As seen in Figure *5-12*, the eutectic Si particles broke down into smaller fragments and became spheroidized in both Aural™-3 and 10-II alloys. In addition to Si particles, it is established that no Mg-rich interdendritic particles were observed in the microstructures, indicating that the solution heat treatment lead to dissolution of Mg_2Si particles into α-Al matrix.

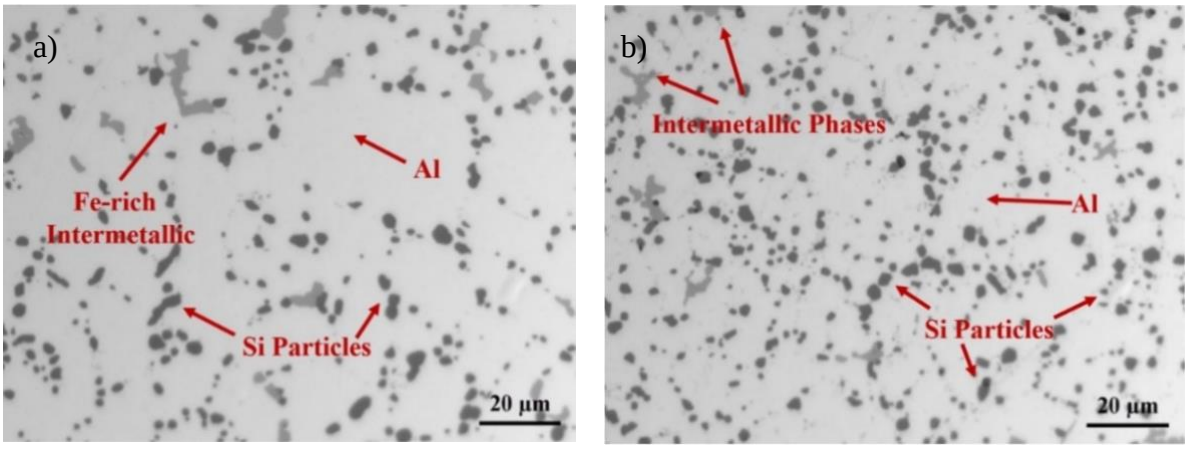

Figure 5-12: Optical microscopic images of Aural^{TM}-3 (a) and 10-II (b) alloys in T6 solution heat treated condition at X500 magnification

Figure *5-13* illustrates the backscattered SEM images of solution heat treated Aural^{TM}-3 and 10-II alloys. According to SEM-EDS results, the presence of block-like Fe-rich intermetallic phase was confirmed in Aural^{TM}-3 alloy whereas dot-like Zr-rich intermetallic phase and block-like Al-Si-Fe-Mn-V containing intermetallic phase were obtained in 10-II (V, Zr) alloy. As distinct from as-cast microstructures, the existence of Mg_2Si phases was not reported in both Aural^{TM}-3 and 10-II alloy which is attributed to the complete dissolution of Mg_2Si phases. The main phases, phase morphologies and their response during T6 heat treatment are given in *Table 5-4* and Table *5-5* for Aural^{TM}-3 and 10-II alloys respectively.

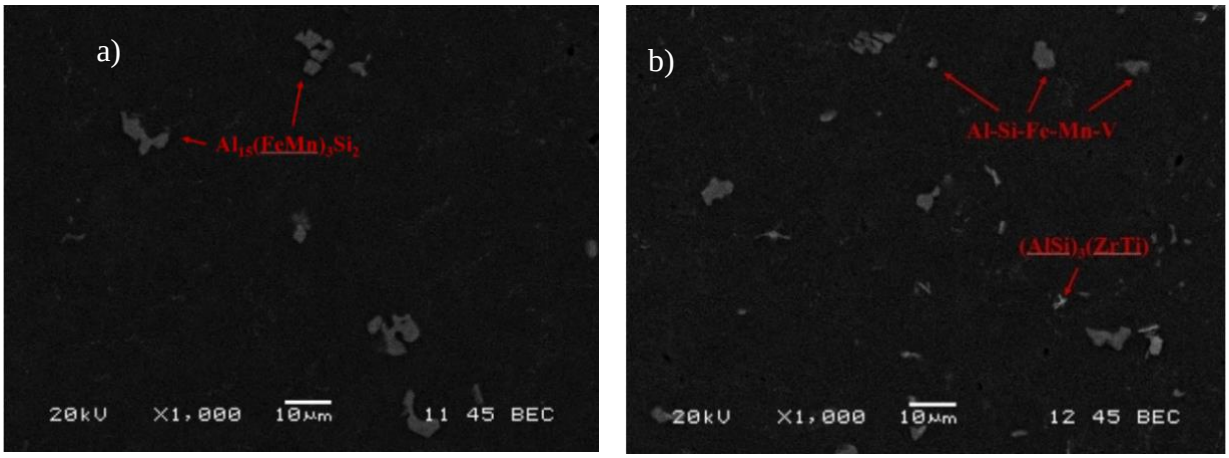

Figure 5-13: Backscattered SEM images of AuralTM-3 (a) and 10-II (b) inT6 heat treated condition

Table 5-4: The main phases and their morphology identified using SEM/EDS in AuralTM-3 alloy.

Calculated phase from SEM/ EDS	Response during T6 heat treatment	Phase morphology
α-aluminum	No change	Dendritic
Eutectic silicon	Thermally modified	Spheroidized
Mg_2Si	Dissolved	-
Al-Si-Fe-Mn	Partially dissolved	Block-like

Table 5-5: The main phases and their morphology identified using SEM/EDS in 10-II(V, Zr) alloy.

Calculated phase from SEM/ EDS	Response during T6 heat treatment	Phase morphology
α-aluminum	No change	Dendritic
Eutectic silicon	Thermally modified	Spheroidized
Mg_2Si	Dissolved	-
Al-Si-Fe-Mn-V	Partially dissolved	Block-like
Al-Si-Ti-Zr	Partially dissolved	Dot-like

In order to have a better understanding on the microstructural changes occurred after addition elements and T6 solution heat treatment, intermetallic phases in the microstructures were quantitatively analyzed. *Figure 5-14* represents the aspect ratio (a), equivalent diameter (b) and volume fraction (c) of the intermetallic phases in Aural^{TM}-3 and 10-II alloys in both as-cast and T6 heat treated conditions. It is found that the aspect ratio and equivalent diameter of intermetallic phases in 10-II alloy are smaller than those in Aural^{TM}-3 in both as cast and T6 heat treated conditions. Also, further reduction in the equivalent diameter and aspect ratio can be obtained due to solution heat treatment. This proves the beneficial influence of V and Zr additions and T6 solution heat treatment on the size of intermetallic phases.

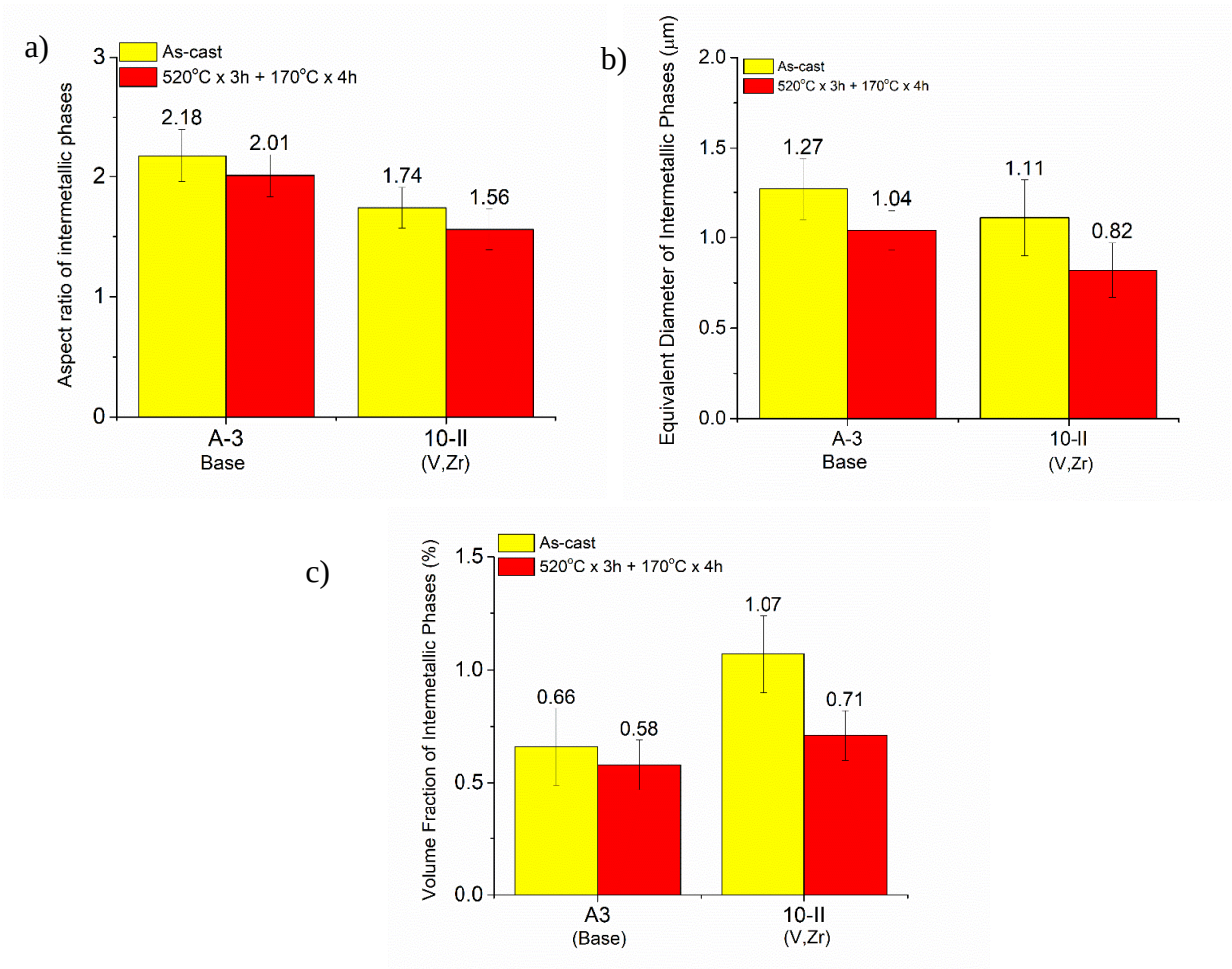

Figure 5-14: Aspect ratio (a) equivalent diameter (b) and volume fraction (c) of intermetallic phases in Aural-3 and 10-II alloys in as-cast and T6 treated conditions

As can be seen in Figure *5-14* (c), the volume fraction of the intermetallic phases was remarkable increased from %0.66 in Aural^{TM}-3 alloy to %1.07 in 10-II (V, Zr) alloy which is attributed to formation of new distinct intermetallic phases due to the additions of V and Zr. On the other hand, following the solution heat treatment, the volume fraction of intermetallic phases in the two alloys becomes less than that on as-cast condition, most likely due to the fragmentation and partial dissolution of intermetallic phases. It is also worthy to note that after solution heat treatment, the reduction in volume fraction of intermetallic phases in the Aural^{TM}-3 alloy is limited in comparison to V and Zr containing alloy (10-II). This implies that the Zr and V addition is

beneficial to the partial dissolution of intermetallic phases during heat treatment, resulting in more solute elements in the aluminum matrix (*Table 5-6*).

Table 5-6: Electrical conductivity of Aural^{TM}-3 and 10-II (V, Zr) alloys on T6 treated condition at 520°C x 3h + 170°C x 4h

Alloy	**Electrical Conductivity (MS/m)**	**Std. Dev.**
Aural^{TM}-3	19.56	0.04
10-II (V, Zr)	18.01	0.02

Solution treatment, which is the first stage of T6 heat treatment, is generally applied to dissolve interdendritic Mg-rich particles into the α-Al matrix, and also spheroidize the eutectic silicon particles. However, it is known that the solutionizing stage can also promote the precipitation of a large volume of Zr / V-rich dispersoids inside α-Al matrix. *Figure 5-15* represents the distribution of dispersoid zone and dispersoid free zone (DFZ) in both Aural^{TM}-3 and 10-II alloys. It is established that following the heat treatment at 520°C for 3h, considerable number of dispersoids precipitated within aluminum grains while the dispersoid free zone formed in interdendritic regions.

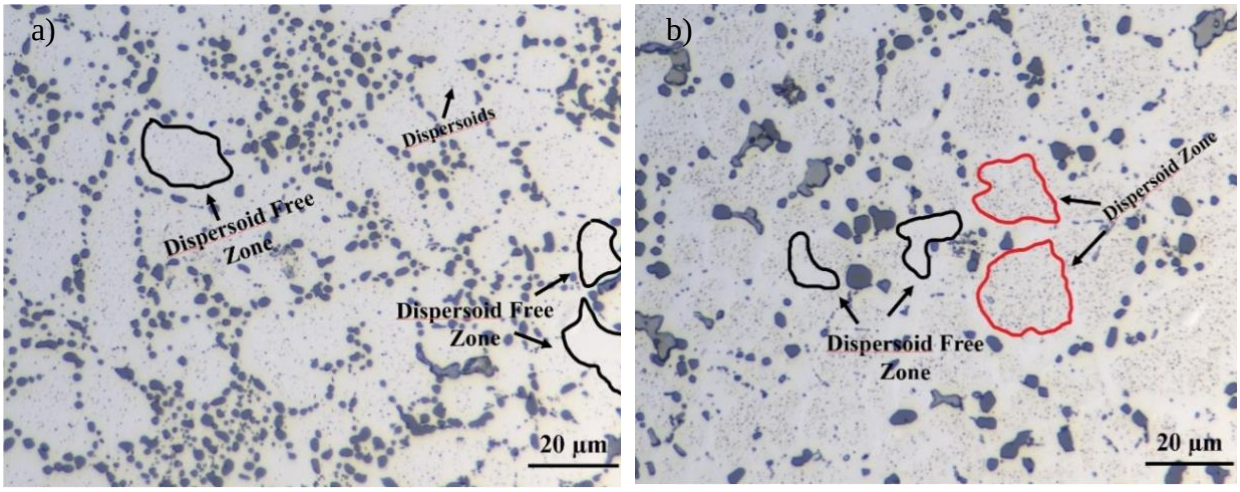

Figure 5-15**:** Distribution of dispersoid zone and dispersoid free zone in Aural^{TM}-3 and 10-II alloys

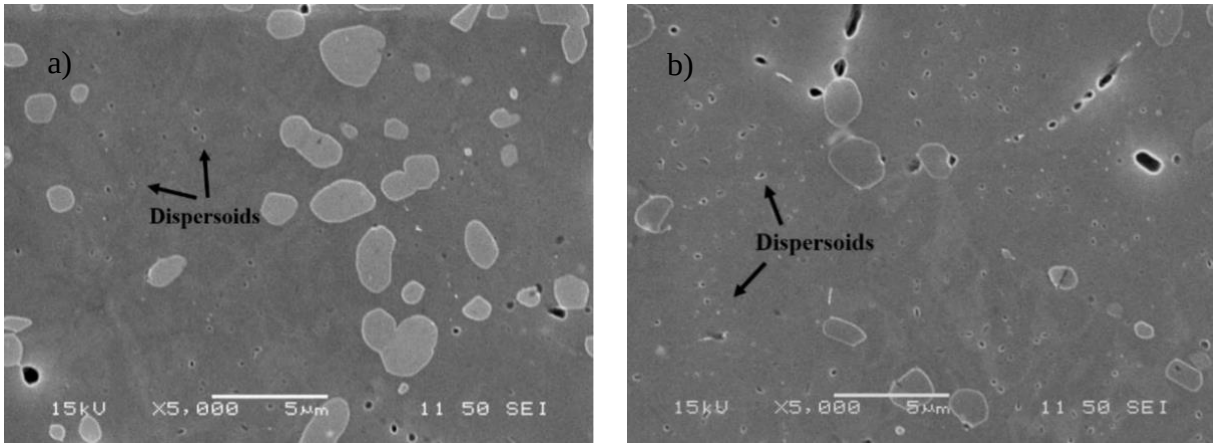

Figure 5-16: Secondary electron images of etched Aural^{TM}-3 (a) and 10-II (b) alloys after solution heat treatment

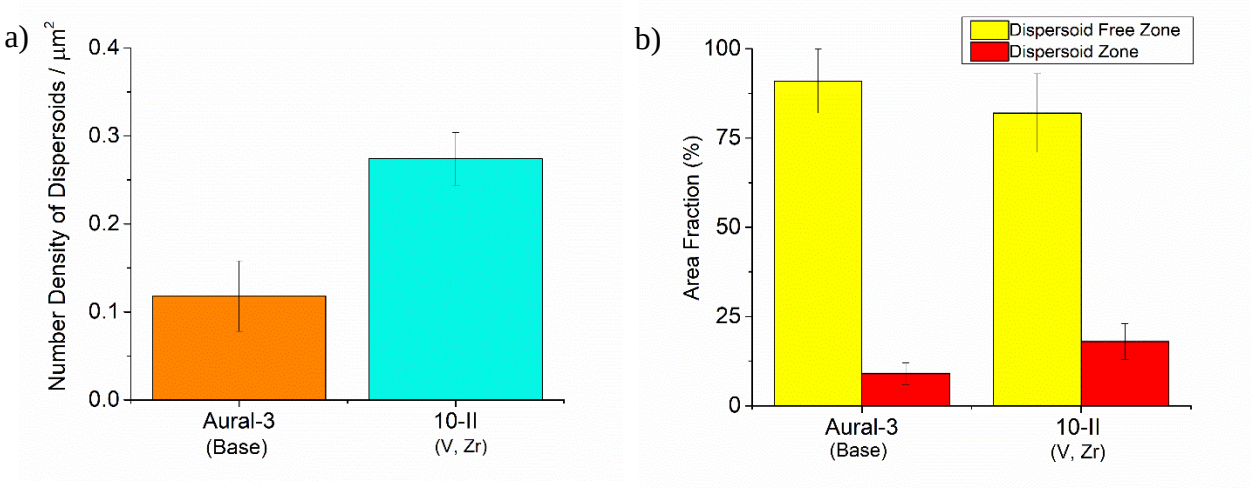

Figure 5-17: Number density of dispersoids (a) and area fraction of DFZ (b) in 10% Si containing alloys

The quantitative analysis of dispersoids (number density of dispersoids and area fraction of dispersoid zone) were carried out to reveal the effect of addition elements on dispersoid formation. As can be seen clearly in Figure *5-17*a, number density of dispersoids significantly increases due to additions of V and Zr metals. Moreover, area fraction of dispersoid free zones decreases while a considerable increase is observed in are fraction of dispersoid zone in 10-II (Figure *5-17*b) alloy. Thus, it can be concluded that the presence of several types of transition metals such as Zr and V in the 10-II alloy yielded the formation of considerable amount of

dispersoids during solution heat treatment stage which can further improve the mechanical properties of the alloy.

5.3.3 Microstructure Analysis of 8%Si Containing Alloys on As-Cast Condition

Figure 5-18 shows the optical microscopic images of 8-I (Base), 8-II (V, Zr) and 8-III (V, Zr, Mo) alloys in as-cast condition. Generally, the as-cast microstructures of base and modified alloys consisted of rosette-like aluminum grains, eutectic silicon particles, primary Mg_2Si and several distinct intermetallic phases.

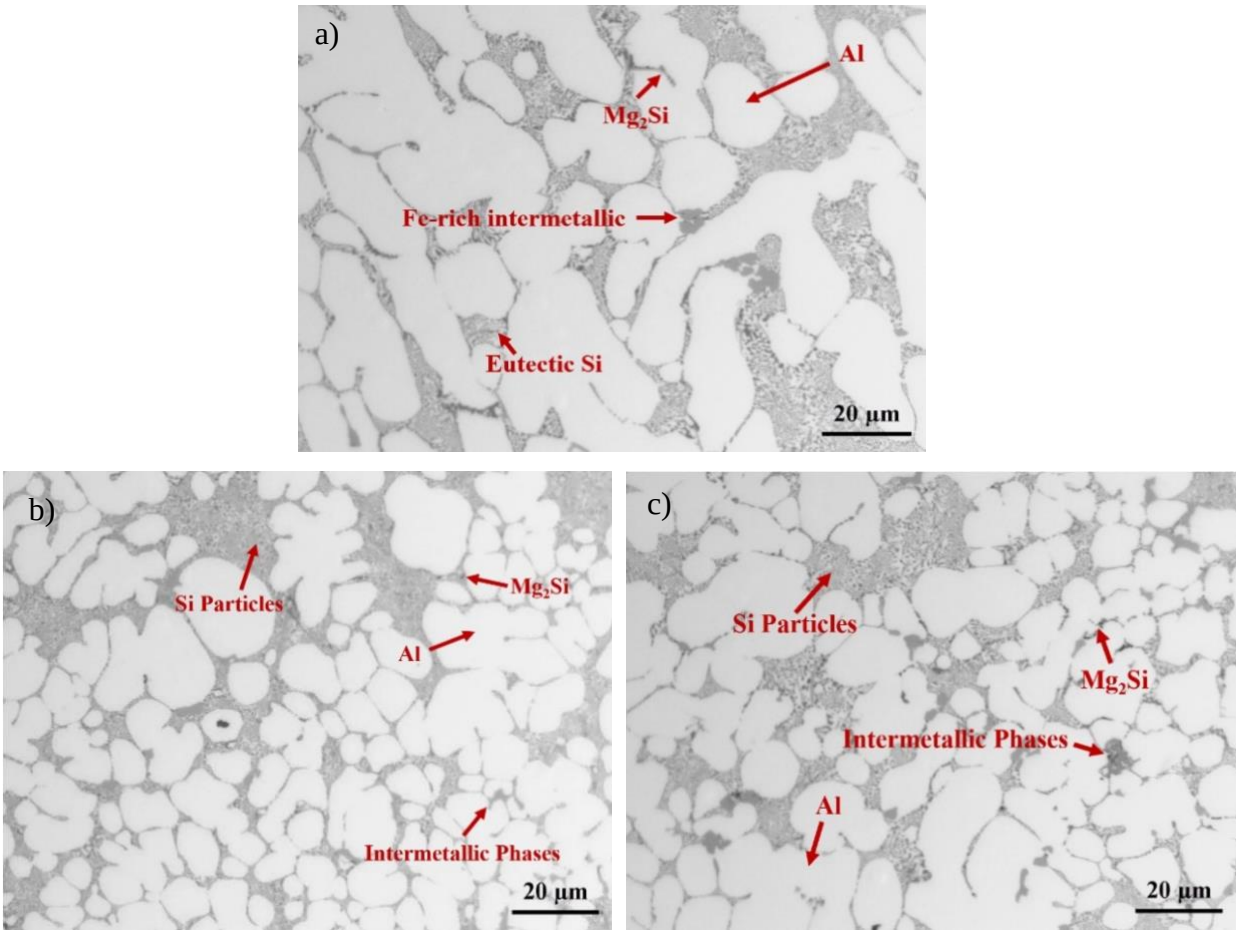

Figure 5-18: Optical microscopic images of 8-I, 8-II (V, Zr) and 8-III (V, Zr, Mo) alloys in as-cast condition

In order to identify the intermetallic phases in the microstructures, SEM-EDS analysis was carried out for each experimental alloy. *Figure 5-19*, *Figure 5-20* and *Figure 5-21* show the intermetallic

phases and their EDS spectrums in the microstructures of 8-I, 8-II and 8-III respectively. As can be seen in Figure-19, the microstructure of 8-I (Base) alloy contains block-like Fe-rich phase which referred as $Al_{15}(FeMn)_3Si_2$ and primary Mg_2Si particles.

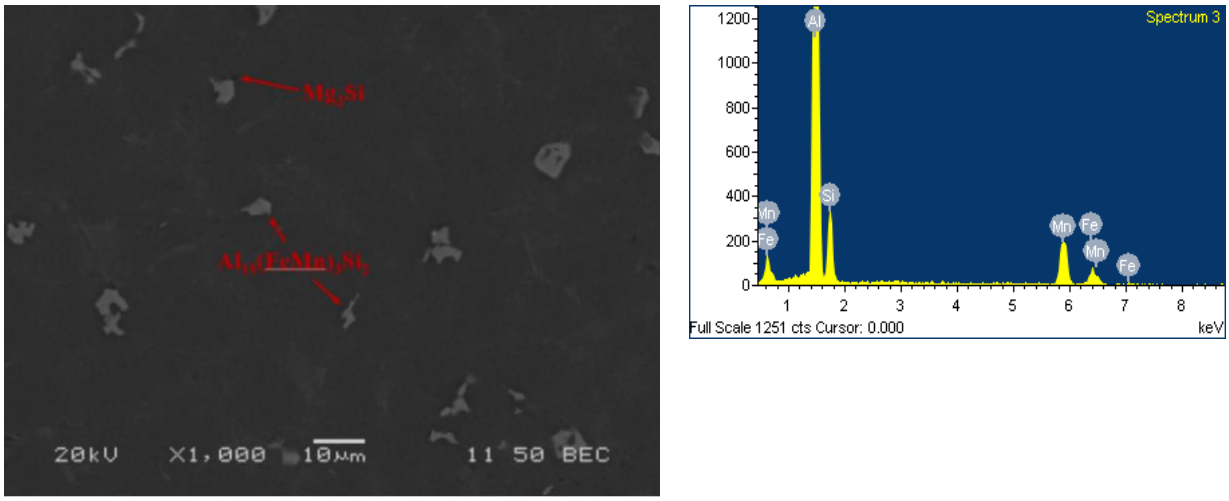

Figure 5-19: Backscattered SEM image (a) of 8-I alloy and EDS spectrum of Fe-rich phase (b)

In 8-II (V, Zr) alloy, two distinct intermetallic phases with different morphologies were found (Figure 20). The corresponding spectrums of these intermetallic phases are shown in Figure 20a and 20b. The dot-like compounds are composed of Al-Si-Ti-Zr and identified as Zr-rich intermetallics. Addition to this, another important phenomenon was identified in the modified alloy microstructure. After addition of V and Zr to 8-I (Base) alloy, Fe-rich (Al-Si-Mn-Fe) phase disappeared from the microstructure. Instead, another type of block-like intermetallic phase was found which is composed of Al-Si-V-Mn-Fe.

On the other hand, presence of two different intermetallic phases was confirmed in 8-III (V, Zr, Mo) alloy. In addition to primary Mg_2Si phase, Zr in generated of its own intermetallic phases with dot-like morphology, referred as $(AlSi)_3(ZrTi)$, whereas the presence of irregular shape Al-Si-Fe-V-Mn-Mo phases was confirmed in the experimental alloy.

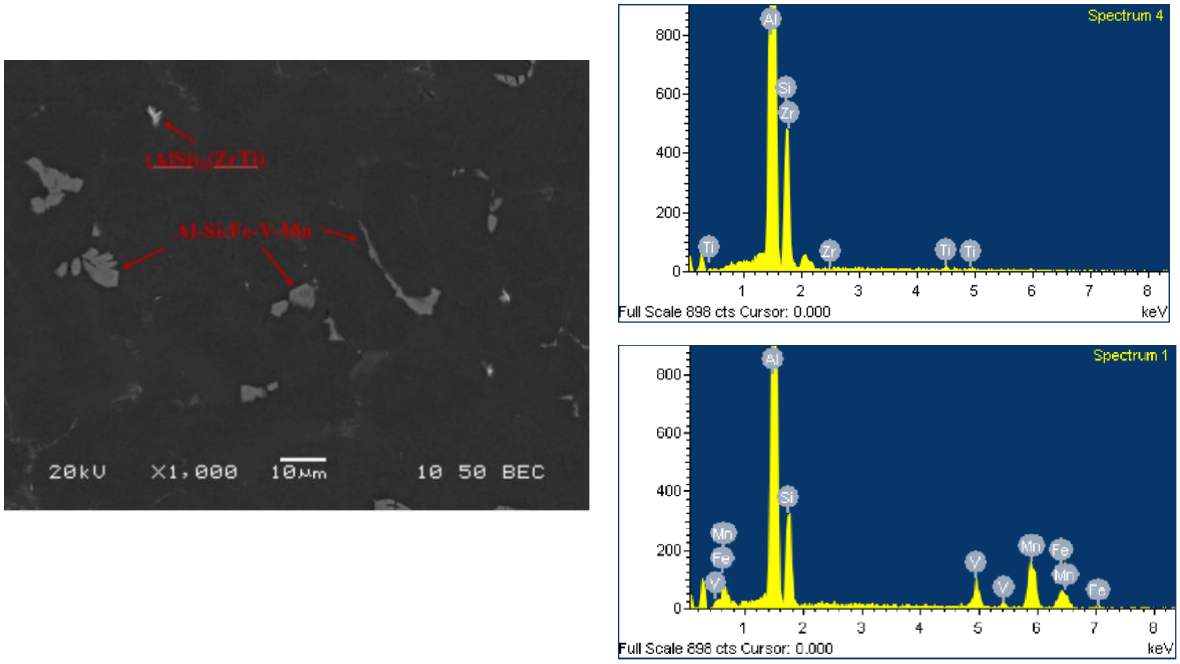

Figure 5-20: Backscattered SEM image of 8-II (V, Zr) alloy and EDS spectrum of intermetallics

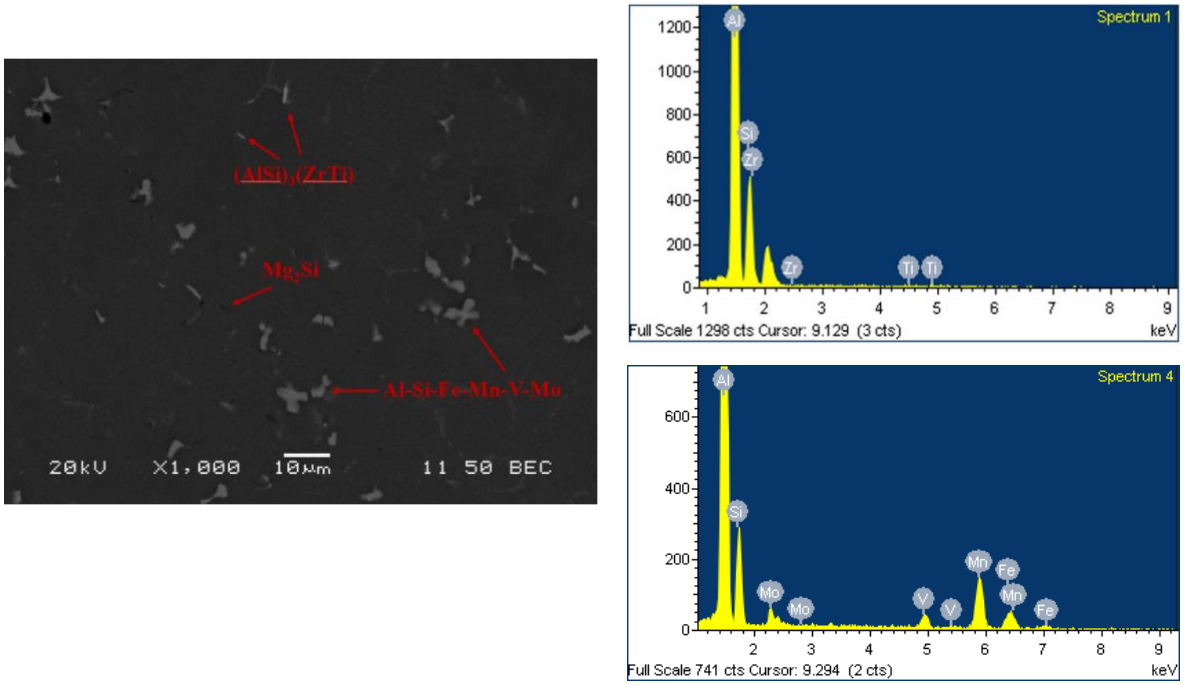

Figure 5-21**:** Backscattered SEM image of 8-III alloy and EDS spectrum of intermetallics

Figure 5-22 represents the EBSD mapping of 8% Si containing alloys in as-cast condition. As similar tendency was also observed in 10% Si containing alloys, average grain diameter of the V and Zr containing alloy (8-II) was smaller than those in Base alloy (8-I), revealing the beneficial

effect of V and Zr additions on grain size. On the other hand, although the average grain diameter in V, Zr and Mo containing alloy (8-III) was found smaller in comparison with base alloy (8-I), no significant difference between 8-II (V, Zr) and 8-III (V, Zr, Mo) alloys were observed, indicating that the Mo addition does not have a significant impact on modification of grain size (Table *5-7*).

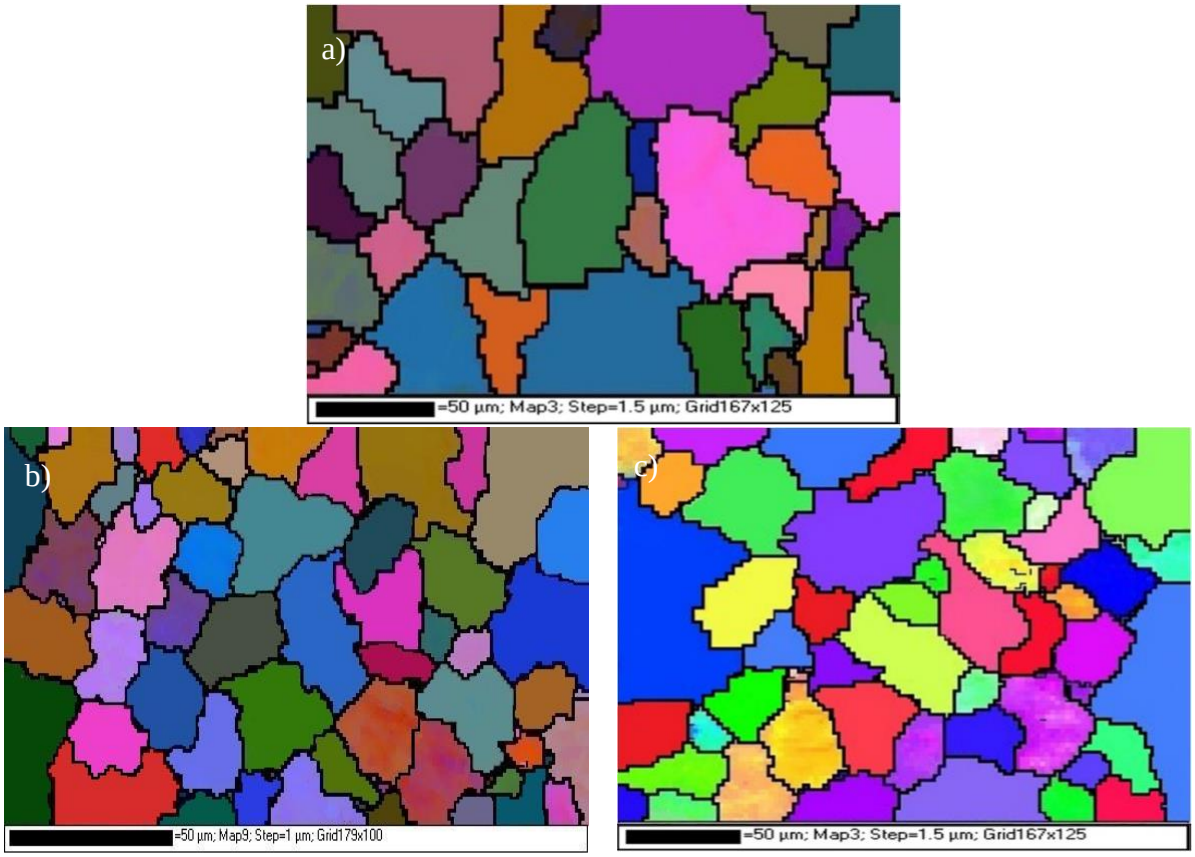

Figure 5-22: EBSD mapping of 8-I (a), 8-II (b) and 8-III (c) alloys at the center on as-cast condition

Table 5-7: The average grain diameter of 8% Si containing HPVD castings

Alloy	Average Grain Diameter (µm)	Standard Deviation
8-I (Base)	83.8	29.7
8-II (V, Zr)	58.5	25.1
8-III (V, Zr, Mo)	64.2	25.3

5.3.4 Microstructure Analysis of 8% Si Containing Alloys on T6 Heat-Treated Condition

Figure *5-23* illustrates the typical solution heat treated (520°C for 3 hours plus 170°C for 4 hours) microstructures of 8-I (Base), 8-II (V, Zr) and 8-III (V, Zr, Mo) alloys. As can be seen clearly, the Si particles thermally modified and became spheroidized in all experimental alloys. The Fe-rich intermetallic phase was still present in the 8-I (Base) alloy whereas α-Al(MnVFe)Si and $(AlSi)_3(ZrTi)$ intermetallics were observed in 8-II (V, Zr) and the presence of two distinct intermetallic phases were confirmed in T6 treated 8-III (V, Zr, Mo) alloy; $(AlSi)_3(ZrTi)$ and Al-Si-Fe-Mn-V-Mo containing intermetallic phases (Figure *5-23*). Due to high thermal stability of those intermetallic phases, the solution treatment at 520 ºC may not lead the complete dissolution of such phases. However, the size of those intermetallic particles after T6 becomes smaller in all three alloys compared to the as-cast condition. In a general view, the T6 treatment can change the Si morphology and reduce the size of intermetallic particles in the experimental alloys.

The backscattered secondary electron microscopic images of the experimental alloys are given in *Figure 5-24*. SEM-EDS studies reveal that there is no Mg_2Si phase present on the T6 heat treated microstructures, indicating the complete dissolution of Mg_2Si phase.

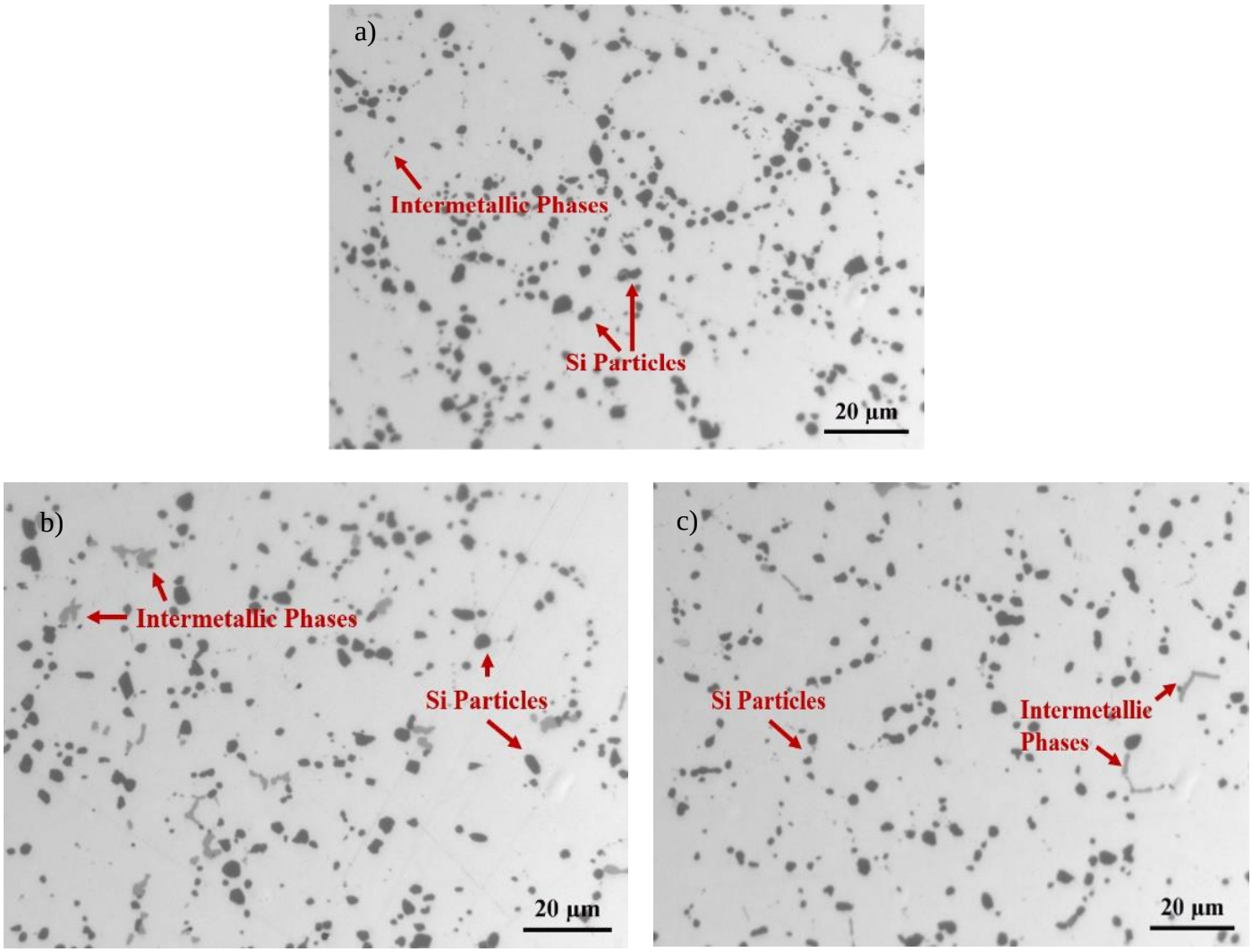

Figure 5-23**:** Optical microscopic images of 8-I (a), 8-II (b) and 8-III (c) alloys at the center of the sample on T6 condition at 520°C x 3h + 170°C x 4h

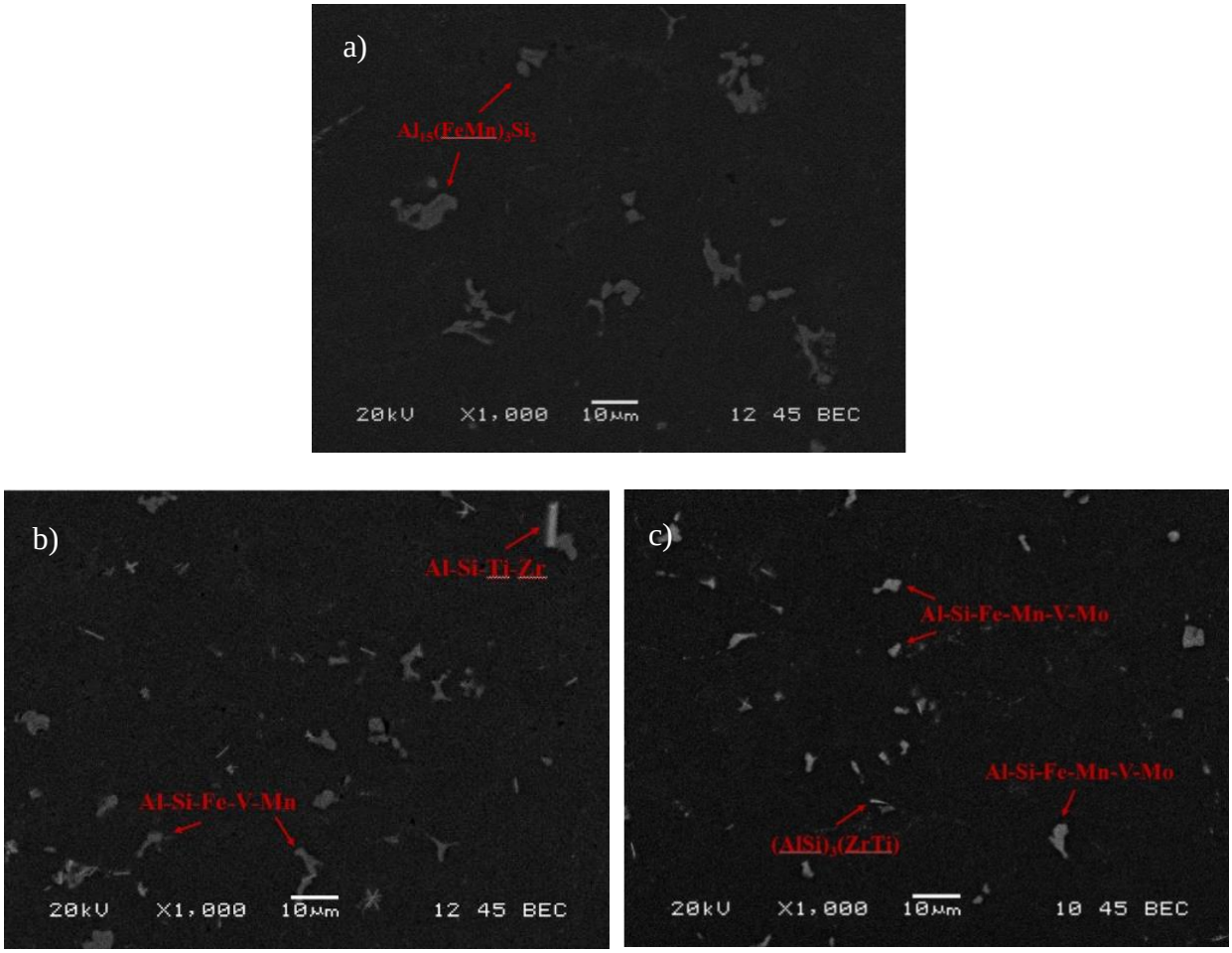

Figure 5-24: Backscattered SEM images of 8-I (a), 8-II (b) and 8-III(c) in T6 heat treated condition.

Quantitative image analysis of intermetallic phases was performed to reveal the effect of Zr, V (in 8-II) and Zr, V and Mo (in 8-III) additions on the phase morphology and size on as-cast and T6 conditions. Figure *5-25* shows the evaluation of the aspect ratio, volume fraction and equivalent diameter of intermetallic particles in all experimental alloys. It is clearly seen that the aspect ratio and equivalent diameter of intermetallic phases in modified alloys (8-II and 8-III) are smaller than those in 8-I (Base) alloy in as-cast state. This implies the beneficial effect of the addition elements on the modification of intermetallic phases. Also, it is reported that further reduction in the size of intermetallics can be achieved due to solution heat treatment which is attributed to partially dissolution of V, Zr and Mo containing intermetallic phases.

Moreover, the quantitative image analysis results show that the volume fraction of intermetallic phases in the 8-II (V, Zr) and 8-III (V, Zr, Mo) as-cast microstructures significantly increases via addition elements. This can be explained by the formation of V, Zr and Mo containing intermetallic phases after the addition of V, Zr and Mo elements. On the other hand, subsequent the T6 treatment, the volume fraction of intermetallics in the experimental alloys becomes less than that on as-cast condition, most likely due to the fragmentation and partial dissolution of intermetallic phases.

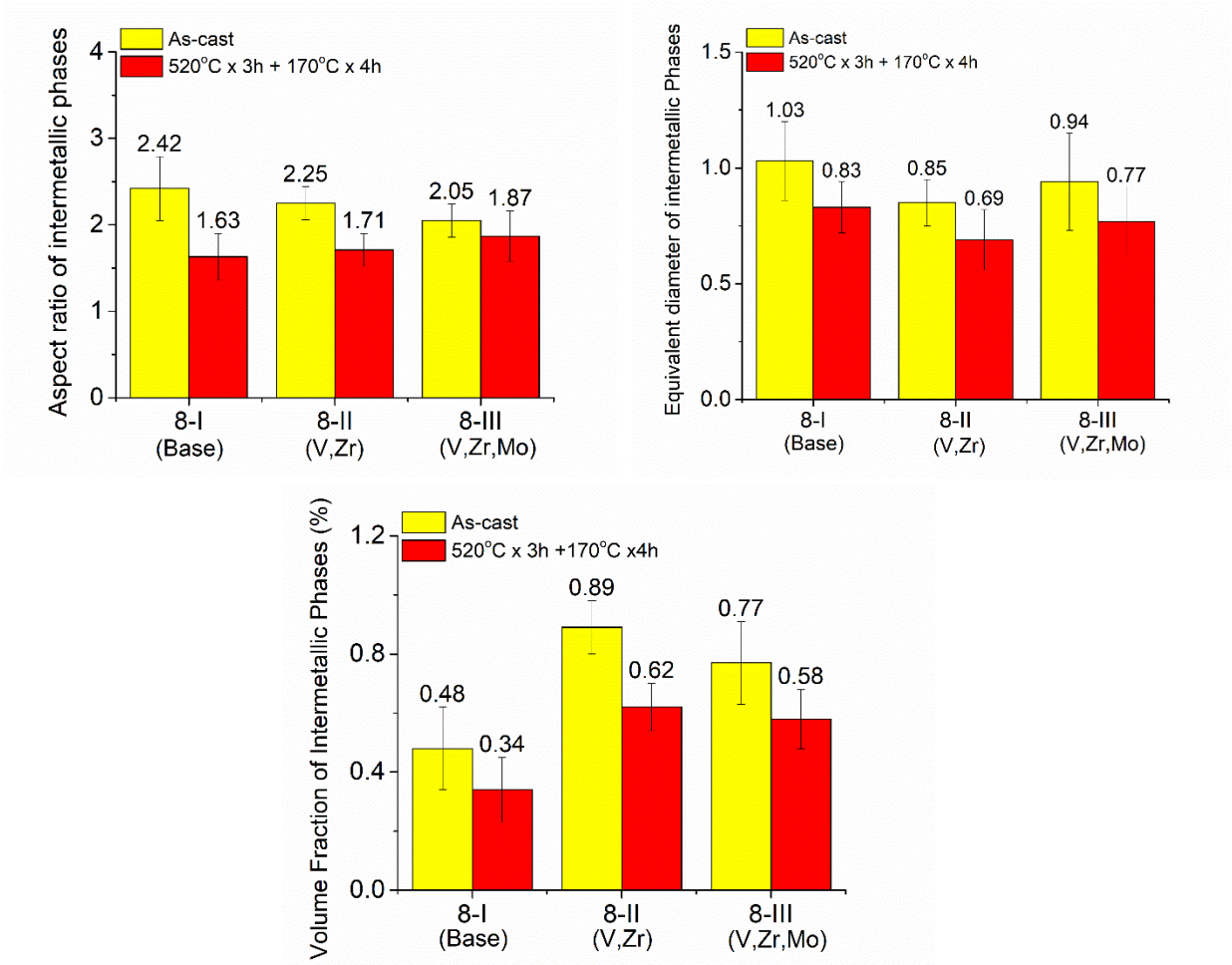

Figure 5-25: Quantitative analysis of intermetallic phases on as-cast and T6 heat treated conditions.

Figure *5-26* shows the distribution of dispersoid zone and dispersoid free zone (DFZ) in 8% Si containing experimental alloys. Following the solution heat treatment at 520°C for 3h,

considerable number of dispersoids precipitated within aluminum grains while the dispersoid free zone formed in interdendritic regions. The qualitative analysis of 8-I, 8-II and 8-III etched microstructures reveals the influence of addition elements on the wideness of dispersoid zone and dispersoid free zone. As it is seen clearly, the number of dispersoids significantly increases due to addition of V, Zr (in 8-II) and V, Zr and Mo (in 8-III) elements whereas limited dispersoids were observed in 8-I (Base) alloy.

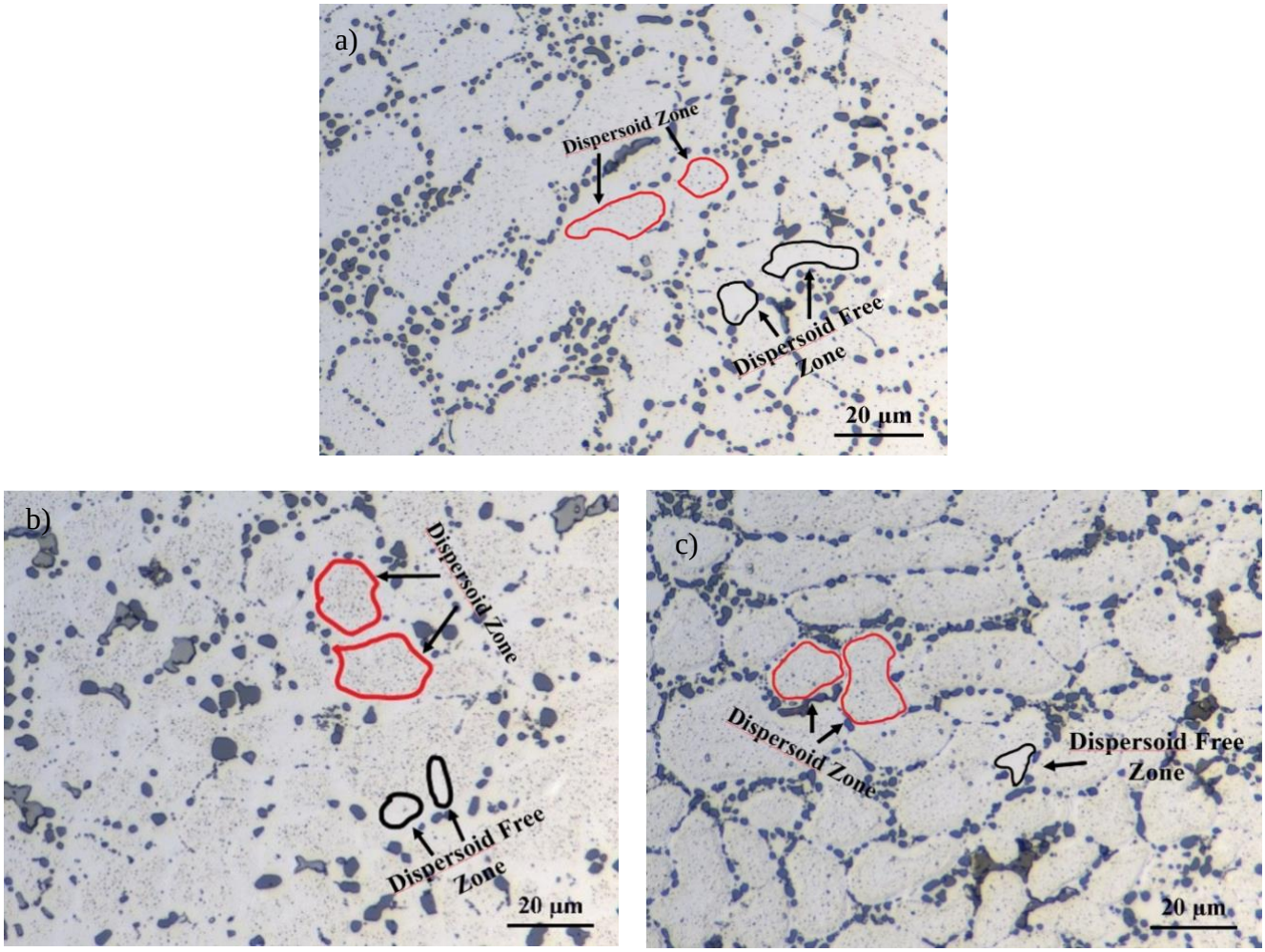

Figure 5-26: Distribution of dispersoid zone and dispersoid free zone in 8-I (a), 8-II (b) and 8-III (c) alloys.

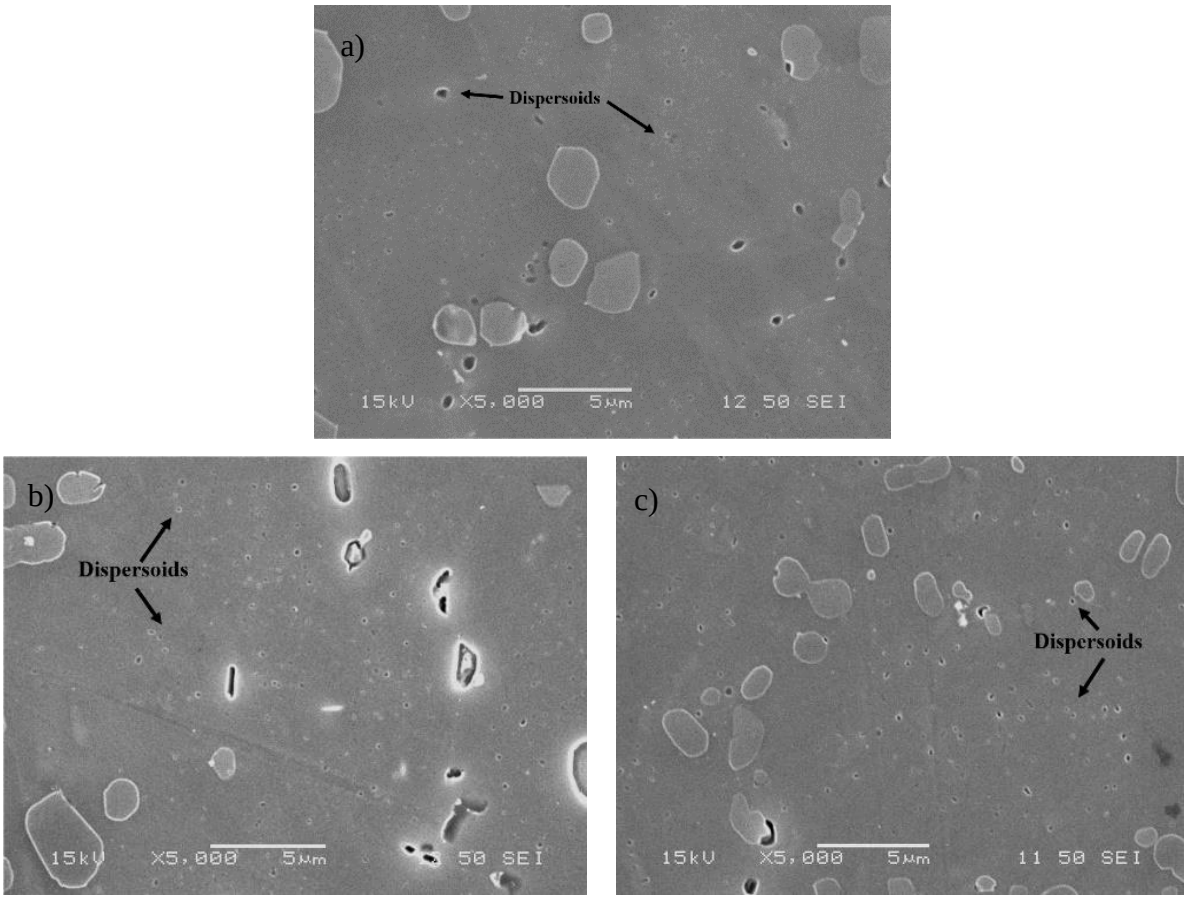

Figure 5-27: Secondary electron images of etched 8-I (a), 8-II (b) and 8-III (c) alloys after solution heat treatment

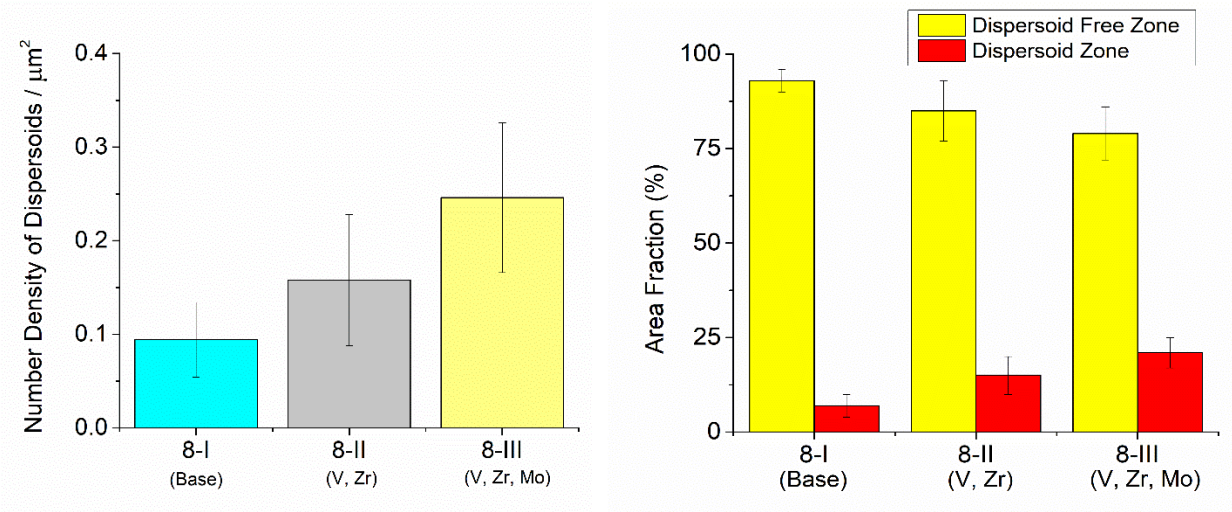

Figure 5-28: Number density of dispersoids and area fraction of DFZ in 8% Si containing alloys

In order to reveal the influence of addition elements on dispersoid formation, quantitative analysis of dispersoids were carried out. Figure *5-28* represents the number density of dispersoids (a) and area fraction of dispersoid zones (b) in 8% Si containing alloys. The results indicate that addition of V and Zr metals to the 8-I alloy, resulted a significant enhancement in the formation of dispersoids (8-II). Additionally, area fraction of dispersoid zone in 8-II alloy was significantly increased while an opposite tendency was seen for dispersoid free zones. This suggests that the presence of V and Zr elements leads the formation of higher amount dispersoids in the 8-II microstructure.

Besides, the results show that the number density of dispersoid in 8-III (V, Zr, Mo) was much higher than those in 8-I (Base) and 8-II (V, Zr) alloys, indicating the great impact of Mo elements on formation of dispersoids. As it is shown in Figure 5, 8-III alloy displays the highest hardness values among the 8% Si containing alloys in T6 heat treated conditions. According to Farkoosh et al. [3], the presence of Mo in Al-Si casting alloys leads formation of thermally stable Mo dispersoids which can hinder dislocation motions, thereby increase the mechanical properties of the alloys.

In brief, V, Zr (8-II) and V, Zr, Mo (8-III) transition elements play vital role on the formation of dispersoids in Al-Si casting alloys. Also, due to high thermally stability of these dispersoids, they can retain their strengthening effect at elevated temperatures.

Table 5-8: Electrical conductivity of HPVD castings on T6 heat treated condition at 520°C x 3h + 170°C x 4h

Alloy	Electrical Conductivity (MS\m) (520°C x 3h + 170°C x 4h)
8-I	22.9
8-II	21.46
8-III	20.78

5.4 Thermal Analysis of High-Pressure Vacuum Die Casting Alloys

As well known, non-isothermal differential scanning calorimetry analysis of solution heat treated samples is generally used to understand the precipitation kinetics of strengthening phases in alloys. *Figure 5-29* represents the DSC heating curves of solution heat treated Aural-3 (a) and 10-II (V, Zr) (b) alloys with 10 ºC / min. heating rate. The analysis reveals the presence of three exothermic peaks in Aural^{TM}-3 alloy whereas five peaks were determined in 10-II (V, Zr) alloy. This implies that the additions of V and Zr metals into Aural^{TM}-3 alloy lead to the formation of two new strengthening phases in 10-II alloy.

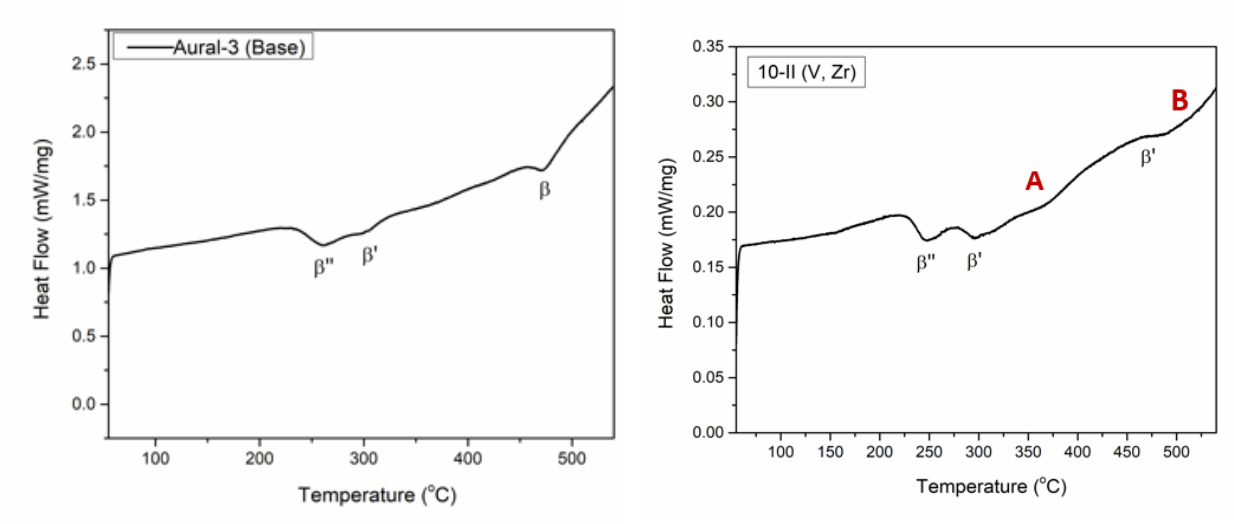

Figure 5-29: Differential scanning calorimetry curves of 10% Si containing alloys

According to the Dutta et al. [4], three peaks in the Aural^{TM}-3 alloys corresponds to β'', β', and β precipitates. These peaks were also observed in 10-II alloy while no reliable data could find for the peaks A and B. Table *5-9* and Table *5-10* are given to show the onset and peak temperatures for the peaks in two experimental alloys. As seen in Table *5-9*, the onset and peak temperatures for β''precipitates are found to be □ 228.2 ℃ and □ 260.6 ℃ respectively in Aural^{TM}-3 alloys, whereas these temperatures determined as 220.1℃ and 248.3 ℃ in 10-II alloy. In addition to that the onset and peak temperatures of β' peak in Aural^{TM}-3 alloy situated at □ 281.2 ℃ and □ 300.4

°C respectively while same peaks observed at □ 277.8 °C and □ 297.7 °C in 10-II alloy. Thus, it can be concluded that the additions of V and Zr metals to Aural™-3 alloy assist to reduce onset and peak temperatures of β'' and β' precipitates.

Table 5-9: The onset and peak temperatures of β'', β' and β phases in 10% Si containing alloys

Casting	β''		β'		β	
HPVDC	Onset (°C)	Peak (°C)	Onset (°C)	Peak (°C)	Onset (°C)	Peak (°C)
Aural™-3	228.2	260.6	281.2	300.4	456.6	472.3
10-II (V,Zr)	220.1	248.3	277.8	297.7	467.1	482.2

Table 5-10: The average values of onset and peak temperatures for A and B peaks in 10-II alloy

	A		B	
Alloy	Onset (°C)	Peak (°C)	Onset (°C)	Peak (°C)
10-II (V,Zr)	333.5	344.6	502.3	518.7

The non-isothermal DSC curves of 8% Si containing high pressure vacuum die casting alloys are given in *Figure **5-30***. In base alloy (8-I), three exothermic peaks were observed and referred as β'', β', and β precipitates. These peaks are also obtained in both 8-II and 8-III modified alloys. In addition to these, two different peaks (A, B) in 8-II (V, Zr) alloy and three different peaks (A, B, C) in 8-III (V, Zr, Mo) alloy were situated. The onset and peak temperatures of β'', β', β as well as A, B and C peaks are listed respectively in Table *5-11* and Table *5-12*.

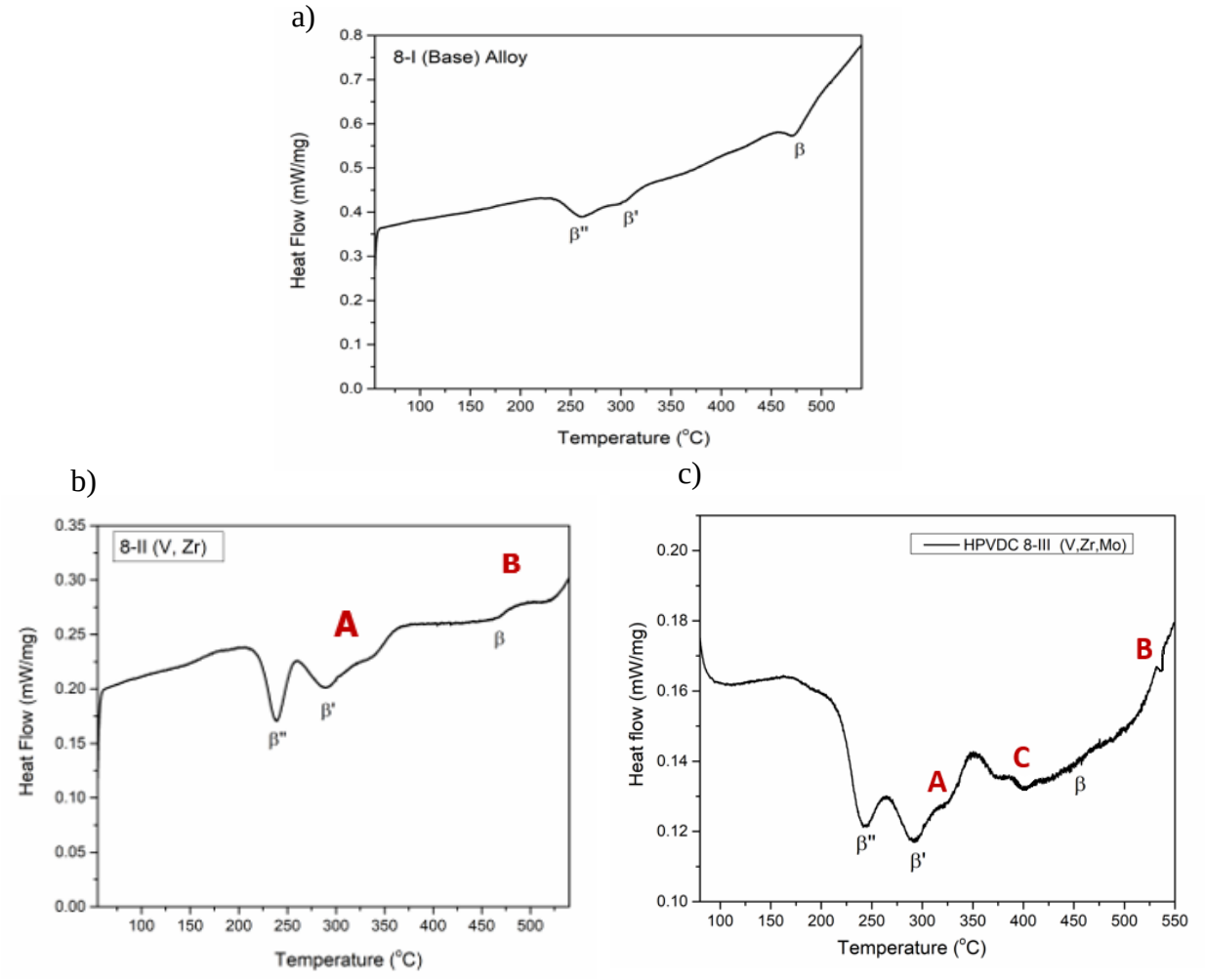

Figure 5-30: Differential scanning calorimetry curves of 8-I (a), 8-II (b) and 8-III (c) alloys

As a similar tendency observed in 10-II alloy, the onset and peak temperatures of β'' and β' precipitates in 8-II alloy are lower than those in base alloy. This indicates that the onset and peak temperatures of β'' and β' precipitates can be reduced via additions of V and Zr. On the other hand, in 8-III alloy, the onset and peak temperatures for β'' precipitates are found to be □ 178.2 °C and □ 243.4 °C respectively whereas these values were observed as □ 227.8 °C and □ 260.1 °C for the base alloy. The analysis also revealed that the onset and peak temperatures of β' and β precipitates in 8-III alloy were lower than those in 8-I (Base) alloy, indicating the beneficial influence of V, Zr and Mo additions on precipitation formation. Moreover, it is reported that the

onset and peak temperatures of β'', β' and β precipitates in 8-III alloy were even lower than those in 8-II alloy which proves that Mo addition can further decrease the onset and peak temperatures of β'', β' and β precipitates.

Table 5-11: The onset and peak temperatures of β'', β' and β phases in 8% Si containing alloys

Casting	β''		β'		β	
HPVDC	Onset (°C)	Peak (°C)	Onset (°C)	Peak (°C)	Onset (°C)	Peak (°C)
8-I (Base)	227.8	260.1	290.5	304.2	455.1	472.5
8-II (V, Zr)	214.7	248.6	273.6	296.5	454.4	472.2
8-III (V,Zr,Mo)	178.2	243.4	262.4	291.6	446.6	471.5

Table 5-12: The average onset and peak temperatures for A and B peaks in 8-II and 8-III alloys.

Casting	A		B		C	
HPVDC	Onset (°C)	Peak (°C)	Onset (°C)	Peak (°C)	Onset (°C)	Peak (°C)
8-II (V,Zr)	327.5	341.0	505.7	520.6	-	-
8-III (V,Zr,Mo)	330.3	337.5	516.2	528.2	385.8	410.9

5.5 Summary

In this chapter, mechanical properties and microstructural features of high-pressure vacuum die castings are discussed. Generally, it is well established that the presence of higher silicon content results in higher hardness of the Al-Si alloy. Following the additions of transition elements (V, Zr and V, Zr, Mo) into base alloys, a noticeable increase in hardness, yield strength and ultimate tensile strength was reported whereas a slight reduction observed in elongation. For instance, in as-cast 10 % Si containing alloys, addition of V and Zr metals into Aural^{TM}-3 alloy was resulted 4 %, 5 % and 6 % improvement in hardness, yield strength and ultimate tensile strength respectively. In contrast, elongation of 10-II alloy was obtained 16 % lower than that in Aural^{TM}-3 alloy.

On the other hand, in 8% Si containing alloys, 4 % hardness improvement was reported after addition of V and Zr (8-II alloy) into 8-I alloy on as-cast condition. It is also established that hardness can be further increased due to addition of V, Zr and Mo additions. Moreover, yield strength of 8-II (V, Zr) and 8-III (V, Zr, Mo) alloys were 13 % and 15% higher than that in 8-I alloy respectively. Also, due to addition metals, ultimate tensile strength of the 8-II and 8-III alloys were found to be 6 % and 7 % higher in comparison to the base alloy.

In order to evaluate precipitation potential of the experimental alloys, T5 and T6 heat treatments were carried out. For T6 tempers, the heat treatment parameters were optimized as 520°C for 3 hours plus 170°C for 4 hours in consideration of blistering effect and high mechanical properties on this condition. The heat-treated hardness and tensile test results indicated that the T6 heat treatment is beneficial to improve the mechanical properties of the alloys. For instance, in 10% Si containing alloys yield strength of the 10-II (V, Zr) alloy, can be increased 80% via T6 solution heat treatment while average of 85 % yield strength improvement was reported for 8% Si containing alloys. In addition to that, a remarkable enhancement in elongation values was observed in modified alloys on T6 heat treated condition, proving the beneficial influence of V, Zr and Mo additions on elongation. It is also found that increasing solution heat treatment temperature results in improvement of the yield and ultimate tensile strength however no significant difference was reported with longer soaking time. On the other hand, for T5 heat treated alloys, a remarkable higher yield strength, and ultimate tensile strength values were reported in comparison to as-cast condition of the experimental alloys. It is also well established that additions of V, Zr and Mo resulted a slight improvement in yield strength and ultimate tensile strength while limited reduction was observed in elongation properties, indicating the beneficial impact of additions elements on tensile properties of the alloys on T5 heat treated conditions.

The microstructure investigation of experimental alloys revealed that the addition of V, Zr and Mo metals resulted a significant reduction in grains size and formation of new intermetallic phases. It is also seen that the heat treatment can induce a reduction in the size and volume fraction of intermetallic phases and results the spherodizitation of the eutectic Si particles. Moreover, it is stated that V, Zr and V, Zr, Mo additions can greatly promote the formation of dispersoids and thereby further increase the mechanical properties of the alloys.

Thermal analysis of high-pressure vacuum die castings showed that V, Zr and Mo additions resulted in formation of three exothermic peaks (A, B, C) in DSC curves of modified alloys. Moreover, it is established that the additions can reduce the onset and peak temperatures of β'', β' and β precipitations in Aural^{TM}-3 and 8-I alloys.

REFERENCES

[1] W. Kasprzak, H. Kurita, G. Birsan, B.Amirkhiz, Hardness control of Al-Si HPDC casting alloy via microstructure refinement and tempering parameters, Materials Design, 103 (2016) 365-376

[2] J. Rakhmonov, G. Timelli, F. Bonollo, Characterization of the solidification path and microstructure of secondary Al-7Si-3Cu-0.3Mg alloy with Zr, V and Ni additions, Mater. Charact.,128 (2017) 100-108.

[3] A.R. Farkoosh, X. Grant-Chen, M. Pekguleryuz, Dispersoid strengthening of a high temperature Al–Si–Cu–Mg alloy via Mo addition, Mater. Sci. Eng.: A 620 (2015) 181–189.

[4] I. Dutta., S. Allen, A calorimetric study of precipitation in commercial aluminium alloy 6061. Journal of Materials Science Letters, 1991. 10(6): p. 323-326.

CHAPTER 6

GENERAL CONCLUSIONS AND RECOMMENDATIONS FOR FUTURE WORK

Chapter 6

GENERAL CONCLUSIONS AND RECOMMENDATIONS FOR FUTURE WORK

6.1 Conclusions

A study on effect of V Zr and Mo additions on mechanical properties and microstructural features of permanent mold casting and high-pressure vacuum die casting Al-Si Mg alloys was carried out. Based on the results obtained from the microstructural analysis and mechanical properties evaluation, the main conclusions could be summarized as follow;

1. The hardness and tensile properties of the AlSi10Mg permanent mold castings can be remarkably improved via addition combinations of (V,Zr), (V, Mo) and (V, Zr, Mo) on as cast condition. Following the V and Zr additions into AlSi10Mg, hardness, yield strength, ultimate tensile strength and elongation values improved by 14%, 28%, 29% 25% respectively. The additions of (V, Mo) resulted 7%, 21%, 12% and 3% improvement in hardness, yield strength, ultimate tensile strength and elongation respectively. On the other hand, the addition combination of (V, Zr, Mo) enhanced these properties by 7%, 21% and 12% respectively while elongation decreased 2% on as-cast condition.

2. Due to lower Si content, the additions of V, Zr and Mo into AlSi8Mg permanent mold casting alloy result in even higher elongation values with relatively lower hardness, yield strength and ultimate tensile strength than those in AlSi10Mg alloy. The additions of V, Zr resulted in 24%, 27%, 33% increase in yield strength, ultimate tensile strength and

elongation respectively, while 19%, 23% and 23% improvement were reported with additions of V, Mo. Meanwhile, the additions of V, Zr, Mo into AlSi8Mg results an outstanding improvement in yield strength, ultimate tensile strength and elongation values with increase of 27%, 32% and 61% respectively.

3. Due to higher hardness results and shorter soaking times, the optimum heat treatment parameters are defined as 540°C x 2h + 170°C x 4h for permanent mold casting alloys.

4. The addition combination of Zr, V into AlSi10Mg and AlSi8Mg permanent mold casting alloys have beneficial influence on the modification of eutectic Si particles and the intermetallic phases on both as-cast and T6 (540°C x 2h + 170°C x 4h) heat treatment conditions. In AlSi10Mg alloy, the equivalent diameter of Si particles decreased from 1.82 µm to 1.48 µm after addition of V and Zr. Also, length of the Fe-rich intermetallic phases decreased by 20%. Meanwhile, in 8% Si containing alloys, additions of V and Zr reduced equivalent diameter of Si particles, aspect ratio and length of intermetallic phases by 19%, 20% and 26% respectively. Besides, V and Zr addition into both AlSi10Mg and AlSi8Mg alloys generates their own intermetallic phases; $(AlSi)_3(ZrTi)$ and Al-Si-V, thus increases the volume fraction of intermetallic phases.

5. The additions of V, Zr, Mo into AlSi8Mg permanent mold castings can decrease equivalent diameter of Si particles and length of intermetallic phases by 22% and 40% respectively. In addition to that due to newly generated Al-Si-Fe-Mn-V-Mo and $(AlSi)_3(ZrTi)$ intermetallics, volume fraction of intermetallic phases significantly increases.

6. The addition combinations of (V, Zr) and (V, Zr, Mo) promote partial dissolution of the intermetallic phases during solution heat treatment at 540°C for 2 hours. The number density of dispersoids increased via addition of V and Zr while dispersoid free zones remarkably decreases. The combination of V, Zr and Mo additions induces even further increase in number density of dispersoids, thus further improve the mechanical properties on T6 (540°C x 2h + 170°C x 4h) heat treated condition.

7. In high pressure vacuum die (HPVD) castings, the additions of V, Zr into AlSi10Mg and AlSi8Mg alloys can improve hardness, yield strength and ultimate tensile strength however it slightly reduces elongation on as cast condition. In 10% Si containing HPVD castings, the additions of (V, Zr) resulted in improvement up to 12%, 10% and 10% in hardness, yield strength and ultimate tensile strength while a negligible reduction observed in elongation. Meanwhile, V and Zr additions into AlSi8Mg resulted 5%, 13% and 5% increase in hardness, yield strength and ultimate tensile strength respectively.

8. The additions of V, Zr, Mo into HPVD castings can remarkably increase hardness, yield strength, ultimate tensile strength while it also considerably increases elongation values on as-cast condition. Following V, Zr and Mo additions into AlSi8Mg alloy, hardness, yield strength, ultimate tensile strength and elongation of AlSi8Mg alloy increased by 9%, 15%, 8% and 6%.

9. Although highest hardness values in HPVD castings were achieved via solution heat treatment at 540°C x 3h + WQ + 170°C x 4 h, the optimum T6 heat treatment parameters are defined as 520°C x 3h + WQ + 170°C x 4h in order to minimize blistering effect. On the other hand, for T5 temper, two different conditions were selected; (1) 170°C x 4h and (2) 210°C x 1h.

10. In HPVD castings, solution heat treatment at 520°C x 3h + WQ + 170°C x 4h resulted a remarkable higher hardness, yield strength and ultimate tensile strength values in comparison to as-cast condition. On the other hand, the additions of V, Zr and V, Zr, Mo did not further improve the yield strength and ultimate tensile strength of the experimental alloys in comparison to base alloy. However, elongation values of modified alloys were significantly higher than those in base alloy on T6 heat treated condition.

11. In HPVD castings, the ultimate tensile strength of T5 heat treated V, Zr and V, Zr, Mo modified alloys were slightly higher than those in base alloys, proving the beneficial impact of addition elements. On the other hand, following the T5 heat treatment at 210°C and 170°C, no significant improvement was observed in yield strength of the modified alloys. Besides, the addition of V, Zr and V, Zr, Mo metals can provide 20% - 40% higher elongation values on T5 condition.

12. In 10% Si containing alloys, the addition of V, Zr into HPVD castings result a significant reduction in grains size, aspect ratio and equivalent diameter of intermetallic phases while volume fraction of intermetallic phases increases. Following the V, Zr additions in

AlSi10Mg alloy, the average grain diameter reduced from 87.7 µm to 43.1 µm. Besides, aspect ratio and equivalent diameter of intermetallics decreased by 20% and 15%. Moreover, solution heat treatment (520°C x 3h + 170°C x 4h) can further induce a reduction in size and volume fraction of the intermetallic phases due to dissolution of intermetallic phases.

13. In 8% Si containing HPVD castings, additions of V, Zr resulted in 35% reduction in average grain diameter while 30% reduction was reported with addition of V, Zr, Mo metals. Besides, aspect ratio of intermetallic phases reduced from 2.42 to 2.25 and 2.05 with additions of (V, Zr) and (V, Zr, Mo) respectively. Moreover, volume fraction of intermetallic phases was increased by 45% and 32% with additions of (V, Zr) and (V, Zr, Mo)

14. In HPVD castings, the number density of dispersoids increases up to 130% due to addition of V and Zr while dispersoid free zones significantly decreases. On the other hand, the V, Zr and Mo additions result even higher (145%) number density of dispersoids, therefore, further improve the mechanical properties on T6 (540°C x 2h + 170°C x 4h) heat treated condition.

6.2 Recommendation for future work

In order to establish a complete understanding of the effects of V, Zr, and Mo additions and casting processes on the microstructure features and mechanical properties of Al-Si-Mg alloys, the following work may be suggested;

1. Further TEM studies can be performed to arrive fully understanding on the role of V, Zr and Mo additions in permanent mold casting and high-pressure vacuum die casting alloys.

2. The content of V, Zr and Mo additions can be changed to reveal the influence of additions content on mechanical properties of Al-Si-Mg alloys and also optimize the amount of additions in order to achieve highest mechanical properties.

3. In this thesis, DSC curves of HPVD castings were studied and discussed. However, no detailed information on the peaks of A'', B'' and C' could be given due to very limited studies in literature. Therefore, further TEM studies may focus on the identification of these peaks and thus it would be easier to explain the effect of transition elements on the precipitation kinetics.